

Peptide Nucleic Acids (PNA) as a versatile tool for modulation of biological systems with visible light.

Zur Erlangung des akademischen Grades eines

DOKTORS DER NATURWISSENSCHAFTEN

(Dr. rer. nat.)

von der KIT-Fakultät für Chemie und Biowissenschaften

des Karlsruher Instituts für Technologie (KIT) – Universitätsbereich

genehmigte

DISSERTATION

von

M. Sc. Tobias Bantle

aus Karlsruhe

KIT-Dekan: Prof. Dr. Manfred Wilhelm

Referent: Dr. Zbigniew L. Pianowski

Korreferent I: Prof. Dr. Hans-Achim Wagenknecht

Korreferent II: Prof. Dr. Frank Breitling

Tag der mündlichen Prüfung: 21.07.2020

Nihil invitus facit sapiens. Necessitatem effugit, quia vult, quod coactura est.

The wise man does nothing against his will. He defies necessity because he wants to force him to do so.

Der Weise tut nichts gegen seinen Willen. Er entzieht sich der Notwendigkeit, weil er will, wozu sie ihn zwingen wird.

The present work was carried out at the Karlsruhe Institute of Technology, Faculty of Chemistry and Biosciences, Institute of Organic Chemistry in the period from May 1st 2017 to June 10th 2020 under supervision of Dr. Zbigniew L.Pianowski.

Die vorliegende Arbeit wurde in der Zeit von 01.05.2017 bis 10.06.2020 am Institut für Organische Chemie Fakultät für Chemie und Biowissenschaften am Karlsruher Institut für Technologie (KIT) unter der Leitung von Dr. Zbigniew L.Pianowski durchgeführt.

I hereby certify that I have written this dissertation independently and made it without any illicit means, that I have not used any other sources and aids and that I have identified the sources taken from the source or content as such. So far, the work has not been submitted to any other examination authority in the same or similar form, nor has it been published. I have observed the rules to ensure good scientific practice in the Karlsruhe Institute of Technology (KIT) in the current version. The document submitted in writing corresponds to the one on the digital carriers (CD). Furthermore, all primary data are stored at the institute (IOC, KIT).

Hiermit versichere ich, dass die vorliegende Dissertation selbstständig verfasst und ohne unerlaubte Hilfsmittel angefertigt wurde. Es wurden ausschließlich die angegebenen Quellen und Hilfsmittel verwendet und die wörtlich oder inhaltlich entnommenen Stellen als solche kenntlich gemacht. Die Arbeit wurde in gleicher oder ähnlicher Form noch keiner anderen Prüfungsbehörde vorgelegt oder woanders veröffentlicht. Ich habe die Regeln zur Sicherung guter wissenschaftlicher Praxis im Karlsruher Institut für Technologie (KIT) in der gültigen Fassung beachtet. Das schriftlich vorgelegte Dokument entspricht dem, welche sich jeweils auf den digitalen Trägern (CD) befindet. Darüber hinaus sind alle Primärdaten beim Institut (IOC, KIT) gespeichert.

Ort, Datum

Unterschrift

Table of contents

Abstract	IV
Kurzfassung	V
1 Introduction	1
1.1 Molecular photoswitches in nature and research	1
1.1.1 Stilbenes	1
1.1.2 Diarylethenes	4
1.1.3 Spiropyrans	7
1.1.4 Azobenzenes	10
1.2 Natural and Artificial Nucleotides	16
1.2.1 Short introduction to DNA	16
1.2.2 Short Introduction to RNA	19
1.2.3 Modification of Nucleobases	20
1.2.4 Modification of the Backbone	21
1.2.5 Peptide Nucleic Acid (PNA)	23
1.2.6 Guanidinium Peptide Nucleic Acid (GPNA)	26
1.2.7 Application examples for PNA	27
2 Aim of the project	33
3 Results and Discussion	34
3.1 Synthesis of PNA-, α -GPNA- and γ -GPNA-backbone	34
3.2 Synthesis of modified nucleobases	42
3.3 Synthesis of PNA and GPNA building blocks	43
3.4 Azobenzene derivatives	45
3.5 Indole-derived fluorescent dyes	51
3.6 Novel fluorinated Spiropyranes	52

3.7	(G)PNA oligomers for knock down experiments in Zebrafish.....	58
3.8	(G)PNA oligomers for hybridization experiments against HIV	60
4	Conclusion and outlook.....	66
4.1	Synthesis of γ -GPNA.....	66
4.2	Novel fluorinated Spiropyranes	66
4.3	Azobenzene Derivatives.....	67
4.4	PNA/GPNA	67
5	Experimental part.....	68
5.1	Origin of compounds, chemicals and data.....	68
5.1.1	Solvents and reagents.....	68
5.1.2	Thin layer chromatography (TLC)	68
5.1.3	High performance liquid chromatography (HPLC).....	68
5.1.4	Column chromatography.....	69
5.1.5	Nuclear magnetic resonance (NMR) spectroscopy	69
5.1.6	UV-Vis spectroscopy	69
5.1.7	Solid phase synthesis.....	70
5.1.8	Lyophilization	70
5.1.9	Mass spectrometry (EI, FAB, MALDI)	70
5.1.10	Analytical balance	71
5.1.11	Preparative work	71
5.1.12	RNase free working conditions.....	71
5.2	Synthesis of literature known procedures.....	72
5.2.1	Synthesis of the modified nucleobases	72
5.2.2	Synthesis of PNA and GPNA monomers	78
5.2.3	Synthesis of modified Azobenzenes	87
5.2.4	Synthesis of Nitro-Spyropyranes	94

5.2.5	Synthesis of cyano-dyes	96
5.2.6	Synthesis of Ribonucleic cleaver.....	98
5.3	New products	102
5.3.1	Synthesis of α -GPNA	102
5.3.2	Synthesis of γ -GPNA	120
5.3.3	Synthesis of Novel Spiropyranes	122
5.3.4	Synthesis of Azobenzenes	127
5.3.5	Synthesis of Dye-PNA	130
5.3.6	Synthesis of PNA-Oligomers and Oligo-Peptides	134
6	Abbreviation index.....	149
7	Literature index.....	151
8	Appendix.....	VIII
8.1	Curriculum Vitae	VIII
9	Acknowledgements.....	X

Abstract

The main goal of this thesis was to combine novel photoswitchable molecules, possibly operational in the visible light range, with PNA (peptidonucleic acids) – artificial oligonucleotide analogues with high hybridisation affinity and sequence selectivity towards complementary DNA and RNA strands. The binding is so strong, that under optimal conditions gene expressions (antigene) and translations into proteins (antisense) can be prevented *in vivo*. Due to a highly specific hybridisation with an oligomer of >10 nucleobases, short PNA oligomers can selectively target particular targets inside living cells or organisms without interfering with the rest of cell's biosynthetic machinery. The long-term goal of this work was implementation of photoswitchable units, like the azobenzene or a spiropyrane, to achieve reversible switching of the antigen or antisense effect with visible light.

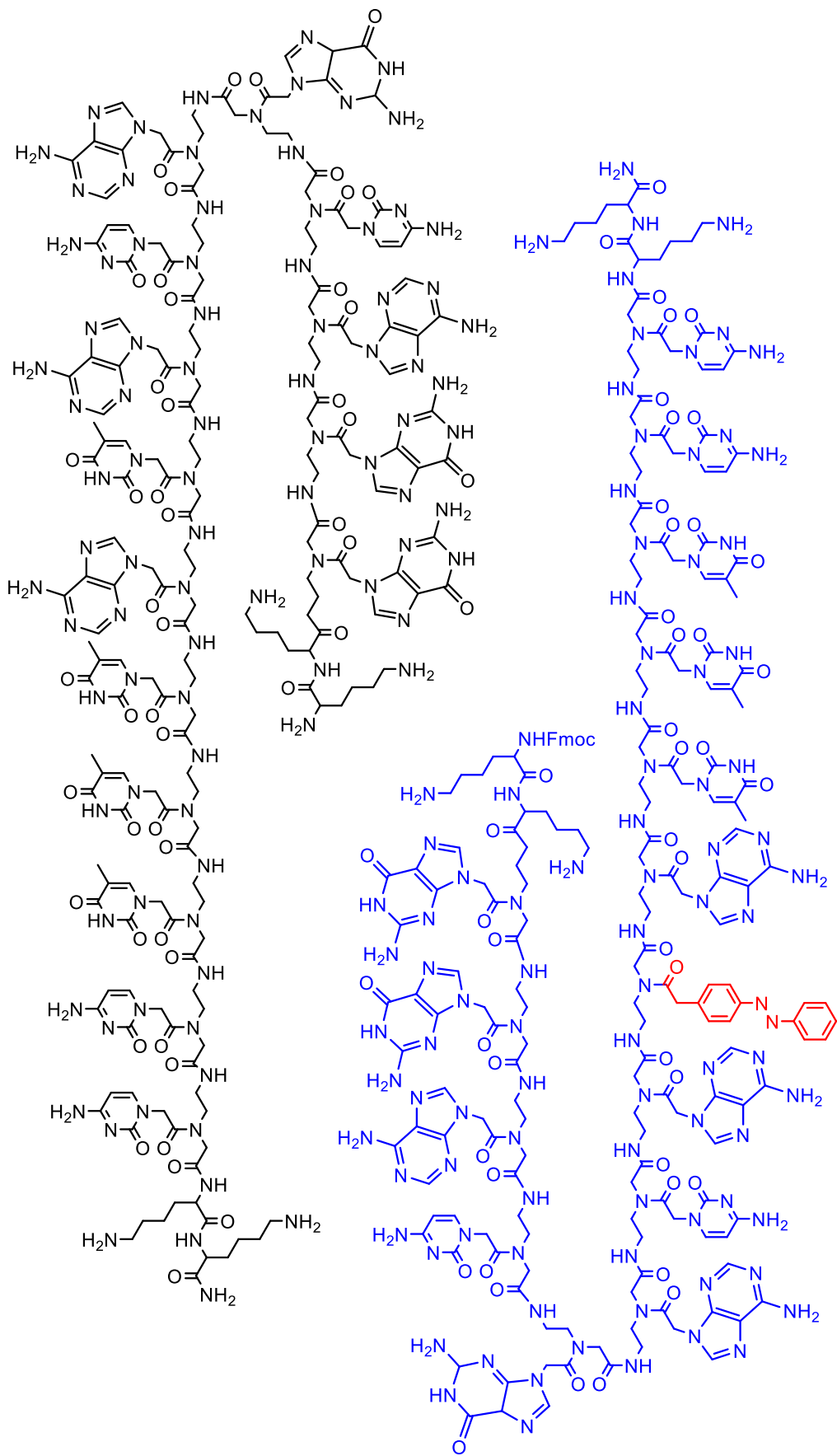
In an offspring project, the PNA was implemented for investigations against the HIV (human immunodeficiency virus). HIV causes AIDS, which is currently one of the most demanding diseases. The virus itself attacks the immune system and systematically destroys it. Since the virus uses our DNA to reproduce itself it is not recognized as an 'invader'. It spreads easily and a commercially available cure is not known yet, although recently introduced antiretroviral therapies can temporarily reduce the virus' level under detection limits. The current hypothesis is that the virus is preserved somewhere in the organism, where the common drugs cannot reach it. Since there are fluorescent dyes which exhibit an increase of the fluorescence intensity (a light-up effect) while hybridized inside of a double oligonucleotide strand (RNA/RNA; RNA/DNA; DNA/DNA; PNA/DNA; PNA/RNA) we attempted to construct an analytical tool to detect HIV-RNA. Fluorescent localization of the HIV viruses would, in turn, help to design drugs that can reach the last reservoirs of the virus, and efficiently eradicate it from the organism. The region of the HIV RNA, which we want to target with PNA sequences, is known of to be the most important region for multiplying. Blocking this region with a complementary PNA would prevent it from assuming the correct fold. This would lead to a knockdown, which hinder the virus to spread further. Another strategy was to decorate the end of the PNA sequences with a chemical ribonuclease. Such a PNA oligomer would cut the complementary RNA in a sequence-specific manner, thus destroying the RNA of the virus and hereby the virus itself.

Kurzfassung

Das Hauptziel dieser Arbeit war die Kombination neuartiger photoschaltbarer Moleküle, die möglicherweise im Bereich des sichtbaren Lichts operieren, mit PNA (Peptidonukleinsäuren) - künstlichen Oligonukleotidanaloga mit hoher Hybridisierungsaffinität und Sequenzselektivität gegenüber komplementären DNA- und RNA-Strängen. Die Bindung ist so stark, dass unter optimalen Bedingungen Genexpressionen (Antigene) und Übersetzungen in Proteine (Antisense) in vivo verhindert werden können. Aufgrund einer hochspezifischen Hybridisierung mit einem Oligomer von >10 Nukleobasen können kurze PNA-Oligomere selektiv auf bestimmte Ziele innerhalb lebender Zellen oder Organismen abzielen, ohne die übrige biosynthetische Maschinerie der Zelle zu stören. Das langfristige Ziel dieser Arbeit war die Implementierung photoschaltbarer Einheiten, wie das Azobenzol oder ein Spiropyran, um ein reversibles Schalten des Antigens oder des Antisense-Effekts mit sichtbarem Licht zu erreichen.

In einem Nachfolgeprojekt wurde die PNA für Untersuchungen gegen das HIV (humanes Immunschwächevirus) eingesetzt. HIV verursacht AIDS, eine der derzeit anspruchsvollsten Krankheiten. Das Virus selbst greift das Immunsystem an und vernichtet es systematisch. Da das Virus unsere DNA benutzt, um sich zu reproduzieren, wird es nicht als "Eindringling" erkannt. Es breitet sich leicht aus, und eine kommerziell verfügbare Heilung ist noch nicht bekannt, obwohl kürzlich eingeführte antiretrovirale Therapien die Virusmenge vorübergehend unter die Nachweisgrenze senken können. Die derzeitige Hypothese ist, dass das Virus irgendwo im Organismus konserviert wird, wo es von den üblichen Medikamenten nicht erreicht werden kann. Da es Fluoreszenzfarbstoffe gibt, die eine Erhöhung der Fluoreszenzintensität (einen Aufhellungseffekt) zeigen, während sie innerhalb eines Doppel-Oligonukleotidstrangs (RNA/RNA; RNA/DNA; DNA/DNA; PNA/DNA; PNA/RNA) hybridisiert sind, haben wir versucht, ein analytisches Werkzeug zum Nachweis von HIV-RNA zu konstruieren. Die fluoreszierende Lokalisierung der HI-Viren würde wiederum dazu beitragen, Medikamente zu entwickeln, die die letzten Reservoirs des Virus erreichen und es effizient aus dem Organismus ausrotten können. Die Region der HIV-RNA, auf die wir mit PNA-Sequenzen abzielen wollen, ist bekanntlich die wichtigste Region für die Vermehrung. Eine Blockierung dieser Region mit einer

komplementären PNA würde verhindern, dass sie die richtige Faltung annimmt. Dies würde zu einem Knockdown führen, was die weitere Ausbreitung des Virus behindern würde. Eine andere Strategie bestand darin, das Ende der PNA-Sequenzen mit einer chemischen Ribonuklease zu dekorieren. Ein solches PNA-Oligomer würde die komplementäre RNA sequenzspezifisch ausschneiden und so die RNA des Virus und damit das Virus selbst zerstören.



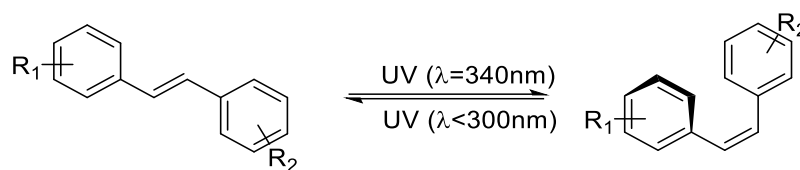
1 Introduction

1.1 Molecular photoswitches in nature and research

For centuries, scientists have been investigating materials and systems that reversibly respond to environmental stimuli. Molecular photoswitches are molecules with the ability to reversibly change their properties (geometry, polarity, charge, flexibility) under light irradiation. Herein the pH-value, temperature and the solvent influence the states. In most common examples, the change occurs due to reversible light-induced E/Z-isomerization of double bonds, or due to electrocyclizations. Most common classes of molecular photoswitches are azobenzenes, stilbenes, diarylethenes, and spiropyrans.

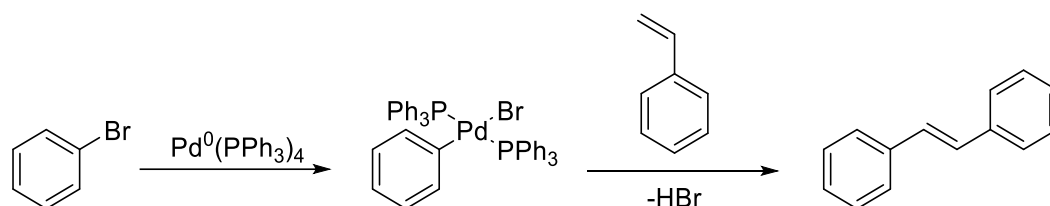
1.1.1 Stilbenes

The first major class of molecular photoswitches are stilbenes. The stilbene consists of two phenyl rings connected *via* an ethylene linker. Under irradiation with UV light at the wavelength of $\lambda = 340$ nm the molecule depicted in scheme 1 changes its conformation from *trans* to *cis*. The reverse reaction takes place under irradiation with UV-light at a wavelength of $\lambda < 300$ nm. Due to the thermal instability of the *cis*-isomer, thermal relaxation is observed. The half-lifetime of the *cis* isomer depends on the substituents at the phenyl ring. It spans from milliseconds to days. This characteristic is based on the fact that the 6π electron system of the two phenyl rings in the *cis*-configuration are in a non-planar arrangement. This means that they interfere with each other and therefore promote thermal relaxation. Electron withdrawing substituents like fluorine decrease the electron density in the 6π system, which elongates the lifetime of the *cis* isomer. On top, the characteristic wavelength for switching can be shifted towards the visible light, but for a fast relaxation UV-light is required.



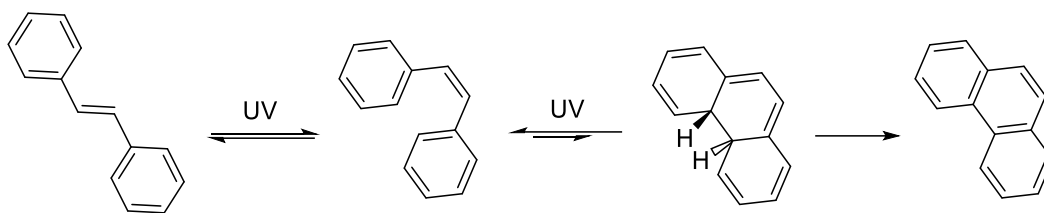
Scheme 1: Stilbenes (left) switch their conformation from *trans* to the less stable *cis*-conformation under irradiation of UV light at the wavelength of ~340 nm. The reverse process is triggered with wavelength below 300 nm. Thermal relaxation to the *trans*-isomer is observed in darkness as well.

The core structure of stilbene can be synthesized in a Horner-Wadsworth-Emmons[1] reaction. Industrial scale reaction is e.g. catalytic dimerization of toluene. The core structure can be modified in the electrophilic aromatic substitution reaction. This leads to symmetric stilbenes. To obtain non-symmetrical stilbene derivatives, cross-coupling reactions like the Heck- (scheme 2) or the Stille-coupling are possible pathways. In these reactions a various number of substituents are tolerated, however they are not optimal for bio-application due to contamination with heavy metals from the catalysts.



Scheme 2: Simplified schematic representation of the Heck cross-coupling reaction starting with bromobenzene. After the activation of the halogen-aryl compound with Pd(PPh₃)₄ the compound d reacts with styrene to *trans*-stilbene.

Stilbenes are a natural product. Their derivatives can be found in many plants. Over the last two decades more and more derivatives were extracted and characterized. The variety of applications ranges from antioxidants over phytoestrogens to anti-cancer drugs.[2] Pinoslivin, a *meta* di- hydroxyl-substituted stilbene is known as an antifungal agent that is synthesized in plants, e.g. wine grapes. The biosynthesis is initiated when the plant is experiencing fungal infestation or physical stress.[3] Other examples for stilbene derivatives with pharmaceutical importance is (figure 2) resveratrol, which differs only by a hydroxyl-group from pinoslivin, is a well-known antioxidant. It was extracted from more than 72 plants all over the world. It was found to inhibit the iron-catalyzed lipid peroxidation by more than 80%.[4] It has not clearly been proven, if this derivate has an anti-cancer effect. The assumption is, that it interferes or supports interactions with specific proteins, which are necessary for the surviving of cancer cells.

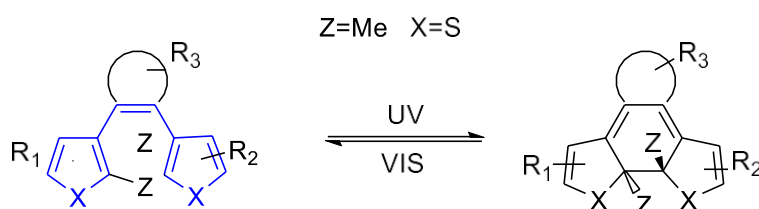


Scheme 3: Reaction of *trans*-stilbene (left) to phenanthrene (right). After the light-triggered transformation to *cis*-stilbene (middle-left), an electrocyclization reaction between the π -electron systems of both aryl rings can occur. The product is unstable and can re-open to the *cis*-stilbene, or can be dehydrogenated to phenanthrene e.g. under the presence of oxygen. Phenanthrene is stable and not photoswitchable.

This ‘quenching’ of the photoswitch in the presence of oxygen is not desired, since after a couple of switching cycles the photochrome is fully degraded. Nevertheless, this disadvantage was exploited to become an advantage in the following photoswitchable scaffold, the diarylethenes - a subclass of stilbenes.

1.1.2 Diarylethenes

The core structure of diarylethenes (DEAs) is derived from the stilbene core structure. In contrast to stilbenes, the double bond between the aryl systems is fixed in the *cis*-configuration. Due to configurational stabilization within the adjacent ring, rotation along the C-C double bond does not occur (scheme 4). Instead, irradiation causes only the reversible electrocyclization process.



Scheme 4: Schematic structure of diarylethenes. Two aryl rings are linked with a C-C double bond which is similar to the *cis*-stilbene structure (blue, left). Under irradiation with UV light the acyclic 6π -electron system cyclizes to the more rigid closed form (a 6-membered ring). The back-reaction is triggered with visible light. The Z-groups (methyl or ethyl) prevent the dehydrogenation to the aromatic phenanthrene analogue according to the pathway described in 1.1.1. Heteroatoms like oxygen, sulfur and nitrogen (X) are implemented to favor the cyclisation and stabilize the closed form to prevent a thermal relaxation.

The open form of diarylethenes is more flexible due to free rotation of the aryl rings. This rotation is not possible after the ring closure. Furthermore, the oxidative dehydrogenation to the stable and irreversible aromatic derivative is prevented by the attached alkyl groups at the C-atoms involved

at the cyclisation process (scheme 4). In literature, methyl and ethyl groups are reported.[8] A 5-membered ring suppresses the *cis/trans*-isomerization along the C-C double bond of this stilbene analogue. To favor the cyclization reaction upon irradiation with UV light, a heteroatom-bearing 5-membered-ring aromatic system is preferred. These can be sulfur, oxygen or nitrogen. [9] Due to the ring tension and a stabilized transition state, UV-light will trigger the cyclization reaction. Following the Woodward–Hoffmann rules, the photochemical 6π cyclization takes place in a conrotatory fashion, leading to products with an anti configuration of the methyl substituents. As both methyl groups are attached to a stereogenic center, two enantiomers (R,R and S,S) are formed, normally as a racemic mixture. This approach also has the advantage that the thermal (disrotatory) ring closure cannot take place because of steric hindrance between the substitution groups.[10] Furthermore, the aromatic rings are substituted with linker groups like carboxylic acids, amines, azides or alcohols. The aromatic system can be elongated with e.g. indole derived aromatic systems, which changes the photophysical properties and may cause bathochromic shift of the absorption maxima. Although most diarylethenes are nonfluorescent in both, the open- and the closed-ring conformation, fluorescent diarylethene derivatives were prepared by introducing fluorescent units, such as indole,[11] furan,[12] oxazole,[13]pyrazole[14] and oligothiophene[15] as the aryl group. Disubstituted indoles are well-known to exhibit strong fluorescence.[16] Nevertheless, low photostability in aqueous solutions is the main drawback of these synthetic photochromic dyes, which limits their switching performance and utility for biological applications. Even the most promising reversibly photoswitchable DAEs with fluorescent „closed “ forms-are known to undergo only several switching cycles in aqueous solutions. In **2019** Hell et al.[17] introduced new fluorescent DEA-dyes capable of alternating under irradiation with UV (365 nm) and visible light (470 nm) over one hundred times.

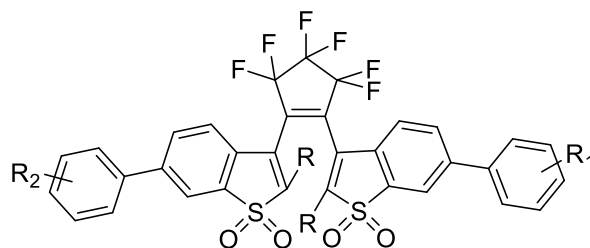


Figure 2: Schematic DEA provided by Hell et al.[18] The two aromatic systems are linked with a perfluorinated cyclopentene.

In literature, the DEAs with perfluorocyclopentene rings undergo 1.4×10^4 switching cycles in methylcyclohexane. Both conformers are thermally stable and a large separation between absorption bands has been observed. The new water-soluble DEAs fulfill switching cycles in aqueous solutions without exclusion of air oxygen, which make them realistically applicable under biological conditions.[19]

One example for the biological application of the DEAs was demonstrated by Babii et al. [8]. They incorporated a DEA in the cyclic peptide structure of gramicidin S (GS), an antibiotic (figure 3) and showed that the antibiotic effect of this photochromic cyclic peptide could be reversibly modulated with light.

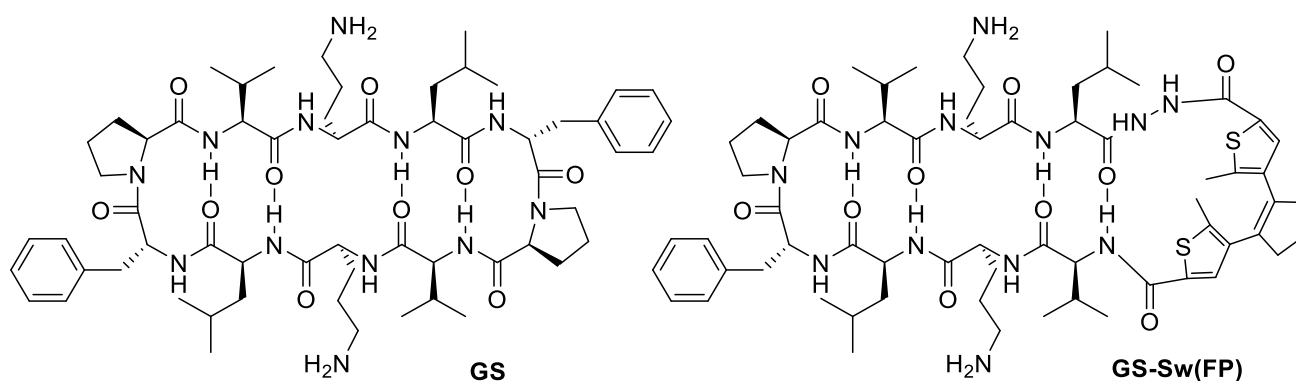
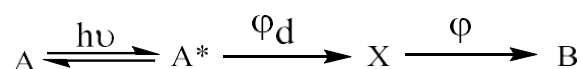


Figure 3: Gramicidin S (GS, left) is a decaameric cyclic peptide consisting of valine, ornithine, leucine, D-phenylalanine, and proline. Two of the β -turn amino acids were replaced with a DEA (right).

In figure 3 one of three photochromic gramicidin derivatives investigated by Babii et al.[8] is shown. This natural antibiotic has a highly amphiphilic structure and is thereby able to permeabilize membranes and kill bacteria. The antibacterial activity photomodulation against *S. xylosus* was shown under irradiation of a Petri dish with UV light using a template. In the dark, bacteria were nearly unaffected while the part exposed to light showed no presence of the bacteria. The DEAs have many advantages. The switching is fast and has a good quantum yield to the respective form. With suitable residues/substituents, the photooxidation can be prevented to the high degree. Some aryl systems render DEAs useful as switchable fluorescent dyes. However, most DEAs need UV-light to switch, which makes them not fully compatible with *in vivo* applications.

1.1.3 Spiropyrans

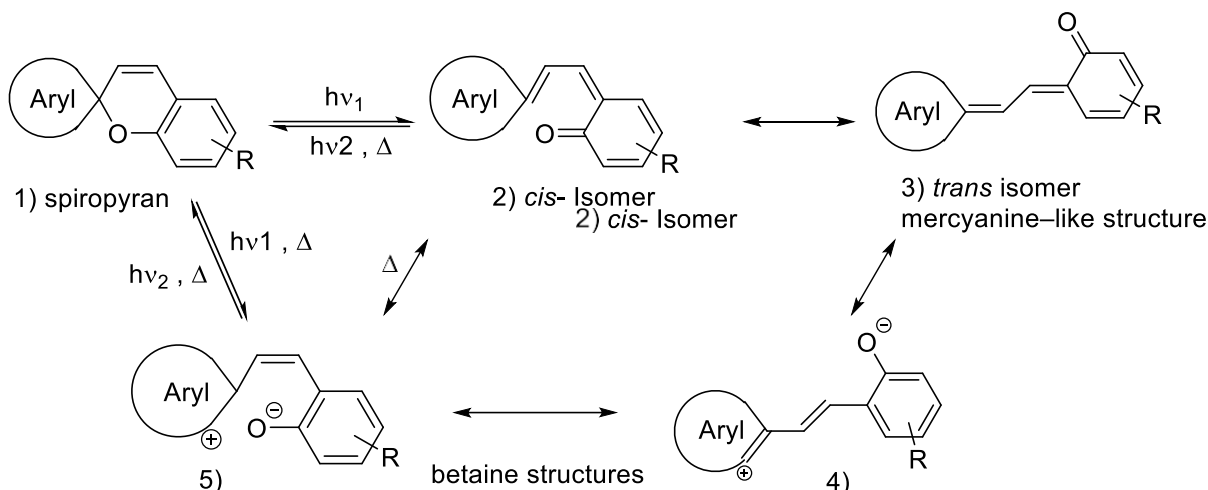
Alike some DEAs, spiropyrans can be fluorescent in their open form. DEAs on the other hand are fluorescent when they are closed. The interest in spiropyrans began in the 1920's.[20] First, the reversible thermochromic properties were discovered. After certain time, the photochromic properties of these molecules were verified, which led to a more careful examination.[21] Spiropyrans are now very widespread as photochromes and have a wide variety of demonstrated applications. The photochemical activity and luminescence of spiropyrans are determined by the position of the energy levels and the nature of the orbital of the lowest electronically excited state. In addition to understanding the mechanism of photodissociation, it is necessary to account for involvement of the electrons of heteroatoms in configuration of the excited states, and the interaction of the orbitals of the orthogonal heterocycles in ground state as well as in the excited state. The process of photocoloration of spiropyrans can be roughly represented in a reaction as follows. [22]



Scheme 5: The starting material (A) is the colorless initial spiropyran, A* is the electronically excited state, X is the cis-isomer of the colored form arising after dissociation of the bond but still preserving the orthogonality of the heterocycles, B is the planar colored form of the spiropyran; ϕ_d is the quantum yield in the bond dissociation process and ϕ is the quantum yield in the formation reaction to the B form.

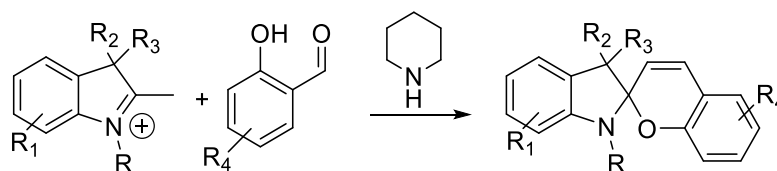
An interesting subset of these compounds are spiropyrans with an absorption maximum shift to the visible light band. The shift can be achieved by introducing a π -accepting substituent such as a nitro group at the benzene ring of the chromene part.[23] The same effect can be achieved by replacing the oxygen with a sulfur atom in the pyran fragment.

The general structure of the spiropyrans consists of two aromatic systems linked over a spiro-center with heteroatoms (nitrogen, oxygen) next to it. The bonds next to the oxygen (scheme 6) can break homo- or heterolytically to the respective *cis*-ketone or *cis*-enolate. These are in equilibrium with their *trans*-isomer, whereas both keto forms are in equilibrium with the enolate forms.



Scheme 6: General structure of spiropyranes (1), bearing different substituents on one or both heterocycles. Light-induced reaction can lead to either a homolytic cleavage of the spiro-bond to a *cis*-ketone (2) with switchable double bonds or to a heterolytic cleavage to a *cis*-enolate-form (5) with one double bond. Both *cis*-isomers (2, 5) are in equilibrium with their respective *trans*-isomer as well as the (*cis*-*trans*) keto-form (2/3) is in equilibrium with the respectively (*cis*-*trans*) enolate-form (5/4).[24, 25]

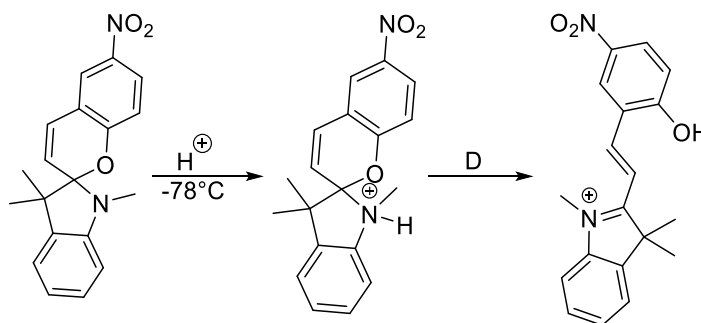
The standard synthesis methods towards spiropyranes can be divided into two main groups: condensations of methylene bases (or their precursor) with *o*-hydroxy aromatic aldehydes and condensations of *o*-hydroxy aromatic aldehydes with the salts of heterocyclic cations containing active methylene groups or isolation of the intermediate styryl salts and subsequent removal of the elements of the acid[24]. The first method is most commonly in use for the synthesis of spiropyranes of the indole series, which remained unchanged from the paper of Wizinger et al.[26] Unfortunately, overcondensation can occur what leads to many side products. The second method (scheme 7) is due to the cationic character of the precursor is not prone to overcondensation, but the turnover rates are lower.



Scheme 7: Condensation reaction of an indolenylium salt (left) with an *o*-hydroxy aromatic aldehyde and piperidine as an organic base. Through this reaction it is only possible to obtain spiropyranes of the indole series type.[24]

One of the characteristic properties of spiropyranes is the ability to transform reversibly into its open form, dubbed merocyanine, which is always colorful. Such transformation can be observed in polar solvents (solvatochromism), upon heating (thermochromism) or under the influence of activating irradiation (photochromism).[27]

The transformation usually occurs in a general scheme in which, during the cleavage of the C_{spiro}-O bond of a [2H]chromene fragment, the bipolar form can be transformed into a quinoid form with a different configuration of the polymethine chain.[28] As an example of solvatochromism and thermochromism, a solution of HCl was added to a solution of 6'-nitro-1,3,3-trimethylspiro(indoline-2,2'-[2H]chromene) and it was possible to isolate two salts with different physical characteristics. In toluene at -78 °C a yellowish salt formed and this converted completely into the isomer during storage or when boiling in alcohol for 10 min (scheme 8).[29]



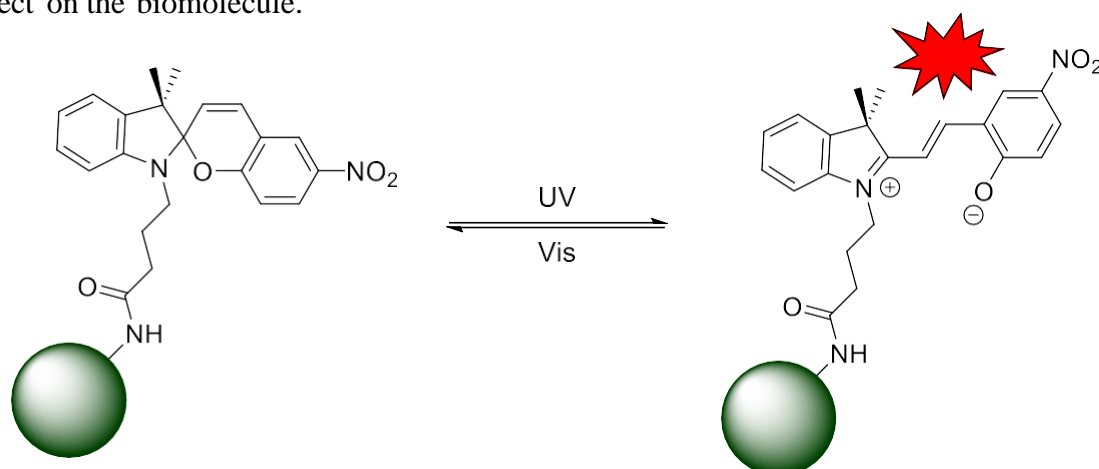
Scheme 8: 6'-Nitro-1,3,3-trimethylspiro(indoline-2,2'-[2 H]chromene is dissolved in toluene with the addition of HCl at -78 °C. During the action of acids on solutions of spiroyrans opening of the [2H]-pyran ring may be accompanied by the addition of a proton to the phenolate oxygen atom of the bipolar form.[24]

Biological applications, which require covalent attachment of spiroyrans to biopolymers or other bioactive molecules, require a linker. Common linkers are alcohols, halogens, amines and acids as well as azides. First four groups can undergo condensation reactions, while azides participate in 1,3-dipolarcycloadditions (e.g. the metal-free with strained cyclooctyne derivatives).

Putri et al.[23] reported (figure 12) the attachment of a spiropyran equipped with a butyric acid linker to a protein encapsulin with a succinimide activated carbon acid. The free amines of the lysine operate as the corresponding reaction partner of the spiropyran. Light-triggered switching lead to the open form which was tracked *via* fluorescence spectroscopy. Hereby it was shown that with an increasing numbers of opening/closing cycles the fluorescence, as well as the absolute absorbance in UV-Vis measurements, decreases. Within 5 cycles the resulting fluorescence drops by ~50%. Under intense irradiation, most organic dyes tend to degrade. This so-called photobleaching is the result of a reaction between the dye in a long-living photoexcited state, such as a triplet state, and molecules in the environment. These can be molecules like solvents or even oxygen. In sum, it was shown that biomolecules can be decorated with spiroyrans with photoswitchable fluorescence, which enables superresolution imaging of the labelled biomolecule.

MOLECULAR PHOTOSWITCHES IN NATURE AND RESEARCH

After multiple switching cycles the encapsulin was not degraded, which means neither the fluorescence spectroscopy measurements nor the formation of the unstable excited states have an effect on the biomolecule.

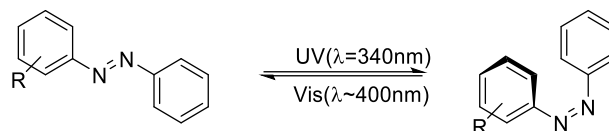


Scheme 9 Schematic visualization of attachment of a spiropyran to encapsulin (shown as a green cycle) *via* an amine derived from lysine in the encapsulin. Light triggered switching lead to the open/closed form of the spiropyran. While the closed form (left) is not fluorescent the open form indeed is fluorescent (right) due to the modification of the nitro group.[23]

Another implementation of spiropyranes was done by Wang et al.[30] The attachment was done over an ester bound to pullulan, a linear polysaccharide polymer consisting of maltotriose units. Three glucose units in maltotriose are connected by an α -1,4 glycosidic bond, whereas consecutive maltotriose units are connected to each other by an α -1,6 glycosidic bond. They showed that the hydrodynamic radius of this biopolymer can be increased by switching the spiropyranes to the corresponding open forms. According to the authors, this more polar form shall allow the uptake of drugs to the polymer. An isomerisation to the closed form will cause shrinking of the polymer and shall encapsulate the desired drug.

1.1.4 Azobenzenes

The last class of molecular photoswitches described in this work are the azobenzenes (AB). The core structure is similar to the stilbene structure, but the aryl rings are linked with a diazo bridge instead of a C=C bond (scheme 10).



Scheme 10: Core structure of azobenzenes. The unsubstituted *trans*-azobenzene changes its geometry upon UV-light irradiation due to isomerization around the N–N double bond. The back - isomerization of the resulting *cis*-isomer is triggered with visible light, or occurs spontaneously by thermal relaxation.

Under irradiation with UV light at the wavelength of $\lambda = 340$ nm ABs can change their conformation from *trans*- to *cis*-isomer (scheme 10). In contrast to stilbenes, the reverse reaction of the azobenzene (AB) can occur under visible light ($\lambda = 400$ nm) irradiation. Thermal relaxation occurs in both classes. The two AB isomers show significant differences in their physical properties like polarity. While stilbenes need highly energetic UV light for efficient photoisomerization, which is not compatible with experiments in living organisms, azobenzenes became most popular molecular photoswitches for modulation of biological systems, since the efficient photoisomerization frequencies can be shifted to the visible light, and sometimes even near-infrared range, as described in more details below. [31, 32] The planar non-polar *trans* isomer of the AB is thermodynamically stable. Upon UV irradiation (320–430 nm) it can isomerize (to about 80%) to the polar *cis*-isomer ($\mu_D = 3D$) with twisted phenyl rings.[33] The reverse process occurs quantitatively upon irradiation with visible light (>460 nm) or by thermal relaxation in darkness. The geometry changes and energy difference between photoisomers can influence adjacent biomolecules e.g. to cause reversible blocking of the active site, or conformational changes and folding modulation in adjacent proteins.[34] UV light used to switch the *trans*-AB is strongly scattered and absorbed, and in certain frequency range also harmful to living organisms. These facts seriously limit the scope of its potential *in vivo* applications. Yet it is known that various substituents can strongly influence both, the absorption maxima and the lifetime of the *cis* isomer (thermal relaxation). [35] Reduction of the azo bond under biological conditions (equivalent to 10 M solution of reduced glutathione), which rate also strongly depends on the substitution pattern, is another concern for potential *in vivo* applications. Tetra-*ortho*-substituted azobenzenes (the substituents are located in the *ortho* positions relative to the azo bond in the respective phenyl rings) were recently demonstrated to be promising molecular photoswitches for biological applications – they combine isomerization in the visible light range with relatively long relaxation times. [27, 36-38] Moreover, with thioalkyl- or chloro- substituents in the *ortho* positions, sufficient resistance on intracellular reducing agents was observed, which renders these derivatives practically applicable *in vivo*.

MOLECULAR PHOTOSWITCHES IN NATURE AND RESEARCH

Several examples of using azobenzenes for photocontrol of oligonucleotide-containing systems have been demonstrated below. Right after the first crosslinking of stilbenes to DNA Yamana et al.[39] showed the same for ABs. Many backbone linkers followed by Wang et al., but these linkers differ only in the length of the side chain attached to the *para* position of both aryl systems of the AB (figure 4).

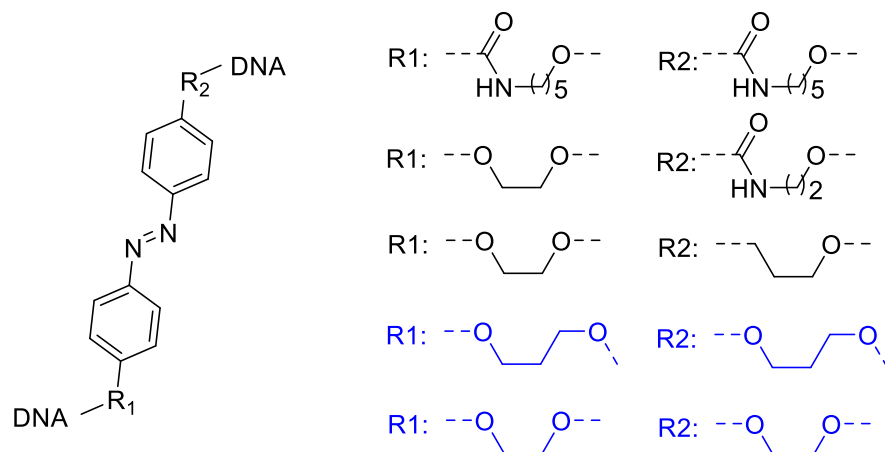


Figure 4: Scheme of the crosslinking ABs provided by Yamana et al. (black) and Wang et al. (blue). They differ at the structure and length of the respectively side chain attached to the *para* position of the AB.

Yamana et al.[39] synthesized azobenzene linkers with spacer units of different functionality and length between the switch and the DNA strands. In organic solvents and with unfolded strands, isomerization was fully reversible. However, in the folded state the isomerization efficiency from *trans* to *cis* was reduced. Wang et al.[30] showed with ethyl and propyl ether linker (blue highlighted in figure 16) that only subtle change of the linker can have a significant effect on the switching properties.

Beside crosslinking DNA strands with ABs with different functional linker systems, Asanuma et al. showed the sequence-specific incorporation of ABs into the DNA strand by means of solid phase synthesis - using a phosphoramidite-functionalized switch as nucleoside surrogate. The method has been generally applied for installation of azobenzene and other photoswitches into a DNA sequence in place of a single nucleoside (figure 5)[39].

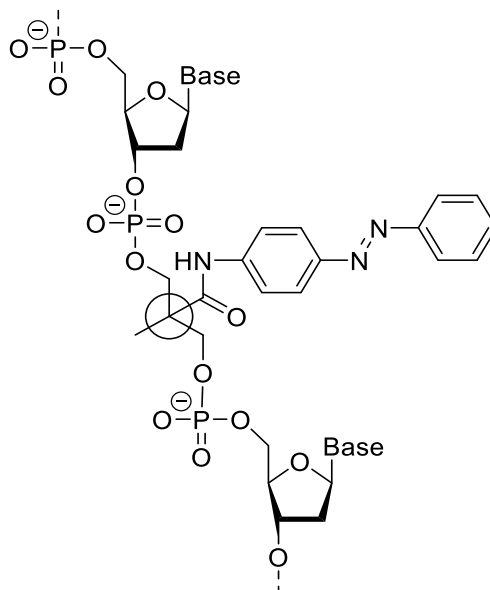


Figure 5: A fragment of Asanuma's et al. photochromic AB-decorated DNA "first generation". Schematic sequence of the incorporation of an AB in to an nucleic acid strand. The strand was synthesized with solid phase support following the phosphoramidate synthesis protocol. Here a racemic mixture was obtained on the stereocenter marked with the cycle.

Azobenzene intercalates between the neighboring pairing bases in the *trans* form. Upon irradiation, the newly produced *cis* form destabilized the duplex due to its increased polarity and changed geometry. There were two generations of the azobenzene-based nucleoside analogs. The first generation was implemented and led to a racemic mixture of two strands with the difference of one stereocenter at the position where the AB was bound (figure 5). When incorporated into the middle of a poly-deoxyadenine 7mer, one diastereomeric oligomer induced an increase in T_m ($\sim +1$ °C) in comparison to the hybrid of the native strand with its full-size complement. The other diastereomer reduced the duplex stability (~ -4 °C). Upon irradiation a reduction in T_m values was observed. The more stable diastereomeric duplex showed a shift of 8.9 °C (24.8 to 15.9 °C) in T_m , and the less stable diastereomeric duplex shifted 5.2 °C (19.9 to 14.7 °C).[39] The process was also shown to be reversible with melting curves obtained following the reverse isomerization. Structural evidence supported the notion that the *trans* isomer of azobenzene readily intercalated between two pairing bases.

One major aspect for the switching of the ABs is the back-isomerization with visible light or the thermal relaxation. To make these switches operational under biological conditions, the 'on-off' switching needs to occur in the visible light range for both forward and backward isomerization reactions. ABs functionalized with four fluorine atoms in the *ortho* positions have a lower energy of the n-orbital of the *cis*-isomer, resulting in a separation of the *trans* and *cis* absorption bands. Green and violet light can therefore be used to induce *trans* to *cis* and *cis* to *trans* isomerizations, respectively.

These new AB derivatives can be switched in both ways with high photoconversions, and their *cis*-isomers display a remarkably long thermal half-life.

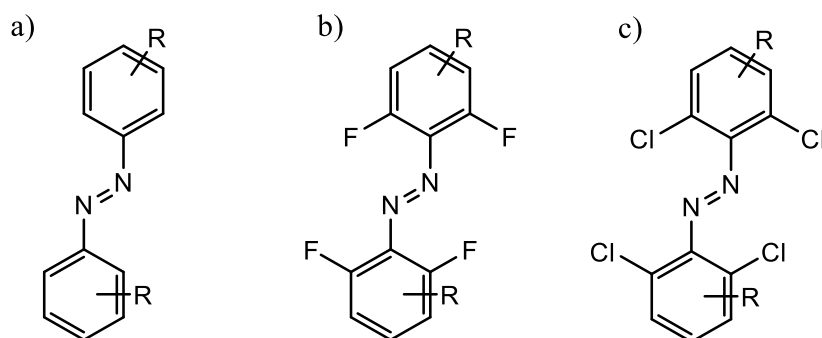


Figure 6 Schematic structure of different ABs. The core structure (a) AB gives much variance for the modification at the aryl rings. Due to their photophysical properties the isomerization to the *cis* isomer is UV-light triggered. This limitation can be overcome with the implementation of *ortho*-fluorine substituents, which causes photoisomerization with green light (b). Another possible modification of AB is the incorporation of chlorine atoms in the *ortho* position. These compounds are switchable with red light.

Due to their stability, *ortho*-fluorosubstituted azobenzenes found significant applications in photopharmacology. Azobenzenes, as well as the other photoswitches mentioned above, can be covalently attached to biopolymers and bioactive molecules using functional groups mentioned above (amines, carboxylic acids, alcohols). While previously reported *ortho*-fluorosubstituted azobenzenes were triggered with green light (500-570 nm), our group recently discovered that a sp^2 hybridized substituent, an aldehyde in this case, at the *para*-position of one or both aryl rings allow them to switch the conformation at wavelengths >630 nm (red light). This discovery is important, as red light frequencies can deeply penetrate human skin and soft tissues, which in turn enables therapeutic applications of such switches on the organismal scale. As an alternative, the fluorine atoms can be replaced with chlorine. However, these derivatives are more synthetically challenging and were used to much lower extent. First attempts by Wooley et al.[36], who tried to build the chlorinated parts first, only gave small yields. They suggested that the poor outcome reported in the azo-coupling reaction results from the steric repulsion between the *ortho*-chloro atoms that shield the reacting sites. To circumvent this, a late-stage functionalization was implemented by Konrad et al.[40] whereby palladium-catalyzed chlorination is carried out after the construction of the AB core. Replacement of fluorine with chlorine is profitable in terms of bathochromic photoisomerization shift, but brings serious disadvantages. The latter system is sterically more hindered, and cannot occur in the planar form (which e.g. hampers efficient intercalation between nucleobases).

The switching efficiency, even under irradiation with intense light, ranges between 50-80%, whereas fluorinated ABs switch almost completely to the *cis*- form. On top, the half-life span decreases from days to hours.

In general, azobenzenes are the most common and predictable class of photoswitches. They are often used for photomodulation of biological systems. Unsubstituted ABs are stable against acids and bases, and the switching rates are high. Depending on the substituents at the aryl rings, or even the aryl rings structure itself (e.g. pyridine- or imidazole- derived aromatic systems) the life time ranges from milliseconds up to weeks. When bound to a target molecule, the energy difference between AB photoisomers is sufficient to force the entire biomolecule (e.g. DNA) to change its conformation. Appending halogen atoms shifts the switching wavelength from the UV to the visible light range. Chlorine substituents allow photoisomerization with red light, which is desirable for living organisms, since red light can enter deep into the body.

1.2 Natural and Artificial Nucleotides

Deoxyribonucleic acid (DNA) and ribonucleic acid (RNA) are biopolymers which assume central roles in storage and transmission of genetic information in all living organisms on Earth. They consist of small building units with uniform structure, the nucleotides. The general structure of a DNA monomer (a deoxyribonucleotide) is depicted in figure 7. These monomers contain a phosphate and a sugar unit which is attached to a nucleobase. In DNA, the sugar unit is *D*-deoxyribose, whereas RNA consists of *D*-ribose.

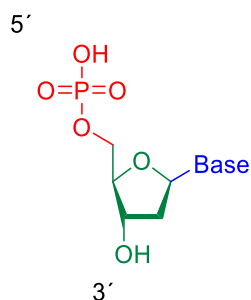


Figure 7: Monomeric structure of a DNA unit a deoxyribonucleotide. The nucleotide consists of the phosphate (red), the sugar (green) and the nucleobase (blue). At these positions, modifications are possible.[41] For different research purposes and applications, these nucleotides can be modified and implemented in synthetic biomolecules.

1.2.1 Short introduction to DNA

In eukaryotic organisms, DNA oligomers are located inside a cell's nucleus as double-stranded, right handed helical structures, supercoiled with histones (positively charged proteins) into chromatin. The strands consist of nucleotide units. The genetic information is encrypted in a code of alternating patterns of the four nucleobases: Adenine (A), Cytosine (C), Guanine (G), Thymine (T). [42, 43]

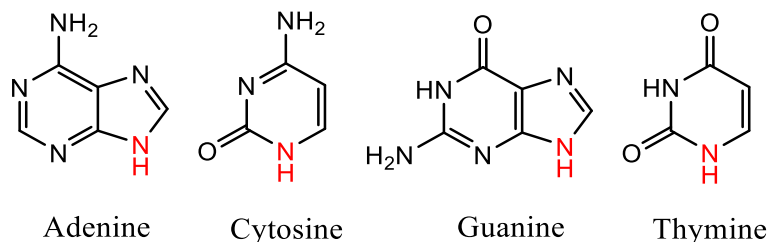


Figure 8: Structure of the nucleobases Adenine (A), Cytosine (C), Guanine (G) and Thymine (T). The red heteroatoms form covalent *N*-glycosidic bonds with the C1-atom of the deoxyribose ring.

The backbone itself consists of alternating phosphate and deoxyribose units. The base is connected *via* a glycosidic bond between the anomeric C₁-atom and an amine moiety of the purine or pyrimidine ring (marked red in Figure 8). Overall, DNA is a long biopolymer containing thousands of nucleotides complementarily aligned in form of a double helix which is stabilized by hydrogen bonds between the bases' heteroatoms as well as the hydrophobic interactions among the stacking aromatic systems. The nucleobases can be divided into the purines (adenine and guanine) and the pyrimidines (cytosine and thymine), based on their heterocyclic core. The bases always hybridize according to the same pattern – the so-called Watson-Crick rules: A-T, G-C: a purine base always binds with a pyrimidine base – adenine with thymine and guanine with cytosine. Therefore, the distance between the two DNA-backbones is equal along the entire helix. A DNA-strand terminates with a 3'-OH group on one end (3'-end) and with a phosphate group on the 5'-OH group (5'-end). Two complementary strands hybridize in the antiparallel fashion, meaning that the 3'-end of one strand faces the 5'-end of the complementary strand.[44, 45]

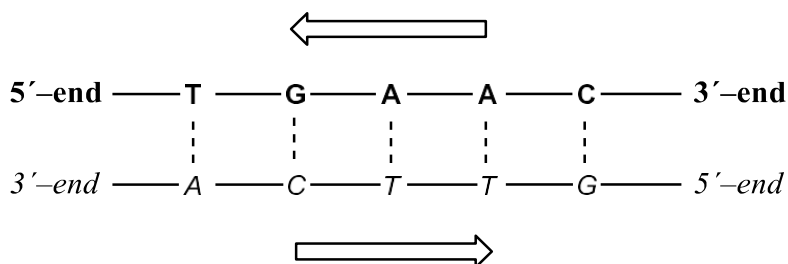


Figure 9: Example of a DNA-strand (*bold*) with five nucleotide units and the corresponding DNA-strand with the complementary nucleotide units (*italic*).

There are three biologically active structures of DNA-double helices (A-, B- and Z-type). [43, 46] Due to the free rotation of the single bonds in the ribose part and its glycosidic bond to the base, several conformations are possible. The Z-type is an example for a left-handed DNA-structure. The most common B-type is the “ideal” form of the DNA, in which every base pair is oriented in a 90° angle to the helix' axis. Thus, the space inside the helix is densely occupied (top view). In contrast to this, the A-type instead is more densely packed and shorter. Here, the base pairs are orientated in a relative angle of ~ 75° to the helix' axis, allowing more base pairs per turn than in the B-form. Therefore, more space inside the DNA-helix is unoccupied. The A-type prevails when the relative humidity drops below 75%.

NATURAL AND ARTIFICIAL NUCLEOTIDES

Due to the angle difference of $\sim 15^\circ$, the A-DNA can bind less water than other forms.[47] Thus, the A-form is favored upon dehydration. It is unclear whether the A- and Z-type play a role in normal cellular processes, but presence of A-type DNA was detected *e.g.* in some DNA-RNA hybrids.

Before cell division, the double-stranded DNA unwinds to single strands through the enzyme helicase. Usually, the replication starts near the middle of the strand. The enzyme DNA polymerase starts to incorporate new nucleotides at the positions where the DNA-helix was divided into single strands. Both new strands are synthesized simultaneously. The synthesis proceeds until every existing nucleotide has its complementary partner. The reliability of the replication process is very high, though fully not perfect. Therefore, living organisms developed many specific ways to correct mistakes like the incorporation of a wrong nucleotide, to ensure the genetic information to be correctly replicated.[48, 49]

1.2.2 Short Introduction to RNA

Ribonucleic acid (RNA) is also a natural genetic polymer. It exhibits a much higher shape and functional polymorphism than DNA. RNA serves for various regulatory and informational roles inside cells and organisms. Its most pronounced function is to transcribe the genetic information from DNA and translate it into functional proteins (enzymes, structural proteins, etc.) in the ribosomes. Several different RNA-forms are involved in particular stages of this process: mRNA, rRNA and tRNA. For the biosynthesis of proteins, 20 different amino acids are available. Their position during ribosomal protein synthesis is encoded by triplets of subsequent RNA-nucleobases, so-called 'codons'. There are 64 (4^3) various codons available in the 'genetic alphabet'. This genetic code is partially degenerated, which means that more than one codon may stand for the same amino acid.[29, 50] Moreover, RNA performs regulatory roles (siRNA) and stores genetic information in certain classes of viruses. Recently discovered catalytic ability of RNA folds (ribozymes; T. Cech, S. Altman, Chemistry Nobel prize 1989) strongly supports the hypothesis that on the onset of life on Earth, RNA oligomers might have been the primordial molecules combining genotype and phenotype (storing genetic information in protocells and performing metabolic reactions currently catalyzed by protein enzymes). This hypothesis, called 'the RNA world' is strongly supported by 'molecular fossils' like ATP or NADP which are still ubiquitous as co-factors in numerous metabolic processes in every living organism and evidently originate from ancient bigger catalytic RNA-peptide complexes or covalently bound primordial nucleopeptides.[51]

RNA-oligomers are composed of a 5'-3'-ribose-phosphodiester backbone. Nucleobases are bound to the anomeric 1'-carbon as β -*N*-glycosides. Apart from thymine being replaced by uracil, the other nucleobases are identical with those present in DNA. The free 2'-OH group, absent in DNA, is responsible for the higher catalytic activity and lower stability of RNA-oligomers compared to DNA-oligomers with identical nucleobase sequences.

DNA most likely evolved from RNA to improve the stability of long-term genetic information storage and ultimately replaced all RNA-oligomers that served as an information storage.[52]

NATURAL AND ARTIFICIAL NUCLEOTIDES

However, some viruses (e.g. retroviruses, like HIV or influenza) still use RNA-strands as genetic oligomers. In most organisms, unless stabilized as conjugates with proteins (e.g. ribosome), RNA-oligomers mainly fulfill regulatory and transport roles and undergo prompt degradation after use. The degradation process is supported with ubiquitously present RNAses (RNA-degrading enzymes) which, aside from pH-dependent depurination, are additional degrading factors for *in vitro* experiments on RNA oligomers.

RNA can be also blocked or degraded *in vivo* in a sequence-specific manner. The first mechanism, called antisense blocking, involves tight hybridization of a complementary oligonucleotide chain (called the 'antisense' strand, because it is complementary to the endogenous/'sense' RNA-sequence) to the particular fragment of an mRNA-transcript. The antisense strand blocks further access of the ribosome to the mRNA strand and thus prevents the translation process. Additionally, some antisense agents hybridized to mRNAs are recognized in form of the heteroduplex by RNAses and cut off which leads to rapid and irreversible degradation of the original mRNA before the translation process can even start. Antisense oligomers are either of natural origin (miRNA) or externally delivered, including unnatural oligonucleotide analogues.

The other regulatory mechanism, called RNA interference, involves short double-stranded RNA-sequences (ca. 20-nb, called siRNA), which are actively recognized by specific enzymatic complexes (e.g. RISC). They acquire sequence-specific RNase activity determined by the initial siRNA-sequence. The activated complex catalytically cleaves all available mRNA strands bearing the identified sequence, and thus prevents the cell from expressing proteins of supposing viral origin. RNA double strands do not naturally occur in eukaryotes, but are pretty common in viruses. Therefore, very likely is that this mechanism was developed by primitive eukaryotes as a primordial immune system against viruses trying to hijack their replicatory machinery. Due to steric issues, double-stranded RNA only exists in the A-type helix.[53, 54]

1.2.3 Modification of Nucleobases

In literature, many nucleobase modifications are described. In the simplest way, modifications of the core structure are replacements of carbon or heteroatoms through other heteroatoms. One example is 6-aza-2-thiothymine which is used as a common matrix-assisted laser desorption/ionization (MALDI) matrix. This molecule co-crystalizes with acids and bases due to the ability to act as a proton acceptor as well as a proton donor. In figure 10, more examples are shown.

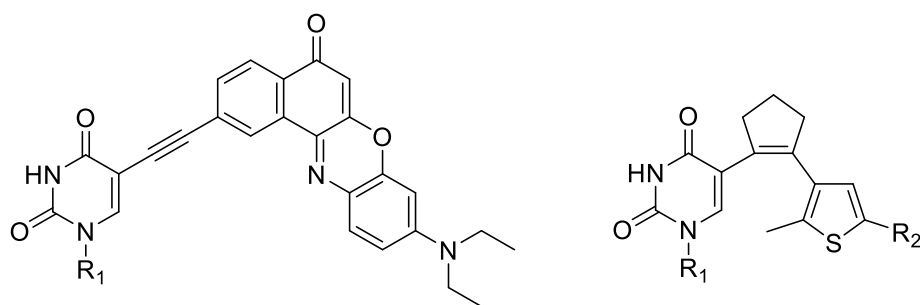


Figure 10: Example of nucleobase modification of thymine. Through cross coupling, a dye was attached to the methyl group of the thymine (left). This building block was implemented into DNA. The second example (right) is a thymine connected to a DEA, where the C-C double bond of the thymine core structure acts as one of the electron pairs in the cyclisation reaction described in 1.1.2. The residue R_1 is the sugar of DNA.

Through cross-coupling reactions, the dye Nile Red was attached to the methyl group of thymine (figure 10, left).[55] The mixed assemblies of this compound with another chromophore are highly ordered, show left-handed chirality and yield dual fluorescence. The strong excitonic coupling indicates assemblies with a high degree of order. Another example was shown by BUCKUP *et al.* [56] who investigated the photoswitching properties of thymine incorporated into the structure of a DEA with four different modifications (Figure 21, right, R^2 = modifications). All four photoswitches investigated with femtosecond transient absorption showed a fast ballistic excited - state deactivation within less than 500 fs towards the S_1/S_0 conical intersection.

Within this work, nucleobases were modified with an acetic acid linker attached to the nitrogen atom, which is normally linked to the sugar, or replaced with photoswitchable units or fluorescent dyes.

1.2.4 Modification of the Backbone

Aside from alterations of the nucleobases, there are many reported modifications of the phosphate/sugar backbone. The field of application ranges from basic research over development of new artificial data storage media to engineering of drugs. Two examples, locked nucleic acid (LNA) and morpholino are shown in figure 11 and will be briefly discussed. They belong to a broad class of artificial genetic polymers of non-biological origin, called xenonucleic acids (XNA).

NATURAL AND ARTIFICIAL NUCLEOTIDES

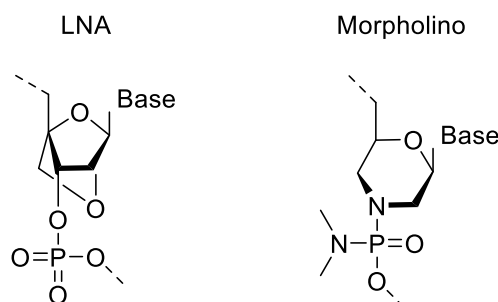


Figure 11: Monomeric structure of LNA (left) and morpholino (right). LNA is linked (“locked”) with a CH₂-bridge between the 2-OH group and the 4-carbon atom of the sugar ring, which is the only difference to natural RNA. Morpholino, on the other side, substitutes the sugar with a morpholine ring. The backbone is aligned at the nitrogen atom and the 5'-carbon atom of the ring. These cyclic sugar analogues are linked by dimethyl substituted phosphate linkers.

LNA is an important xenonucleic acid. Here, the ribose unit possesses an additional CH₂-bridge between the 2'-oxygen and 4'-carbon. As a result, the ribose is less flexible than the unmodified analogue. This significantly increases the hybridization strength (melting point) and sequence selectivity, as well as the affinity for base stacking. Due to its structure, the LNA is stable against *exo*- and *endo*- nucleases which makes it applicable for *in vitro* and *in vivo* experiments.

Another artificial structure worth mentioning is the morpholino oligomer (MO) structure. Here, the sugar is substituted by a morpholine ring. The backbone is connected with dimethyl-substituted phosphate. The nucleobases are attached to the C₁ atom of the ring. The backbone itself is connected *via* the nitrogen atom of the ring and the C₅-atom through a CH₂-bridge to the modified phosphate. MOs were first developed by JAMES SUMMERTON as a way to inhibit the translation of RNA-transcripts *in vivo*. MOs are typically employed as oligomers of 25 morpholine bases, which are targeted *via* complementary base pairing to the RNA of interest. The neutrally charged phosphorodiamidate backbone results in a high binding affinity for RNA, enabling steric hindrance of proper transcript processing or translation.[] Additionally, MOs are the most widely used anti-sense knockdown tools in the zebrafish community. However, MOs are not cell-permeable which makes micro-injections mandatory. Moreover, MOs potentially lack specificity which can lead to false positive results. Another example of XNA is the peptide nucleic acid (PNA). PNA oligomers are investigated in this work and will be discussed in the next chapter.[57-62]

1.2.5 Peptide Nucleic Acid (PNA)

Similar to LNA and morpholinos, peptide nucleic acid (PNA) is a synthetic mimic of DNA and RNA. In contrary to the other XNA examples, the phosphate-sugar polynucleotide backbone is entirely replaced by a pseudo-peptide polymer. In addition, acetic acid modified nucleobases are linked to the amino group of the PNA-backbone. The modification with acetic acid is necessary to imitate the distances of the nucleobases to the backbone. PNA itself is not known to occur naturally, but the PNA-backbone, *N*-(2-aminoethyl) glycine (AEG), has been hypothesized to be among the earliest molecules of biological origin on Earth. AEG is produced in cyanobacteria and is known for its extreme robustness, simple formation and possible spontaneous polymerization at 100 °C.[63, 64]

First artificial synthesis of PNAs was achieved in 1991 by NIELSEN *et al.*[65] Structurally speaking, PNA consists of a backbone of repeating AEG units. These units form a polymeric chain *via* pseudo-peptide bonds. To every secondary amine, a nucleobase (A, C, G, T, U) is added through an acetate group to mimic the distances that are found in DNA/RNA molecules (figure 12).

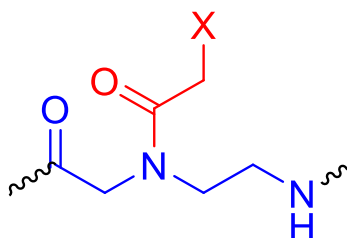


Figure 12: Structure of a PNA monomer. AEG units (blue) form the PNA backbone *via* pseudo-peptide bonds. The acetic acid-modified nucleobase X (red) is linked to every secondary amine. X symbolizes the natural nucleobases adenine (A), cytosine (C), guanine (G), thymine (T).

In comparison to the DNA- and RNA-backbone, the PNA-backbone has no charge, resulting in the PNA's ability to hybridize with high affinity and specificity to complementary sequences of DNA and RNA (lack of charge repulsion, which normally occurs between negatively charged phosphates in DNA or RNA homodimers) (figure 13). This also causes a remarkable resistance to deoxyribonucleases (DNAses) and proteases. PNA shows an exceptional acid stability towards TFA and base stability during its synthesis. These unique physicochemical characteristics of PNAs have led to the development of a wide range of biological arrays, like the development of anti- gene and anti-sense drugs, modulating polymerase chain reactions (PCRs), detecting genomic mutation or labelling chromosomes *in situ*.[64, 66-68]

NATURAL AND ARTIFICIAL NUCLEOTIDES

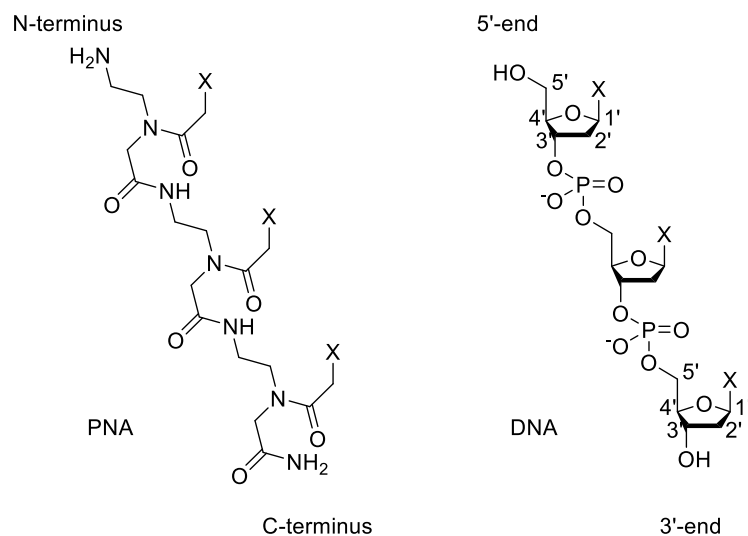


Figure 13: Cut-out of a PNA (left) oligomer and a DNA (right) polymer. The PNA consists of an uncharged peptide-like backbone with repetitive *N*-(2-aminoethyl) glycine (AEG) units. To every secondary amine a nucleobase is attached *via* an acetic acid linker to mimic the distance from the backbone to the nucleobase compared to the DNA. The backbone follows the direction from the N-terminus to the C-terminus. The backbone of DNA-polymers is negatively charged due to the phosphate group. On each 1' C-atom a nucleobase is attached, which forms the DNA-sequence. The direction of the DNA backbone is shown in the direction from the 5'-end to the 3'-end. X symbolizes the nucleobases adenine (A), cytosine (C), guanine (G) and thymine (T). In RNA, thymine is exchanged with uracil (U).

Due to the lack of phosphate groups, the PNA backbone is uncharged. This leads to a higher binding strength between PNA/DNA compared to DNA/DNA or DNA/RNA strands. One reason is the lack of electrostatic repulsion and the resulting strengthened hydrogen bonds as well as the π - π stacking of the nucleobases in a helical order. The formation of sequence-specific hybrids of PNA/DNA or PNA/RNA is achieved through complementary base pairing. However, an undesirable side-effect is the hydrophobic nature of PNAs, lowering their bioavailability. PNA oligomers are usually synthesized from its monomeric building blocks *via* solid phase peptide synthesis (SPPS) using robust protocols and well-established protecting groups developed for peptide synthesis. The acetic acid-modified nucleobases can be attached *via* a coupling reagent like diisopropylcarbodiimid (DIC) or similar coupling setups to the secondary amine of the PNA backbone (protected AEG)., STAFFORST AND HILVERT[69] implemented an unsubstituted AB to the PNA-backbone. Herein, they showed the formation of PNA₂/DNA triplexes. Triplex-forming PNA-structures are potentially interesting as antigene agents since strand invasion of double-stranded DNA has been shown to stop transcription *in vivo*. The implementation of an AB made the system switchable. In the *cis*-conformation, the anti-gene effect decreases due to the lack of destabilized π - π -stacking.

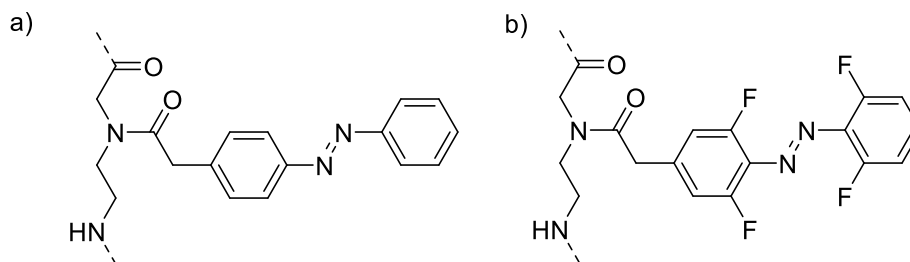


Figure 14: Structure of azobenzene-building blocks for solid phase synthesis, which are unsubstituted (a) or substituted with four fluorine atoms in the *ortho*-position of the AB (b).

As described in 1.1.4, the plain AB is not favorable for biological applications as switching demands harmful UV-light. VASQUEZ *et al.*[70] implemented a tetrafluoro-substituted AB to the PNA backbone. In comparison to the setup of STAFFORST *et al.*, the AB is switchable with visible light. However, the main disadvantage of fluorinated azobenzenes is their base lability. Unfortunately, for almost every coupling reaction a base catalyst is necessary. Moreover, the cleavage of some protecting groups like Fmoc also need basic conditions. The chemical half-life of a tetrafluoro-AB under these conditions is below five minutes. Therefore, VASQUEZ *et al.* protected the secondary amine with an Alloc-protecting group which was cleaved in the last step of the strand synthesis to leave a secondary amine for subsequent coupling to the corresponding AB-acetic acid. These ABs are stable under acidic conditions.

Aside from azobenzenes, many molecules can be attached to the secondary amine. Another example was shown by SONAR *et al.*[71] who implemented a fluorescent dye within the oligomeric structure of the PNA (figure 26).

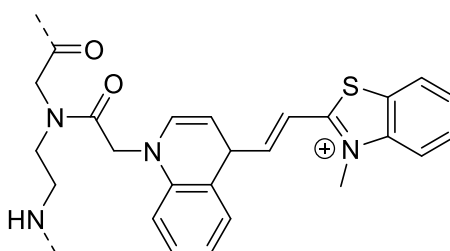


Figure 15: Cut-out of the PNA sequence with a fluorescent dye attached to the secondary amine of the PNA-backbone. One property of this dye is the 'light up'-effect while hybridized in a PNA/DNA or RNA dimer.

With this dye inside a PNA-sequence, it was possible to detect specific RNA of cancer cells. Herein, the fluorescent intensity increases up to the five-fold compared to the single-strand PNA.

All in all, PNA is suitable for antigenic and antisense applications. The hybridisation with complementary DNA/RNA is highly specific. It is possible to incorporate photoswitchable units

NATURAL AND ARTIFICIAL NUCLEOTIDES

like azobenzenes without disturbing the hybridisation process. Fluorescent dyes were implemented with a light-up effect, making them a tool for detecting complementary DNA/RNA, and for the detection of cancer and other diseases. PNA itself is only slightly soluble in water and tends to aggregate in aqueous solutions. To overcome this issue, *D*-Lysine can be attached at the ends of the strands. Another disadvantage of PNA is the poor cellular uptake, which makes further modifications necessary. One example is described in the next chapter.

1.2.6 Guanidinium Peptide Nucleic Acid (GPNA)

Since PNA has a poor cellular uptake into mammalian cells as well as low water solubility, considerable efforts were devoted to developing ways to deliver PNA into cells and improving its intrinsic uptake properties [72]. Several delivery methods have thus far been described, such as DNA-assisted transduction, microinjection, and more recently covalent attachment to carrier peptides.[73, 74]. However, research has shown that only little progress has been made with these methods. Another promising method was the incorporation of positive charges into the PNA-backbone in form of an arginine-derived backbone (GPNA), which was readily taken up by mammalian cells.[75]

GPNA consists of an arginine-derived side chain, which makes the resulting oligomer chiral. LY *et al.* synthesized a GPNA molecule with this side chain in the α -position to show that GPNA has a higher binding strength to DNA than the unmodified PNA with the identical nucleobase sequence. One reason is that the positively charged guanidinium group and the negatively charged phosphate group attract each other electrostatically. Compared to PNA, the level of sequence specificity is consistently high.[75] It was also shown, that GPNA with a *D*-backbone configuration binds specifically selectively to RNA while readily being taken up by both human somatic and embryonic stem (ES) cells.[30] This holds important implications for the future design of cell-permeable antisense molecules and the development of anti-sense technology for *in vivo* applications. Since the arginine-derived side chain in *R*-configuration shows higher binding affinity to DNA than the *S*-configuration, only the expensive, unnatural *D*-arginine (*R*-configured) can be used to synthesize α -GPNA.[41] Therefore, the synthesis of a γ -GPNA backbone with the relatively cheap, natural occurring *L*-arginine is goal for the synthesis of cell-permeable γ -GPNAs. Another advantage would be that γ -GPNA oligomers are already pre-organized into a right-handed helix, which would hybridize with DNA and RNA in the same high affinity and sequence selectivity.[76]

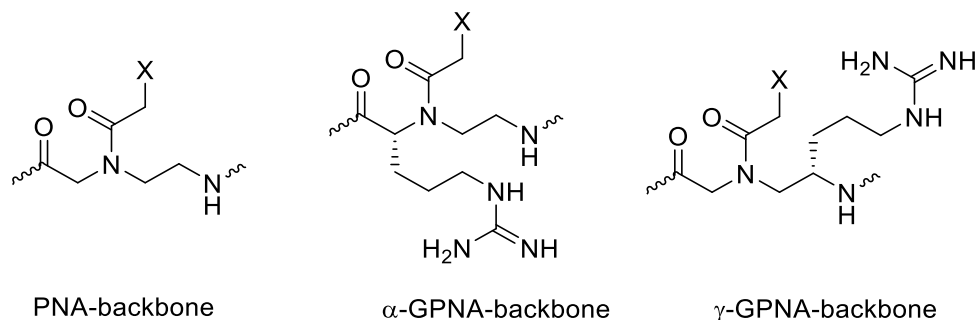


Figure 16: Structures of the unmodified PNA-backbone, α -GPNA-backbone and the γ -GPNA-backbone. The nucleobases are attached to the amine group with an acetate linker, while the monomers are linked with peptide (amide) bonds. In the case of α -GPNA (center), the arginine side chain is attached in α -position, forming an *S*-configured α -GPNA. γ -GPNA can be synthesized from *L*-arginine, adding it to the γ -position of the PNA backbone. X symbolizes the nucleobases adenine (A), cytosine (C), guanine (G), thymine (T).

As well as in the unmodified PNA backbone (AEG), the secondary amine is free for coupling reactions with nucleobases, azobenzenes and many other molecules.

Other than PNA, GPNA is water-soluble and due to the positively charged arginine-derived side chains, the strands do not tend to agglomerate. These modified PNAs are cell-permeable and even the positively charged side chains improve hybridization with complementary DNA/RNA. Unfortunately, α -GPNA is expensive as it is derived from the unnatural *D*-arginine. Due to the position of the stereocenter, not every coupling procedure is suitable as some induce racemization. Here, the γ -position would be favorable, since it is both more resistant to racemization and less expensive as it would be derived from the natural *L*-arginine.

1.2.7 Application examples for PNA

Antigene and antisense PNA

Molecules are designated as antigene/antisense oligonucleotides if they bind specific to the complementary DNA/RNA sequence of the target gene and thereby significantly block the production of the associated RNA/protein. There has been a recent revival in the application of antisense oligonucleotides. The application possibilities are almost limitless and ranges from treat

NATURAL AND ARTIFICIAL NUCLEOTIDES

or prevent numerous genetic disorders or infections. Herein many different ways were achieved to overcome occurring problems like water solubility, cellular uptake and agglomeration.

In the previously described studies, PNA-mediated gene modification was achieved by designing bis-PNAs that bind to homopurine/homopyrimidine tracts, forming a PNA/DNA/PNA triplex. This strategy is limited by the requirement for a polypurine sequence in the target gene to enable triplex formation. To overcome this limitation, Lohse et al. designed pseudo-complementary PNAs (pcPNAs) that were capable of binding mixed purine-pyrimidine sequences to form two PNA/DNA duplexes.[77]

PNA and donor DNAs have also been used to modify additional, disease relevant genomic loci in vitro. Individuals with a naturally occurring 32 bp deletion in CCR5, a chemokine receptor required for intracellular HIV-1 entry, have been shown to be resistant to HIV-1 infection. In 2011, Schleifman et al.[78] co-transfected PNA targeting the CCR5 locus with a 60 nucleotide antisense donor DNA designed to introduce a stop codon, mimicking the delta32 mutation into THP-1 cells, a human acute monocytic leukemia line that expresses CCR5.

Interstrand crosslinking in nucleic acids is another strategy for preparing a stable duplex between PNA and DNA/RNA to be targeted through covalent bond formation either by photolysis or in oxidative conditions. For instance, PNA with 4-amino-6-oxo-2-vinylpyrimidine at terminal position was found to possess excellent and selective crosslinking reactivity with thymine-DNA and a stable PNA-DNA complex formation was observed. [79] This would make PNA to emerge as a new probe for regulation of the gene expression through sequence specific PNA-DNA interactions. In order to explore the clinical applications in fibro-proliferative disorders, PNA as an antigenic reagent was found to decrease mRNA level of the gene, thereby reducing type I collagen production by fibroblast cells.[80]. Recession of RAD51, a central protein in the pathway of homologous recombination may result in resistance to chemotherapy. According to a recently published article, PNA conjugated to NLS (PKKKRKV) was found to suppress RAD51 expression in multiple myeloma and act as potential candidate in multiple myeloma chemotherapy[81]. Furthermore, AgPNAs could also be introduced for the purpose to silence expression with mRNA targeted PNAs or siRNAs. [82]

D. Ly et al.[83] showed that PNA oligomers containing GPNA units at every other position are readily taken-up by mammalian cells.[84, 85] This modification of the PNA (see **2. Structural**

modification) bears an arginine derived guanidinium side chain which enhance the water solubility and prevent agglomeration.

For their research the target sequence lies in the extracellular domain of epidermal growth factor receptor (EGFR), which is responsible for ligand binding. Due to comparing reasons a matching 16mer and a total scrambled GPNA oligomer was synthesized. Because of their ability to enter the cell by themselves GPNAs offer a solution to the problem, that they do not need any transfecting reagents or other mechanical or electrical transductions. These carrier systems could lead to a not correct result.

EGFR plays a critical role in promoting tumor growth. Cetuximab is the only food and drug administration (FDA)-approved EGFR targeted agent for clinical use in head and neck squamous cell carcinoma (HNSCC), but the clinical response rates have been low, in the range of 10–13%.[85]

Results from a phase II trial with a small molecule EGFR inhibitor erlotinib demonstrated a 4% response rate but 38% disease stabilization for 16 weeks.[86] Here, the antitumor effects of cetuximab and erlotinib was compared to the EGFRAS-GPNA in vivo. There was a statistically significant difference in tumor volumes across the erlotinib, cetuximab, and EGFRAS-GPNA groups when compared to the vehicle control group over time. However, there was no significant difference in the response among erlotinib, cetuximab, and EGFRAS-GPNA groups indicating that the antitumor effects were comparable. There is a significant difference in tumor volumes of EGFRAS-GPNA and scrambled GPNA treated mice indicating a sequence specific antitumor effect of EGFRAS-GPNA. The reduction in tumor volume is correlated with reduced EGFR mRNA and protein levels. Although the outcomes of the treatment are similar, GPNA-based therapy has the potential to overcome drug resistance due to mutation in the targeting gene by modifying the nucleobase sequence to match that of the mutant, which is not feasible with small-molecule and antibody inhibitors such as erlotinib and cetuximab.

Antibacterial and antiviral PNA

One of the serious problem which is emerging at an alarming rate is the increasing multidrug resistant bacteria. These bacterial pathogens exhibit resistance towards conventional antibiotics due to excessive use of these antibiotics and resistance genes transfer within the bacteria.

NATURAL AND ARTIFICIAL NUCLEOTIDES

We desperately require new antibacterial drugs for the treatment of patients infected with drug resistant bacteria. Antisense PNAs as antibacterial agents were found to treat infections caused by multidrug resistant bacteria.[87]

Host-defense peptides (HDPs) are a crucial part of the immune system and were detected in a wide range of organisms, including humans. This innate system serves as the first line of defense antibiotics protecting organisms from antimicrobial infection.[88-93] HDPs interacting with the membranes of bacteria in a unique way. On the one hand it depends on the molecular properties of the peptides and on the other hand the composition of the lipid membranes has a huge impact of the activity.[94]

As a result of the nonspecificity of the interactions between HDPs and the anionic components of microbial membranes, many HDPs are broad-spectrum in their antimicrobial activities against both Gram-positive and -negative bacteria and are less prone to the development of antibiotic resistance in bacteria.[89, 95] These unique features present HDPs as a preferable potential source of future antibiotics

Sequences consisting of short (1-4) amphiphilic building blocks had no activity against Gram-positive or Gram-negative bacteria,[96] whereas five and seven amphiphilic building blocks, respectively, were active against *Bacillus subtilis* and *Staphylococcus epidermidis* (Gram-positive bacteria) and *Escherichia coli* (Gram-negative bacteria). Lipidated peptides like polymyxin B64 and daptomycin65 have fatty acid tails that are important for their bactericidal activities. These aliphatic tails are believed to enhance lipophilicity, which promotes membrane interaction.[97, 98]

O. Bolarinwa et al.[87] showed, that cationic lipo- γ -PNAs displayed a broad-spectrum of antimicrobial activity and were even active against the fungus *Candida albicans*. Here the lipophilicity of the alkyl tail is more critical for membrane interaction than cationicity. The lipo - γ -PNA sequences with longer tails were more active than the lipo- γ -PNA oligomers with more cationic charges. This belabors the importance of a good balance between hydrophobicity and cationicity for good antimicrobial activity and selectivity.

The hypothesis that lipo- γ - PNAs could mimic the mechanism of HDPs was supported by fluorescence microscopy and membrane depolarization studies that suggested that lipo- γ -PNA kill bacteria by way of membrane disruption.[99]

Antigene therapy using oligonucleotides have targeted various viral agents at the transcription step. In the race of finding potential antiretroviral agents, PNA oligomer, was found to significantly suppress HIV-1 replication in chronically infected lymphocytes and macrophages. A decrease of HIV RNA expression in PNA treated infected cells also demonstrated the inhibition of HIV-1 replication during transcription. [100]

The *P. aeruginosa* pathogen is a widespread and clinically important one since it has developed resistance to a variety of antibiotics. Antisense PNA, which has the property of conjugating to the carrier peptide, can be a therapeutic tool which can target a large number of genes in this bacterium.[101] Another pathogen worth mentioning is *A. baumannii*, which often causes severe infections in hospitals. Wang et al.[30] established antisense PNAs to carry out gene specific inhibition effects in multiresistant drug against *A. baumannii*. The described PNAs conjugated to the (KFF)₃K peptide targeted the growth of essential gene *gyrA* in *A. baumannii* and showed strong inhibition effects with lowest inhibitory and bactericidal concentration of 5 and 10 μ M, respectively. Recent studies also revealed the potential of duplex DNA-invading γ PNAs for the identification of both bacterial and fungal pathogens directly from blood without any need for culturing which is time consuming. This approach would help in improving patient's health by fast and appropriate antimicrobial intervention.[102]

PNA as antisense molecules when conjugated to a cell penetrating peptide (CPP, i.e. octa-D- lysine) is used as a potential tool for *Plasmodium falciparum* gene silencing and in the development of potential and highly specific antimalarial agents.[103] Antisense PNAs could also be effectively used to restore vulnerability to β -lactams in methicillin-resistant *Staphylococcus aureus* and *Staphylococcus pseudintermedius*. [104] It was also shown that antisense PNA conjugated with antimicrobial peptides could effectively target *acpP* gene (responsible for growth of fatty acid chain in the biosynthesis of fatty acid) in *E. coli* with MIC values of 2–4 μ M.[105] Sadeghizadeh et al.[106] studied the potential of peptide-PNA as antibacterial agent and also considered the uptake efficiency of dendritic cells for PNA treated bacteria. It was found that peptide-PNA may emerge as an excellent candidate in immunological and DNA vaccine. Antisense PNAs also targeted essential genes infected with *Klebsiella pneumoniae* (10^4 CFU) without any significant toxicity to the human cells (Kurupati et al., 2007).[107]

Photochromic PNA

Up to date only few research was done on a reversible hybridization of PNAs upon irradiation. [69, 108, 109] Azobenzene-containing PNA has been successfully used for the photocontrol of transcription by T7 RNA polymerase *in vitro*. However, the wavelengths used for switching are in the UV range, which is not suitable for *in vivo* application. Such results spur the search for further, new azobenzene derivatives which are switchable in visible light and can therefore also be used *in vivo*. Vasquez et al. [70] showed in 2019 that tetra ortho fluoro azobenzene can also be incorporated into PNA. The fluoro substituted azobenzene allows switching in visible light. In their publication they synthesized PNA strands of different lengths and placed the photoresponsive component at different locations. They also included several switchable devices in the sequence (max. 3) and hybridized these strands with complementary RNA. For the hybrids, melting points for cis and trans formation were measured and compared. The difference was 0-3.4 °C depending on the number and position of the photoswitchable units.

Another approach was executed from Hövelmann and Seitz[110] in 2016. They attached thiazole orange to the PNA backbone, which exhibit a strong enhancement of fluorescence emission upon target recognition. The dye itself intercalates similar to the aforementioned Azobenzene. While incorporated in duplex structures it was shown, that these type of dyes can show an increase of the fluorescent emission up to the 50-fold in comparison with single strand PNA. Further it was shown *in vivo* with H1N1-neuramidase infected MDCK cells, that only in infected cells fluorescence was detectable whereas non infected cells and the vehicle control remained dark. This leads to the conclusion of selectively binding to the targeted mRNA. Later Wickstrom and coworkers used similar PNA probes to image *kras2* mRNA in human cancer cells.[71]

2 Aim of the project

As already shown in the introduction, PNA is an extremely lucrative pharmaceutical substance. Due to its antisense effect, it can be used against virtually any kind of disease. Its stability and the almost non-existent cytotoxicity make it even more interesting. The basic structure also consists of relatively simple molecules and modified nucleobases. The required sequences can easily be synthesized in any desired variable way using solid phase synthesis. If important RNA sequences of a virus, for example, are still unknown, it is possible to use various methods for screening. By using the 'split and mix' method already known from DNA, it is possible to synthesize very quickly over 10^9 different PNA strands which can be tested for the unknown sample. Already one strand with 9 units reaches a melting point (depending on the type of composition) of about 40 °C. This property and the high selectivity even allow the use of PNA for micro RNA, which is unfortunately not the case with DNA.

What has been little researched so far is a photo-switchable PNA that can switch the antisense effect on and off by light-induced switching. First approaches were already pursued in the early 2000s, but the photoswitches in PNA could only switch in the UV range, which is not suitable for bio-applications. With new holders that switch in visible light, we want to investigate the antisense properties when intercalated in a PNA/RNA hybrid.

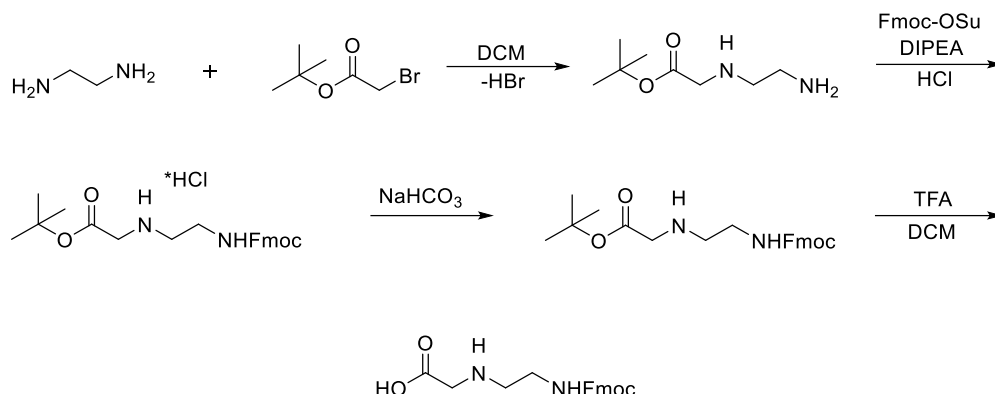
Furthermore, we want to combine new fluorescent dyes with the PNA backbone to obtain new fluorophoric devices. Once intercalated these dyes should have a light up effect. This can be used for the detection of miRNA or mRNA to make HIV infected cells visible.

3 Results and Discussion

3.1. Synthesis of PNA-, α -GPNA- and γ -GPNA-backbone

The PNA backbone synthesis was reproduced as it is described in literature (see experimental part).

The procedures was, however optimized.

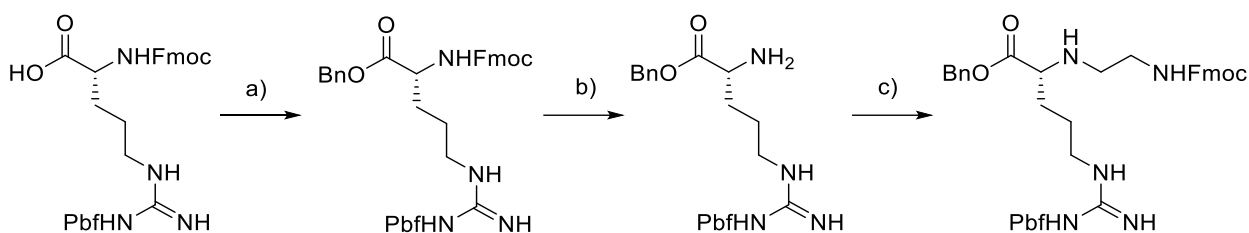


Scheme 11: Synthesis of the PNA backbone. Ethylenediamine is monoalkylated with tert-butyl bromoacetate. The remaining free amine is protected with Fmoc-OSu. After workup with 1 M HCl, the salt was obtained. It was neutralized to the free amine by washing with aq. NaHCO₃ yielding the tert-butyl protected PNA-backbone as a white solid. After ester deprotection with TFA the free acid was obtained.

To obtain the product PNA backbone (a protected AEG), a three step procedure is necessary. First, tert-butyl bromoacetate was diluted in 250 mL of DCM and added dropwise over 5 h to the vigorously stirred diamine in 250 mL DCM cooled with an ice bath. The higher dilution enabled a higher input of equivalents (equiv.) of the alkylating agent, comparing to the published procedure (0.11 equiv.). Yet still, the unwanted bis-alkylation was negligible. The procedure yielded 88% of the monoalkylation product. Here, the ice bath was not removed after the addition. Therefore the reaction mixture reached room temperature (rt) slower than in the literature experiment. The protection of the free amine in the second step with Fmoc-O-succinimide to the product occurs also upon slow addition of the diluted (250 mL) Fmoc-OSu solution to the diluted solution (250 mL) of the monoamine, both in DCM, without cooling. The solvent was evaporated to dryness obtaining a light yellowish solid. The product was obtained with a yield of 85% and was used without further purification. The Fmoc protection should be performed directly after isolation and purification of the monoalkylation intermediate. Otherwise, a degradation of unknown nature (possibly cyclization to a piperazine type of the product) takes place. For the third step, the product was dissolved in chloroform and washed with saturated aqueous NaHCO₃ solution to obtain the tert-butyl protected PNA-backbone, which was used in some coupling reactions due to non-standard coupling conditions. It proceeded always with quantitative yield.

In the final step, the *tert*-butyl ester is cleaved with trifluoroacetic acid (TFA) to the free acid (ω - N-Fmoc-2-aminoethylglycine). TFA (100 mL) was added dropwise over a period of one hour to the solution of ester in DCM (unlike in literature, when it is poured into the mixture at once). This change led to an increase of the yield up to 69%. We also optimized the purification procedure. Instead of crystallization from MeOH/Et₂O solution, the crude product was solved in a small amount of DCM. The mixture was loaded to a syringe and added dropwise to vigorously stirring Et₂O. The precipitate was filtered, washed with Et₂O and dried under high vacuum. The Et₂O of the flowthrough was evaporated under reduced pressure and the sticky residue was solved in a small amount of DCM repeat the same procedure, obtaining a second batch of the solid. The solids were analysed separately by NMR and identified as the same product.

The synthesis of α - GPNA was following the literature procedure.[124] In the course of the synthesis some problems were faced, which forced changes in the synthetic pathway (scheme 12).



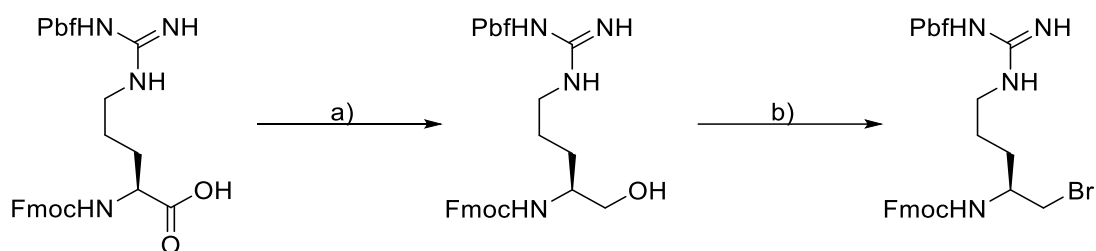
Scheme 12: Schematic reaction pathway from the commercially available Fmoc- and Pbf-protected *D*-arginine starting with an esterification with HBTU and benzyl alcohol (a) followed by a deprotection of the Fmoc-group (b). In the next step, glycinal was brought to reaction with the free amine to get the imine which was immediately reduced to the secondary amine in methanol (c).

The synthesis is well described. The first step (figure 28, a) yields almost quantitative amount of the benzyl-protected arginine derivative. The deprotection of the Fmoc-group (figure 28, b) does not grant a very good conversion (80%) but is sufficient for further reactions. First issue was faced when the free amine reacted with the aldehyde. After reduction to the secondary amine (figure 28, c) the product could be isolated and thin layer chromatography (TLC) indicates a pure product. When checking the purity with reversed phase HPLC analysis two spots were detected in the chromatogram with the ratio of 3:1. After careful analysis, the side product was determined as the methyl ester in the ratio of Bn/Me 3:1.

SYNTHESIS OF PNA-, α -GPNA- AND γ -GPNA-BACKBONE

After purification with HPLC the literature-described procedure could not be reproduced. The catalytic reduction with 5% palladium on charcoal and hydrogen did not lead to the free acid. Even attempts with higher concentration of the palladium catalyst or reaction in the pressure chamber gave no product. At the attempt to remove the benzyl protecting group with LiOH the Fmoc-group was deprotected as well. A re-protection with Fmoc-OSu led to the protection at the secondary amine as well, since it is more nucleophile than the primary terminal amine. The solution was to attach the nucleobases at that stage which covers the secondary amine.

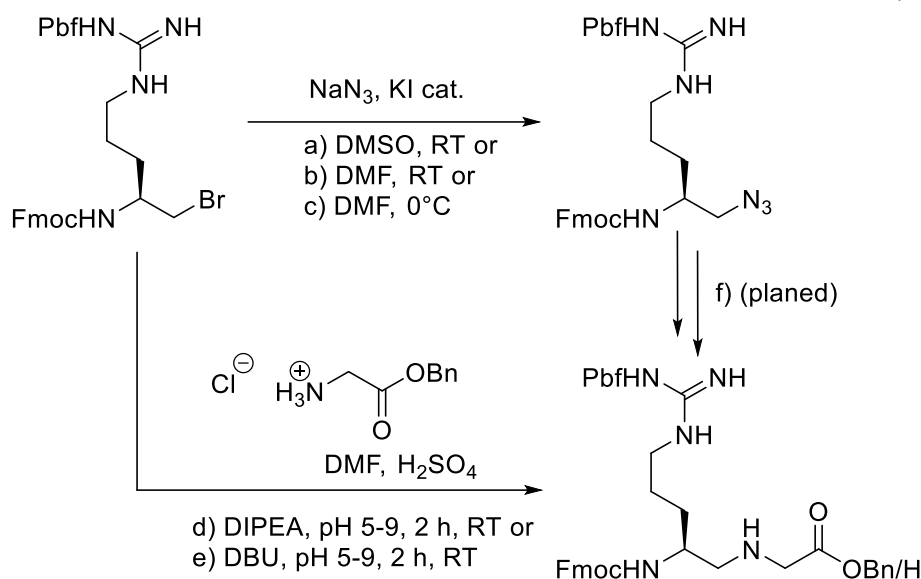
The synthesis of γ -GPNA is desirable due to the reasons mentioned in **1.2.6**, however a respective reaction pathway for the derivative matching our solid-phase protection group pattern is not described in the literature yet. Therefore, we explored several synthetic pathways, which could result in the desired component. A possible pathway was investigated in this work starting with the natural *L*-arginine with an Fmoc-protection at the α -amine and a Pbf-protection at the guanidine side chain.



Scheme 13: Reaction pathway for the transformation of natural arginine to the bromide. NaBH_4 , after activation with NMP and isobutyl chloroformate, yields the alcohol (a). Via Appel reaction using CBr_4 and PPh_3 , the desired bromide was synthesized (b) in an overall yield of 49%.

In the first step, the acid was converted into an alcohol using NMP and isobutyl chloroformate at $-5\text{ }^\circ\text{C}$ in DME followed by a reduction with NaBH_4 (scheme 13, a).[35] In the second step, the alcohol was brominated in an Appel reaction using CBr_4 and PPh_3 in DCM at room temperature to afford a white solid with a yield of 61%. (scheme 13, b).

SYNTHESIS OF PNA-, α -GPNA- AND γ -GPNA-BACKBONE



Scheme 14: Kinetic studies on the formation of an azide intermediate under various conditions: a) in DMSO at room temperature, b) in DMF at room temperature and c) in DMF at 0 °C. Additional kinetic studies for the formation of the γ -GPNA backbone directly with benzyl glycinate and H₂SO₄ in DMF, using different bases and pH values: d) DIPEA as base in a pH- range of five to nine in steps of one, e) DBU as base in a pH-range of five to nine in steps of one. Reaction f) shows a planned pathway for the formation of the γ -GPNA backbone in which the azide is reduced to a primary amine first and then alkylated using bromoacetic acid, leading to a γ -GPNA backbone with an unprotected carboxylic acid.

Before the γ -GPNA backbone was synthesized, kinetic studies were carried out to get an insight in the formation of the γ -GPNA backbone, as well as an azide intermediate, under various conditions (figure 30). In the first study, the formation of the azide intermediate using different solvents and different temperatures was investigated. The reaction was carried out with three equivalents of NaN_3 and a catalytic amount of KI in each variation. This way three reactions were done with the following parameters:

DMSO at room temperature.

DMF at room temperature.

DMF at 0 °C.

The data on the formation of the azide was collected via HPLC-samples every 30 minutes over a period up to 7 h, whereby after 2 h a sample was taken every hour. Afterwards, the area of the signal of the putative product in the relation to the total area was measured at a wavelength of $\lambda = 254 \text{ nm}$ by HPLC and shown graphically (Figure 17).

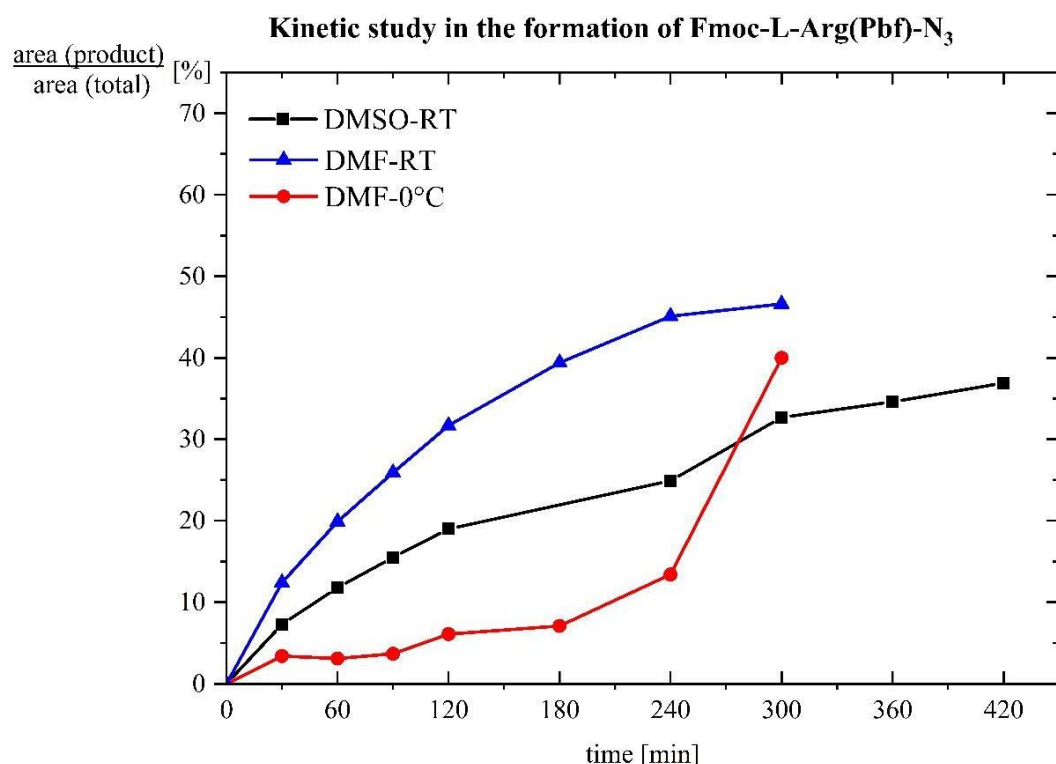
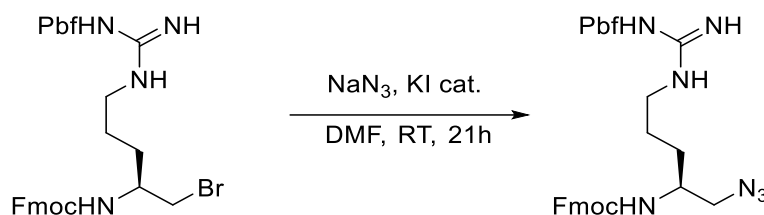


Figure 17: Kinetic study in the formation of Fmoc-L-Arg(Pbf)-N₃ under varying parameters using a) DMSO as solvent at RT (black), HPLC-samples taken every 30 min for 420 min, b) DMF as solvent at RT (blue), HPLC-samples taken every 30 min for 300 min and c) DMF at 0 °C (red), HPLC-samples taken every 30 min for 2 h followed by 1 sample every hour up to 7 h. HPLC signals were measured at a wavelength of $\lambda = 254$ nm.

The reaction in DMF at room temperature is faster than the one in DMSO at room temperature (figure 17), which is indicated by the significantly higher slope of the curve. After 300 min, 47% of the putative product is formed in DMF, while in DMSO only 37% of the supposed product is present. A possible explanation could be a different shielding through the solvation shell of the bromide in DMSO or DMF. If the kinetic is compared at different temperatures in DMF, we find that at 0 °C the reaction is much slower than at room temperature. This was to be expected since the reaction rate decreases with decreasing temperatures. The significant increase of the putative product at 0 °C in DMF after 300 min is attributable to the fact that the reaction was insufficiently cooled after 240 min. In summary, it can be stated that in the case of the tested variations of the reaction conditions, the reaction in DMF at room temperature has been found best conditions of the ones tested formation of the azide.

SYNTHESIS OF PNA-, α -GPNA- AND γ -GPNA-BACKBONE



Scheme 15: Synthesis of Fmoc-*L*-Arg(Pbf)-N₃ by reacting Fmoc-*L*-Arg(Pbf)-Br with NaN₃ and catalytic amounts of KI in DMF at RT for 21 h.

Based on these results we proceeded with a reaction of the bromide to the azide at room temperature using sodium azide and a catalytic amount of potassium iodide for a Finkelstein- type activation of the bromide (scheme 15). Using this conditions, a slightly yellow solid could be isolated with a yield of 73%, which was confirmed to be the desired product using ¹H-NMR, IR and FAB-MS. In addition, HPLC measurements showed, that a slow cleavage of the Fmoc protecting group had occurred. Therefore, it was decided to split the obtained crude product in half to perform a re-protection of the now free amine with Fmoc-OSu. HPLC measurements after the protection showed that the signal for the free amine has indeed become smaller, so it is possible to protect the free amine group again, following the formation of the azide. Test reactions to convert the azide into an amine using reductive conditions afforded the amine in traces, detectable by MALDI-TOF. Unfortunately, the amine is basic enough to deprotect itself, so the free bis-amine was observable too.

For the kinetic study in the formation of the γ -guanidinium PNA backbone by coupling the bromide directly with benzyl glycinate in DMF with H₂SO₄, ten variations were tested. The parameters for the kinetic study are as follows:

- a) DIPEA as base in a pH-range from five to nine in steps of one.
- b) DBU as base in a pH-range from five to nine in steps of one.

The first 5 variations were performed with DIPEA as base with pH-values of five, six, seven, eight and nine to observe the effects of the pH-value for the outcome of the reaction using a comparatively weak base. The reactions were started and quickly brought to the designated pH value. HPLC samples were taken every 30 min until 120 min have passed. The results were obtained by measuring the area of the signal of the putative product in relation to the total area at a wavelength of $\lambda = 254$ nm and graphically plotted (Figure 18).

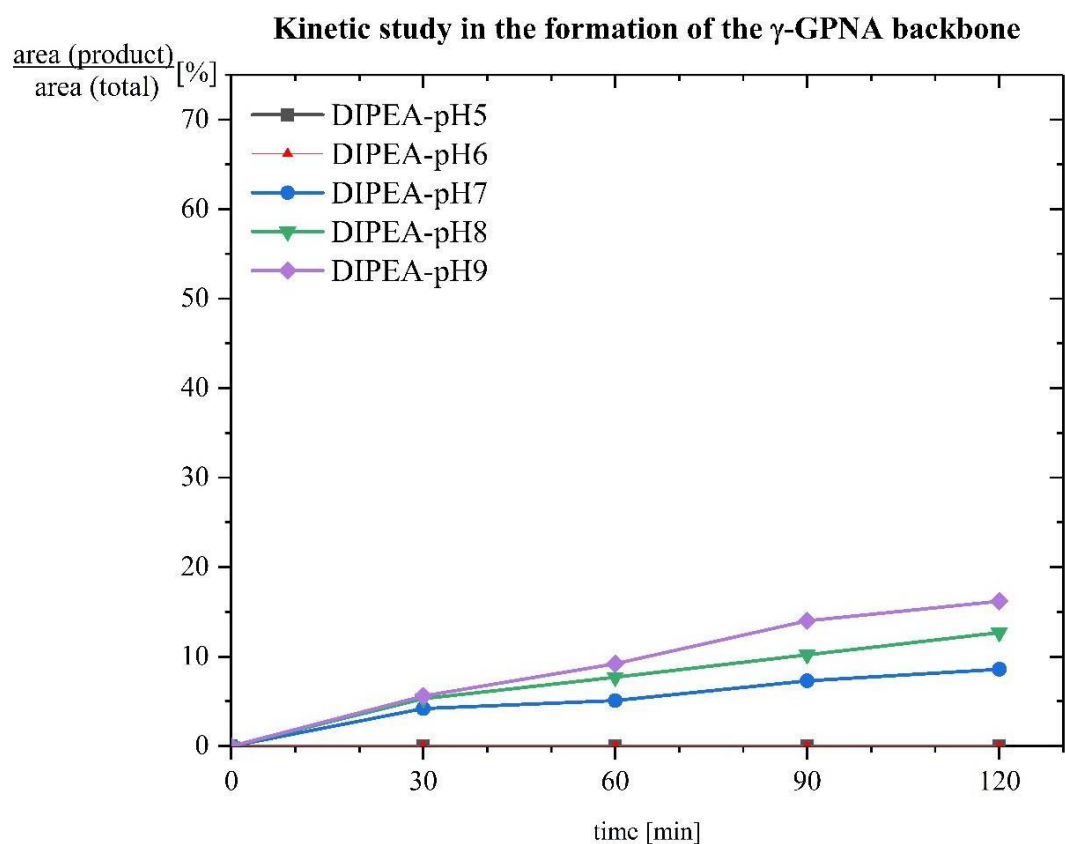


Figure 18: Kinetic study on the formation of the γ -GPNA backbone using benzyl glycinate in DMF and catalytic amounts of H_2SO_4 . DIPEA was utilized as base and the pH adjusted to five (black), six (red), seven (blue), eight (green) and nine (purple) at RT. HPLC samples were taken every 30 min for 120 min. HPLC signals were measured at a wavelength of $\lambda = 254$ nm.

With increasing pH more of the supposed product was formed. As expected, the formation of the putative product only starts from a neutral to basic pH value, since the reaction should only take place in a basic environment. One problem is the overall small amount of supposed product, which may be explained by the usage of the very mild base DIPEA and the relatively short reaction time. Former procedures with longer reaction time were carried out before. The substrate and the product decomposes, respectively deprotect the Fmoc group while stirring under these conditions providing a complex reaction mixture. In order to investigate when the maximum of the putative product is observable while the side products are not, we tested on small scales different conditions with DBU as a stronger base.

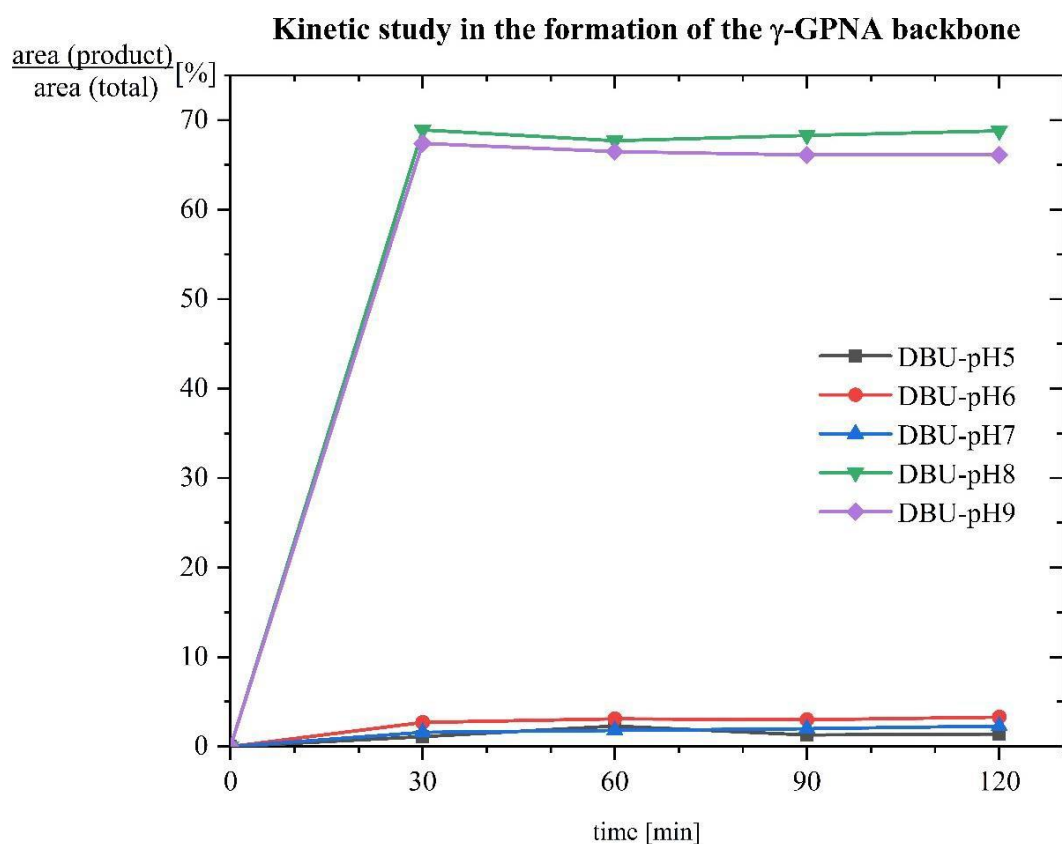


Figure 19: Kinetic study on the formation of the γ -GPNA backbone using benzyl glycinate in DMF and catalytic amounts of H_2SO_4 . DBU was utilized as base and the pH adjusted to five (black), six (red), seven (blue), eight (green) and nine (purple) at RT. HPLC samples were taken every 30 min for 120 min. HPLC signals were measured at a wavelength of $\lambda = 254$ nm.

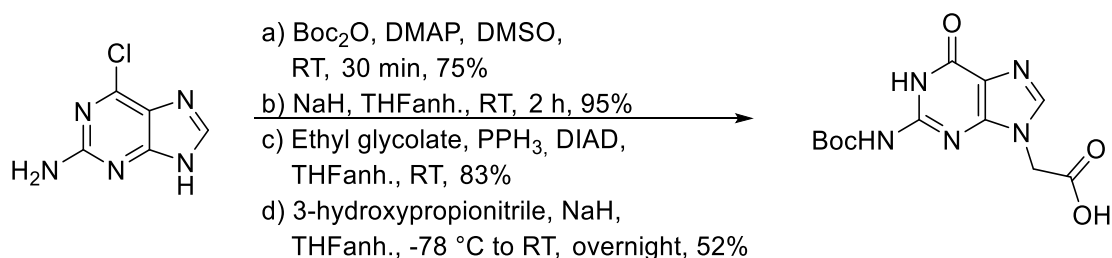
There is no significant formation of putative product at pH values of five, six and seven (Figure 19), which mirrors the results of the kinetic study with DIPEA. This is presumably due to the fact, that the base DBU is comparatively strong the pH increased too fast before it was adjusted with 1 M H_2SO_4 . At higher pH values, eight and nine, the reaction is already finished after 30 min. This observation is not surprising, since DBU is a strong base compared to DIPEA. It was decided to perform a scaled up reaction using DBU with a pH of eight. Unfortunately, the putative product was formed as well as a possible side product with the Fmoc-group cleaved of. This was observable in HPLC samples indicated by a rising peak at lower retention times. Due to the unwanted side reaction, another reaction with DIPEA was set up and run overnight. Unfortunately, the supposed product could not be verified to be the desired product.

Overall, we decided to proceed further syntheses of PNA monomers and oligomers using the unmodified PNA backbone and the α -GPNA backbone, which were obtained in sufficient quantities and purity. The efforts on synthesis of γ -GPNA backbone were discontinued.

SYNTHESIS OF MODIFIED NUCLEOBASES

3.2. Synthesis of modified nucleobases

As already mentioned in 1.2.3, for implementation in PNA oligomer synthesis the nucleobases need a modification with an acetic acid linker at the secondary nitrogen atom. The reactions and the intermediates are known in literature. Schematic synthesis is shown for the modification of guanine (scheme 16). All other modifications of the three remaining nucleobases are stated in chapter 5.2.1 'Synthesis of modified nucleobases'.



Scheme 16: Synthesis of Boc protected acetic acid-modified guanine in four steps. a) Protection of 6-chloro-9H-purin-2-amine in the N^9 -position with Boc_2O with DMAP as base and DMSO as solvent over the course of 30 min at RT, b) Boc transfer reaction to the primary amine of the purine with sodium hydride and anhydrous THF at RT for two hours, c) Functionalization of the free N^9 -amine in a Mitsunobu-reaction^[31] with ethyl glycolate, PPh_3 and DIAD, using anhydrous THF at RT over the course of 20 min, d) Saponification of the resulting acetate ester and concomitant deprotection of the chloride with 3-hydroxypropionitrile and NaH forming the desired Boc-protected acetic acid-modified guanine nucleobase in anhydrous THF. Temperature gradient: -78°C for 30 min, 0°C for 5.5 hours and room temperature overnight.

In the first of four steps the N^9 nitrogen atom of the starting material 6-chloro-9H-purin-2-amine is protected with a Boc-protecting group using Boc_2O as protecting reagent and DMAP as base. The reaction was performed in DMSO near the freezing temperature (18°C) for 30 min. The selective protection of the secondary amine follows the *Hauser*-rule. In the second step the Boc-protecting group is transferred to the primary amine with NaH leaving the secondary amine free for a Mitsunobu reaction with ethyl glycolate to the respective ester. In the last step the ester undergoes a saponification reaction. Simultaneously through the presence of 3-hydroxypropionitrile and NaH the chlorine undergoes a substitution reaction with the alkoxide. In the next step another alcoholate/alkoxide abstracts an H-atom at the fresh attached propionitrile causing a elimination reaction to form the ketone and thus the Boc-protected acetic acid guanine nucleobase.

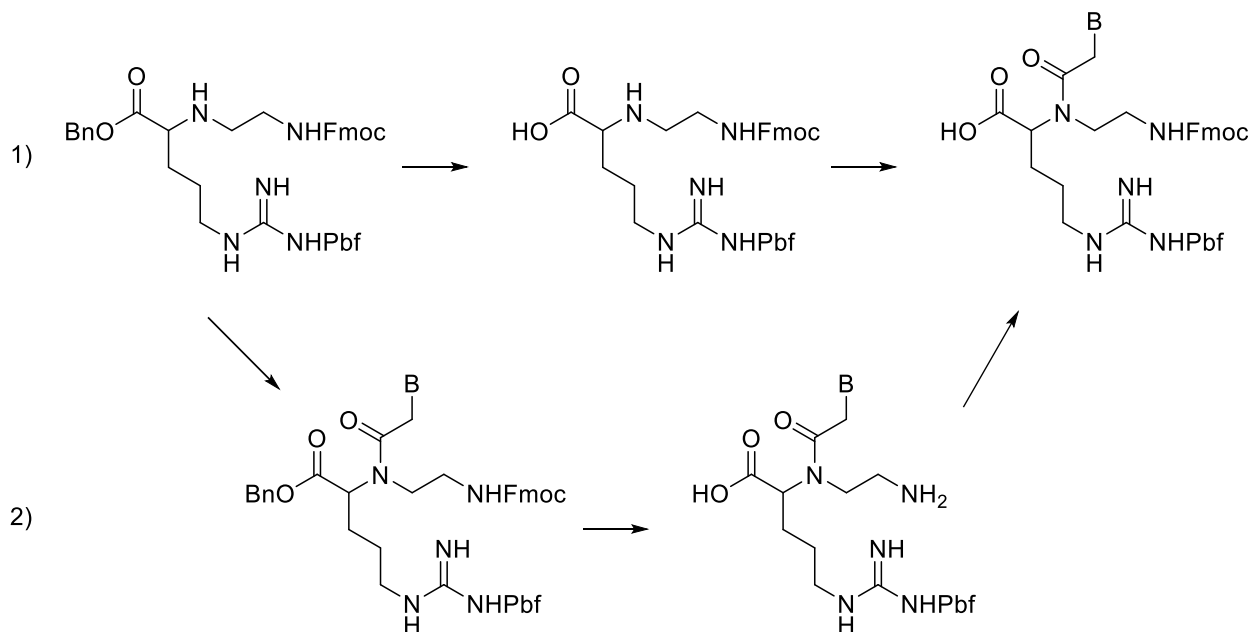
3.3. Synthesis of PNA and GPNA building blocks

For the synthesis of PNA monomeric building blocks fragile α -stereocenters are absent. However, activating agents known from peptide bond synthesis (HBTU, TSTU) are still used for the amide bond formation due to favorable kinetic parameters, wide availability of the reagents, and standardized workup procedures suitable for gram-scale production. As an example, the coupling of an *N*-Boc-protected cytosine-1-acetic acid ('C-acid') to the Fmoc-protected *N*-(2-aminoethyl) glycine ('PNA backbone'). *N,N,N',N'*-Tetramethyl-*O*-(*N*-succinimidyl)uronium tetrafluoroborate (TSTU) is the coupling reagent. *N,N*-diisopropyl-*N*-ethyl amine (DIPEA) is used as catalyst. All reactions were performed in *N,N*-dimethylformamide (DMF) if it is not stated otherwise.

The mechanism starts with a nucleophilic attack of an electron pair of the carboxylic oxygen atom of the C-acid targeting the vinyl C-atom of the TSTU molecule. A positive charge occurs at the former hydroxyl oxygen. After the abstraction of the acidic H-atom by the counter ion BF_4^- the active ester is built. Due to a strong polarization of the carboxylic C-atom of the former acid, there occurs a nucleophilic attack of the electron pair of the secondary amine incorporated in the PNA-backbone, which is added after TSTU. A positive charge occurs at the now tertiary amine and the negative charge is located at the former carboxylic oxygen atom. Through rearrangement of the electron pairs, the C-O bond at the TSTU rest breaks heterolytically, the negative charge remains at the uronium rest since it is stabilized by a highly positive polarized C-atom next to the negative charge. After abstraction of the H-atom at the positive charged amine by the alkoxide, the product is obtained. This reaction was performed with all other modified nucleobases.

As mentioned before, the α -GPNA building blocks were synthesized in a slightly different way as it was described in literature. Since the deprotecting of the benzyl group was insufficient and a cleaving with LiOH also removes the Fmoc-group the nucleobase was attached at this stage (scheme 17).

SYNTHESIS OF PNA AND GPNA BUILDING BLOCKS



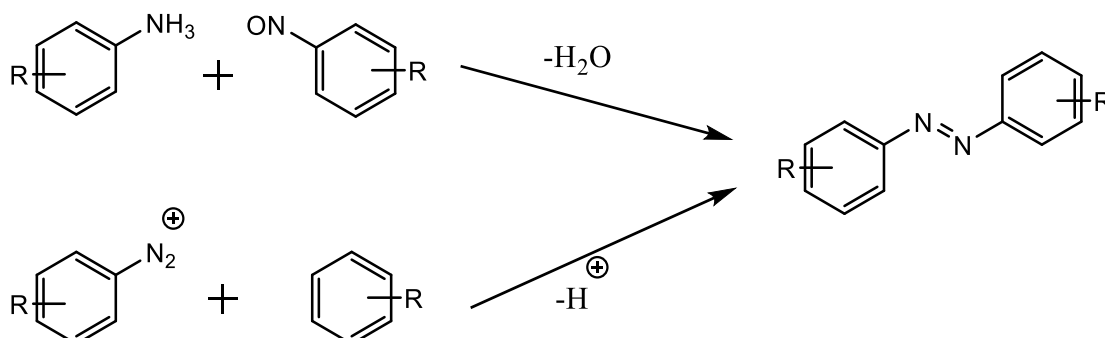
Scheme 17: reaction pathway of the α -GPNA monomers. The literature known procedure (1) follows a Pd/C catalyzed hydrogenation of the benzyl-group followed by the coupling reaction of the modified bases (B = A(Boc), C(Boc), G(Boc) and T) with HBTU. The modified route starts with the coupling of the modified nucleobases with DIC followed the deprotection of the benzyl - and Fmoc- group. After reprotection of the Fmoc-group the α -GPNA monomer building blocks are synthesized.

As described in **3.1**, the deprotection of the benzyl group was challenging. In the reaction to the all protected backbone a trans-methylation from solvent occurred, which gave a mixture of methyl and benzyl ester. These esters were implemented in the coupling reactions with the modified nucleobases. Many coupling mixtures failed but the reaction with DIC gave full conversions. Since a mixture of methyl and benzyl ester was implemented in the reaction with all four modified nucleobases the two products were obtained after purification with preparative reversed phase HPLC. These were analyzed separately and were confirmed as the desired products. The methyl/benzyl ester of the corresponding nucleobase were converted to the free acid and amine with LiOH. In each case, HPLC indicates the formation of only one product which could be confirmed as the desired GPNA monomer with the respective nucleobase. A reprotection of the N-terminal amine with Fmoc-OSu finally gave the desired α -GPNA monomers. The conversion with this synthesis route was always complete. At the stage of the coupling of the nucleobase HPLC checkups showed no starting material in the chromatogram. However, the isolated yield was not in the range of quantitative conversion. These circumstances are justified by small batch reactions (<50 mg) using a preparative HPLC which is designed for larger scales. Here much product was lost in the purification process.

Since the methyl and benzyl group are cleavable with LiOH, the first step of the backbone was performed with methanol instead of the benzyl alcohol to gain the methyl ester. This change led to full conversion and quantitative yield compared to 95% of the benzyl ester. Even the next step, the Fmoc-deprotection gave higher yield (90%) as the corresponding benzyl ester (76%). The followed reductive amination to the secondary amine gave similar yields.

3.4. Azobenzene derivatives

Azobenzenes are accessible by many different synthetic pathways, but not every route is suitable for halogenated derivatives, which are among the most bathochromically shifted modifications – particularly desired for *in vivo* experiments. One of the less demanding reaction setup is the acid catalysed reaction of an amine with a nitroso compound – the Mills reaction. Another possibility is the azo coupling, in which amine first reacts with NaNO₂ to yield the corresponding diazonium salt. In the second part of the reaction the diazonium salt is then coupled to another aromatic compound. Due to steric hindrance, the *para* position is usually favoured (scheme 18).



Scheme 18: Two synthetic pathways towards an azobenzene. Acid-catalysed reaction of an amine and a nitroso compound leads to the azobenzene (top). After conversion of an amine to the corresponding diazonium salt this compound then reacts with another (substituted) aromatic compound. Due to steric hindrance the reaction at the *para* position is usually favoured.

To obtain the desired azobenzenes a MILLS reaction was performed according to HECHT *et al.*[38] For non-halogenated azobenzenes acetic acid as solvent and catalyst is sufficient, whereas for fluorinated compounds additional TFA is needed – the electron-poor substrates require more electrophilic environment. The second reaction pathway implements a diazonium salt produced with e.g. sodium nitrite. *In situ* reaction with another aromatic compound affords the desired azobenzene. This reaction pathway was chosen to provide numerous pyridine derived azobenzenes by M. STEINBISS during his master thesis, whereby one of them was investigated further.

AZOBENZENE DERIVATIVES

In contrast to other ABs, these photoswitches are equipped with a positive charge. Therefore, these molecules exhibit different photochemical properties and increased water solubility.

There were many attempts to synthesize tetra *ortho*-chloroazobenzenes, but the common coupling reactions did not result in satisfying yields. The solution for this problem was to switch to a late-stage chlorination, which is a particular modification of the unsubstituted azobenzene, which was previously synthesized in a 'easy' coupling reaction by the e.g. MILLS-reaction.[111] Here the AB with the pre-installed functional groups was brought to reaction with *N*-Chlorosuccinimide catalysed by Pd(OAc)₂ in acetic acid. As the aim was to attach these switches to the PNA- backbone, this work focused on a precursor which had the acetic acid linker attached in the *para*- position relative to the azo bond (in *meta*-position in case of pyridinium-ABs) (figure 20).

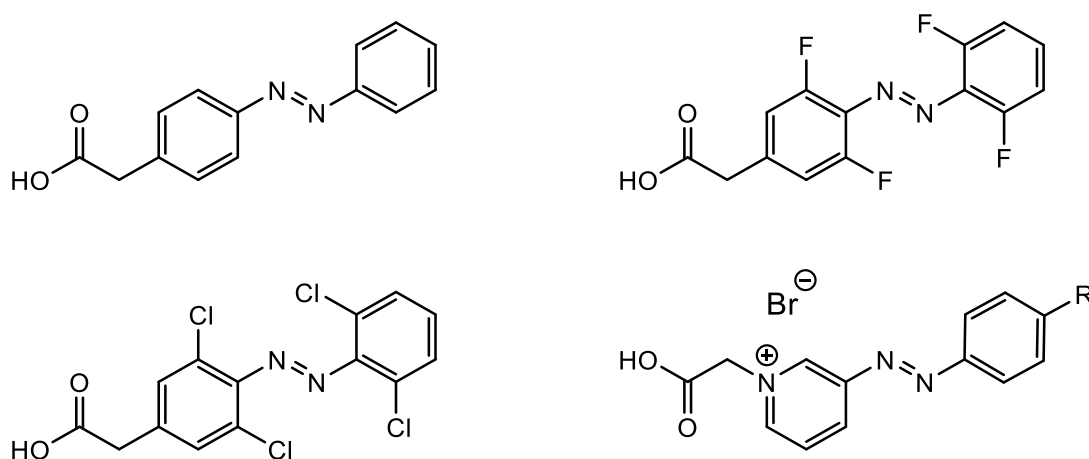


Figure 20: Structure of the azobenzenes synthesized in this work. The unsubstituted AB (top, left) with an acetic acid linker serves as the core structure. ABs tetrafluorinated at the *ortho*-position (top, right) are synthesized in a different way compared to their chlorinated analogues (bottom, left). Pyridinium azobenzenes (bottom, right) are synthesized *via* a diazonium salt.

In collaboration with J. Karcher and M. Bichelberger we investigated the photochemical properties of the pyridine-derived ABs. The task was to show the increased water solubility of the positive ly charged molecules in comparison with the uncharged ones. In order to show the implementation of the pyridine-derived azobenzenes, a peptidic tetramer was synthesized *via* solid phase synthesis following the Fmoc-protocol. (*S*)-Phenylalanine was used as the first building block, (*S*)-2-(((9*H*-fluoren-9-yl)methoxy)carbonyl)amino)-4-azidobutanoic acid was coupled next. Two (*S*)-alanine building blocks were used to complete the tetramer, with a Boc-protecting group at the N-terminus. This sequence was used in order to have an unpolar peptide chain. The tetramer was cleaved from the resin on an analytical scale in order to check the purity of the compound (MALDI, HPLC). Afterwards the azide was reduced to the amine with a 2 M solution of P(^{*t*}Bu)₃ in NMP/THF/water 10:9:1. The unsubstituted AB and the pyridinium azobenzene (shown in figure 20) with an acetylated piperazine attached to the phenyl ring were activated with TSTU and coupled to the free amine.

After cleaving the tetramer from the resin, both tetrameric structures (figure 21) could be obtained and characterized. The 3-arylazopyridinium salts isomerize with green light, the reverse reaction needs no light at all. M. Bichelberger found this is due to the short half-life of these compounds, which is in the millisecond range. Both, the heterocyclic ring of the pyridinium with the positively charged nitrogen and the piperazine moiety, enhance the hydrophilicity.

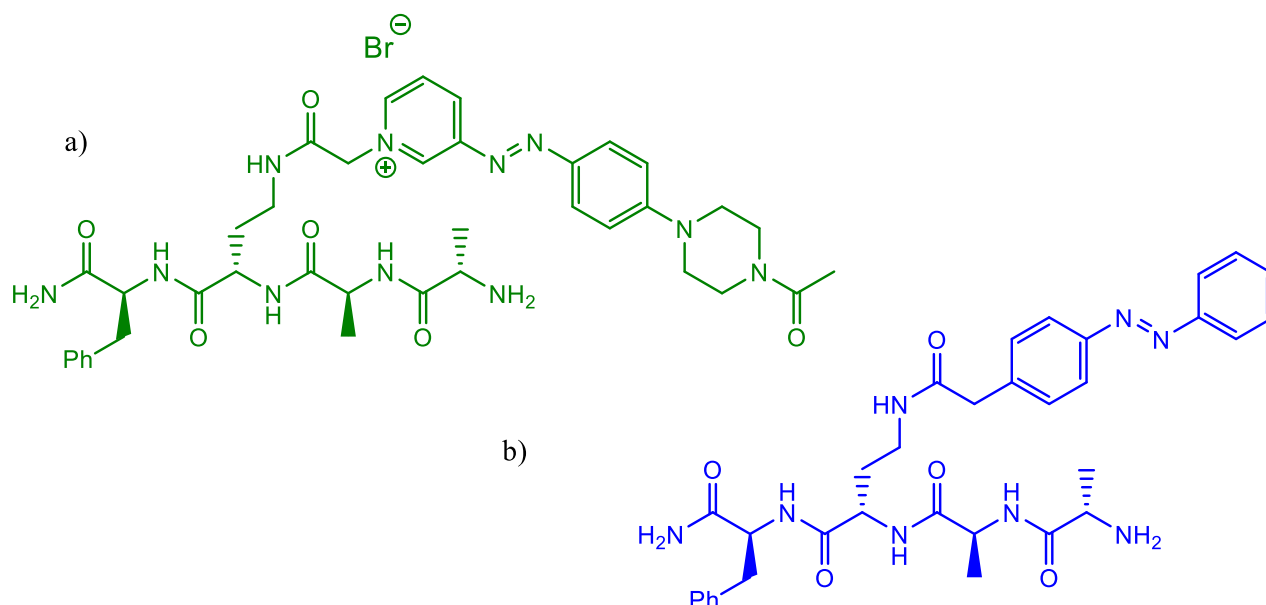


Figure 21: Structures of *tetra*-peptides containing a 3-arylazopyridinium photoswitch (a), which is triggered with green light, and the unsubstituted AB attached to the same peptide (b), where UV light was necessary to switch it to the *cis* conformation.

The hydrophobic AB is expected to agglomerate in water solution. The same oligopeptide with the pyridinium AB should form less aggregates under the same conditions because it is a salt. To investigate this assumption, both oligopeptides were dissolved in diluted aqueous PBS buffer (pH 7.4). To determine the exact concentration of the oligopeptides, a calibration curve with the UV-Vis spectrometer was made. For each of the acetic acid ABs a 1 mM stock solution was prepared and diluted in 200 μM steps. A second calibration curve was done starting at 100 μM in 20 μM steps to 20 μM . The assumption was, that the specific absorption properties in the visible light range of the free acid do not change significantly compared to the properties while attached to the tetramer. The tetramers were measured giving a concentration of $\sim 50 \mu\text{M}$ after fitting the maximum with the calibration curve. After the measurement the solution was passed through a 3 kDa size-exclusion filter. The filtrate was measured again. As expected, the differences in both oligopeptides are significant (Figure 22).

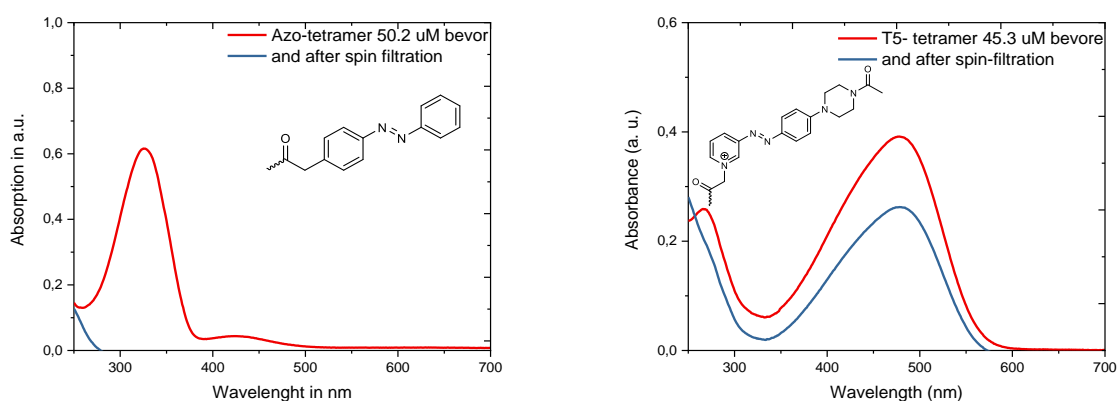


Figure 22. Absorption spectra of solutions ($\sim 50 \mu\text{M}$ in PBS, pH 7.4) of tetrapeptides with the azobenzenes attached to it. Left with the uncharged azobenzene and right with the charged one. The red line indicates the absorption spectra before and the blue line - after spin filtration, respectively.

More than 50% of the positive charged oligopeptide passes through the filter. This shows that even with a rather unpolar peptide structure the charged AB is able to avoid agglomeration in buffer solution, whereas more than 95% of the oligopeptide coupled with the non-polar AB did not pass through the filter. The molar masses of 755 Da for the positive charged AB and 628 Da for the unsubstituted AB are well below the cut-off (3 kDa). The aforementioned assumption of the tendencies to form aggregation, respectively to avoid aggregation in the PBS buffer leads to this interpretation of these results. In a longer peptide this effect might be reduced due to the increased influence of other side chains.

In another task *tetra*-fluoro- and *tetra*-chloro azobenzenes with acetic acid linkers were synthesized following literature procedures. These ABs shall be attached to the PNA respectively the GPNA backbone. Starting with the fluorinated AB, many different coupling conditions were tested but not successful at all. After careful tests it was concluded that these ABs are not stable against bases. Since the products will be implemented in the solid phase synthesis following the Fmoc-protocol, where at last the protecting group is removed with 20% v/v piperidine in DMF, they should be stable for at least 5 min (figure 23).

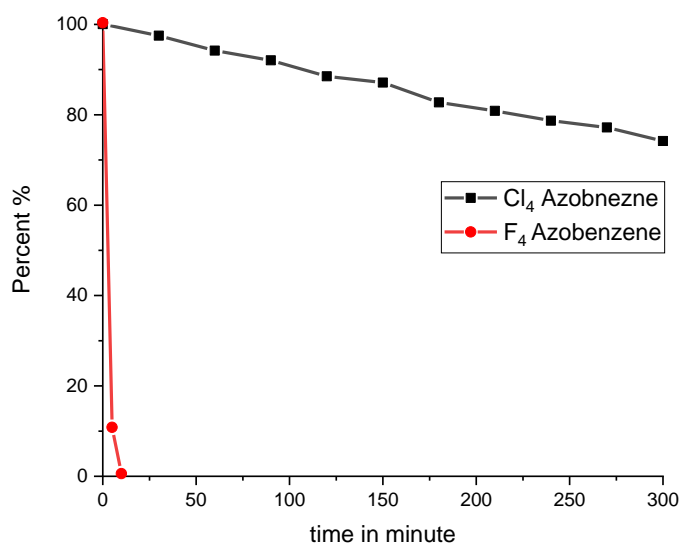
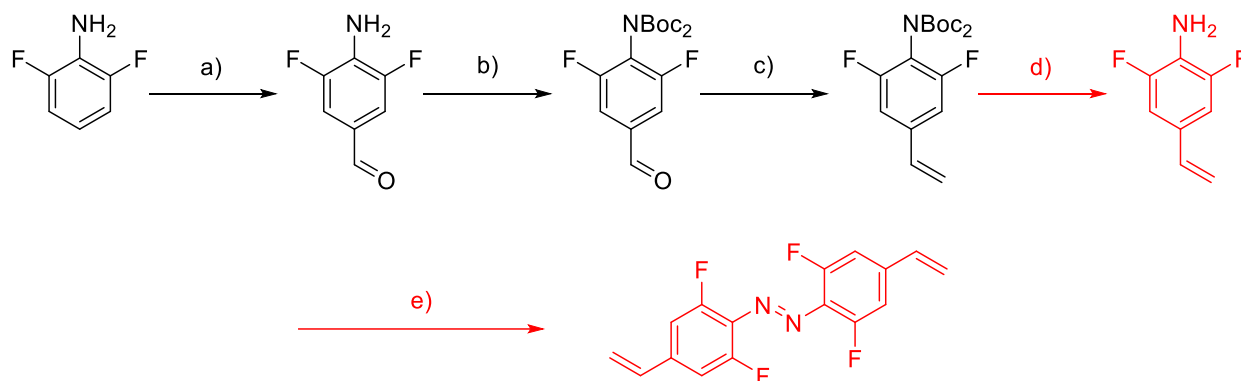


Figure 23: Kinetic studies of the halogenated azobenzenes in 20% v/v piperidine in DMF. While the chlorinated AB (black) is stable against the harshest basic conditions in the SPS, the fluorinated AB (red) is almost fully decomposed after 5 minutes.

These results made it clear, that a switch to the chlorinated ABs was necessary as they show stability against these conditions. The synthesis again followed the route of late-stage chlorination. Here the methyl 2-(4-aminophenyl)acetate was reacted with nitrosobenzene under MILLS reaction conditions to the corresponding AB. The resulting unsubstituted azobenzene was converted with NCS to the corresponding *tetra*-chloro AB. The ester was cleaved with LiOH in acetonitrile/water (3/1) to obtain the desired AB with an overall yield of 9%. As well as with the fluorinated ABs, the coupling reactions were challenging. The common reagents did not work. After implementing the free acid with DIC and the *tert*-butyl protected PNA backbone the coupling to the secondary amine succeeded giving the ester-protected photoswitchable building block.

Together with A.-L. Leistner new red-light switchable ABs were investigated. During her studies, she discovered that fluorinated ABs with sp^2 -hybridized residues at the *para*-positions undergo efficient photoisomerization with red light (>630 nm). To investigate this behaviour further, more sp^2 -hybridized ABs are planned to synthesize (scheme 19), as this was initially demonstrated on aldehydes with intrinsically limited stability.

AZOBENZENE DERIVATIVES



Scheme 19: Schematic synthesis of novel *para* sp^2 -hybridized azobenzenes with *ortho*-fluorinated positions (here a vinyl modification). Starting with a formylation reaction for halogenated aromatic systems with DMSO, CuCl_2 and concentrated HCl, yielding the aldehyde in the *para* position (a). After the bis-Boc-protection of the amine with Boc_2O and DMAP (b) a Wittig conditions afforded the alkene (c). These procedures were carried out during this work. Planned reactions (d+e, red) are the deprotection of the amine followed by an oxidative dimerization with NCS to the desired AB.

The desired product was a bisalkenyl-substituted AB. Starting material was 2,6-difluoroaniline, the synthesis begins with a formylation in the *para*-position of the aniline. LIDHOLM *et al.* developed such a reaction for halogenated aromatic systems, by refluxing the substrate in DMSO, CuCl_2 and conc. HCl. The reaction is highly selective and results in a full conversion and 95% yield. To protect the aniline, the Boc-protecting group was chosen and was installed with Boc_2O and DMAP as transfer reagent obtaining the bis-protected aniline. Under WITTIG conditions the aldehyde was converted to an alkene with sufficient yield. It is planned to remove the protecting groups and dimerize the amine under oxidative conditions.[40] This would provide potentially a red-light- switchable fluoro-AB with the possibility of the implementation *e.g.* in polymer structures due to its two vinyl groups (in analogy to divinylbenzene, which is often used as *e.g.* polystyrene cross- linker). Here it could function as a switchable cross-linker building block.

3.5. Indole-derived fluorescent dyes

In collaboration with C. Schwechheimer we investigated fluorophores which have a light-up effect once they are hybridized in double-stranded DNA or RNA. Therefore we choose two different dyes provided by C. Schwechheimer and one reversed dye where the acetic acid linker and the methyl group switched the position (figure 24).

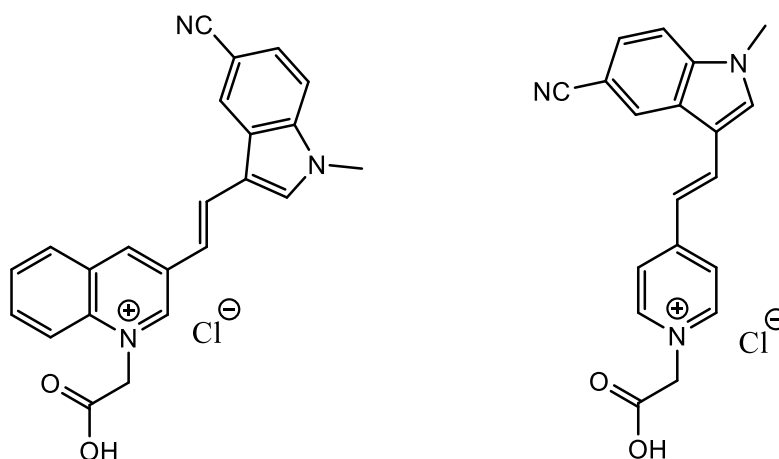


Figure 24: Structures of two dyes provided by C. Schwechheimer. The left structure was not implemented due to the lack of stable fluorescence. The work was continued with the other dye (right).

The first dye showed poor fluorescent activity, respectively the weak triplet state, which resulted in a quick fading of the fluorescence in HeLa cells. Since the other dye did not show this problem, we focused on the second dye shown in figure 42. To investigate the fluorescent behaviour regarding the structure of the dye, the acetic acid linker was synthesized to the indole derivative while the picoline part was methylated with MeI. Many different conditions to couple the free acid to the PNA backbone, respectively to the *tert*-butyl protected PNA backbone were tested, but always afforded a complex mixture with traces of product detected in MALDI-TOF. The solution to this problem was to use only DIC as coupling reagent with the di-protected backbone in acetonitrile. After deprotection of the ester, the fluorescent PNA-building block was ready to be used in solid-phase synthesis.

3.6. Novel fluorinated Spiropyranes

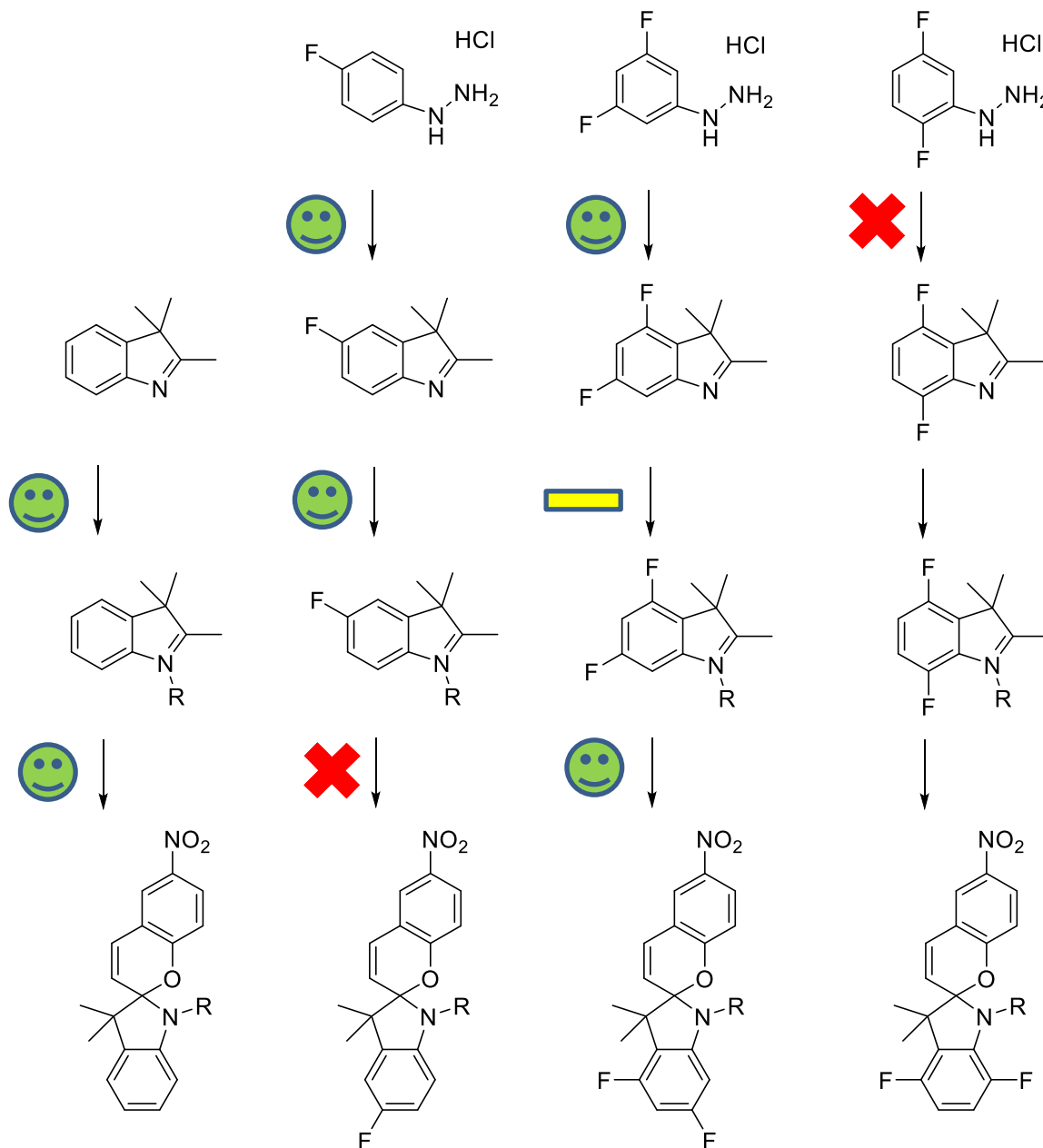
One of the common photoswitchable units are the spiropyrans. KATSONIS *et al.* implemented a fluorescent spiropyran with a nitro-group at one of the aromatic rings. This implementation led to fluorescence in the open form. To investigate if fluorine atoms have the same effect as they have in ABs, a red-light shift in the absorption and therefore a red-light shift in the fluorescence for these molecules, three spiropyran derivatives with one or two fluorine atoms were planned to synthesize. For the synthesis of the literature known non-substituted spiropyran as a reference, the commercially available substrate 2,3,3-trimethylindoline was brought to reaction with the ethyl- 4-bromobutyrate to give the alkylated indole salt. Another cyclisation reaction with 2-hydroxy-5- nitrobenzaldehyde gave the non-fluorinated spiropyrane. Normal column chromatography was not the first choice of purification since there was a chance to switch to the open form, the merocyanine form due to slightly acidic conditions derived by the silica gel.

For the synthesis of the mono-fluorinated spiropyran, the commercially available substrate was 4-(fluorophenyl)hydrazine hydrochloride. To form the indol derivative, a cyclisation reaction with 3-methylbutan-2-one gave the desired ring closure reaction with all similarities (methyl groups) as the non-modified spiropyrane. This reaction succeeded without any problems and the desired product was found after purification through column chromatography. However, the alkylation step resulted in some difficulties during the purification process. The reaction led to the desired product, but NMR indicated numerous impurities. Various attempts of purification were executed, mainly recrystallizations and precipitations. Most of the impurities were removed after recrystallization with toluene which gave the product in a sufficient purity to proceed.

In comparison to the non-fluorinated spiropyrane, the cyclisation with 2-hydroxy-5-nitrobenzaldehyde gave no product within the same conditions. Unfortunately, a more basic environment granted by the addition of piperidine did not perform well. The yield of 10% of a mixture of different species was neither efficient nor sufficient for further tests.

The disubstituted hydrazine compound with fluorine atoms at the 2 and 5 position of the phenyl ring did not react under various conditions to the desired indole derivative. However, the 3,5-fluorospiryran was obtained, but the synthesis of the alkylation step could not be reproduced, yet (scheme 20).

NOVEL FLUORINATED SPIROPYRANES



Scheme 20: Schematic pathway of the synthesis of the spiropyran. The literature-known non-fluorinated spiropyran (left) was obtained in a two-step procedure. Since the fluorinated indole derivatives are not commercially available, the substrates were the respectively fluorinated phenylhydrazines as hydrochlorides (mid left, mid right, right). Except for (2,5-difluorophenyl)hydrazine, all cyclisation reactions with 3-methylbutan-2-one led to the product. The methylation of 4,6-difluoro-2,3,3-trimethyl-3 H-indole was carried out once in a big scale, but the synthesis could not be reproduced. However, the reaction to the respective spiropyran worked for the 4,6 difluoro-alkyl indole but not for the 5 fluoro-alkylindole.

NOVEL FLUORINATED SPIROPYRANES

In order to test the photophysical properties of the new spiropyran, the UV/Vis absorption in acetonitrile was first measured for the known spiropyran. First the desired absorption maximum of 1 of the stock solution was achieved by diluting 1 mL of a 5 mM solution with 9 mL of acetonitrile. This stock solution was measured in a 0.1 cm thick cuvette and results in the black curve shown in Figure 45, which has a maximum at 404 nm. Then 1 mL of the stock solution was taken and irradiated with LEDs of different wavelengths (365 nm, 400 nm, 500 nm, 530 nm, 3 W each) to measure the spiropyran's switching property. It was not surprising that at 400 nm (4 nm below the maximum) the most drastic decrease in absorbance was observed (Table 1). It can be assumed that after one minute of irradiation at this wavelength, almost all molecules have switched to their merocyanine form. The drop was not quite as extreme at 365 nm. Here an absorbance of 0.29 was reached after one minute, which still indicates that most of the molecules have switched. Astonishing here was the extremely good switching at 500 nm. The absorbance is 0.21, which is between 365 nm and 400 nm in terms of efficiency, although the initial state of the stock solution does not suggest this. At 530 nm, the worst switching efficiency was found, but was still around 40% despite the high wavelength.

Despite the comparatively weak LED strengths of the lamps used, it is clear that the unsubstituted spiropyran switches very well and very quickly. Even when irradiated with light of a wavelength that is not necessarily close to the absorption maximum, this molecule switches, which makes it very photosensitive.

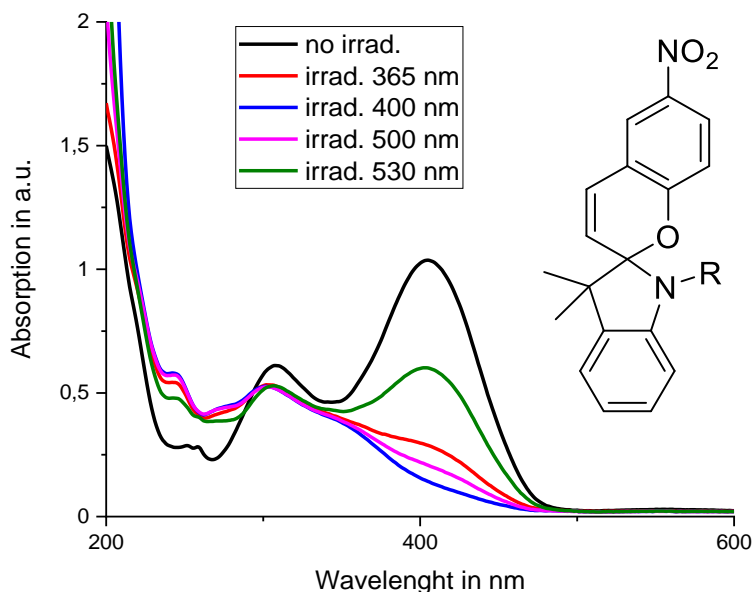


Figure 25: UV-spectrum of the non-substituted spiropyran. Shown in black is the absorption of the stock solution without irradiation. All the measurements were done by taking 1 mL of the stock solution and irradiating it with LEDs of different wavelengths. In red shown the absorption after irradiation with 365 nm, in blue after irradiation with 400 nm, in pink after irradiation with 500 nm and in green after irradiation with 530 nm.

Table 1: maxima of the absorption for the unsubstituted spiropyran at a concentration of 500 μM using a 0.1 cm thick cuvette with no irradiation and with LED irradiation at a wavelength of 365 nm, 400 nm, 500 nm and 530 nm, respectively.

Substance	Irradiation	Max. Absorption (at 404 nm)
Non substituted SP	no irrad.	1.04
Non substituted SP	365 nm	0.29
Non substituted SP	400 nm	0.14
Non substituted SP	500 nm	0.21
Non substituted SP	530 nm	0.60

The same procedure was used for the double-substituted spiropyran. For the UV/Vis measurement, 10 mL of a 342 μM stock solution had to be prepared to obtain the absorbance of 1, which is reflected by the black curve in Figure 46. Unfortunately, we found that the two fluorine atoms on the phenyl ring do not have a red-shifting effect on the absorption maxima, but the exact opposite was the case. The maximum of the difluorinated spiropyran was 346 nm. Nevertheless, 1 mL of the stock solution was irradiated with the same LEDs for 1 min and the result was very interesting in another way. Compared to the unsubstituted spiropyran hardly any change of the curve could be detected at 500 nm and 530 nm. The circuit was virtually non-existent (<3%).

NOVEL FLUORINATED SPIROPYRANES

But also the switching behaviour at the wavelength of 365 nm was not much better, where about 10% of the molecules switched. The efficiency was best at 400 nm where about 25% was in the open form. Although the fluorine atoms unfortunately do not have a redshift, they have a stabilizing effect on the system. With the same irradiation by the LED lamps and at the same time the efficiency was clearly different.

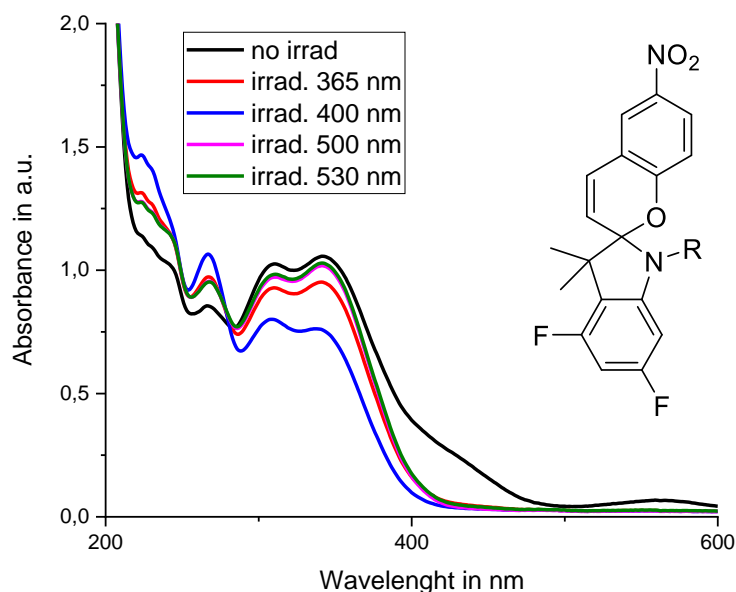


Figure 26: UV-spectrum of the bis-substituted spiropyran. Shown in black is the absorption of the stock solution without irradiation. All the measurements were done by taking 1 mL of the stock solution and irradiating it with LEDs of different wavelengths. In red shown the absorption after irradiation with 365 nm, in blue after irradiation with 400 nm, in pink after irradiation with 500 nm and in green after irradiation with 530 nm.

Table 2: maxima of the absorption for the bis substituted spiropyran at a concentration of 500 μM using a 0.1 cm thick cuvette with no irradiation and with LED irradiation at a wavelength of 365 nm, 400 nm, 500 nm and 530 nm, respectively.

Substance	Irradiation	Max. Absorption at 342 nm
3,5-Difluoro SP	No irrad.	1.06
3,5-Difluoro SP	365 nm	0.95
3,5-Difluoro SP	400 nm	0.76
3,5-Difluoro SP	500 nm	1.02
3,5-Difluoro SP	530 nm	1.03

To further investigate the behaviour of the bis-substituted SP, a 50 μM solution of both compounds in acetonitrile was prepared and after measuring the UV-Vis absorption, these were illuminated for one minute with a stronger LED lamp (380 nm, 15 W).

This wavelength was chosen because it is approximately in the middle of the two absorption maxima of the SP. While the unsubstituted one switches almost completely, the efficiency of the di-fluoro SP is below 15%. Therefore, even stronger lamps are not able to switch this molecule efficiently.

In principle, this property is very desirable, e.g. with a light pulse only a few molecules change into the open and therefore into the fluorescent form. This could be an advantage in single-molecule detection. Unfortunately, the absorption maxima at 346 nm makes these molecules not applicable for *in vivo* experiments and therefore they are not in our interest.

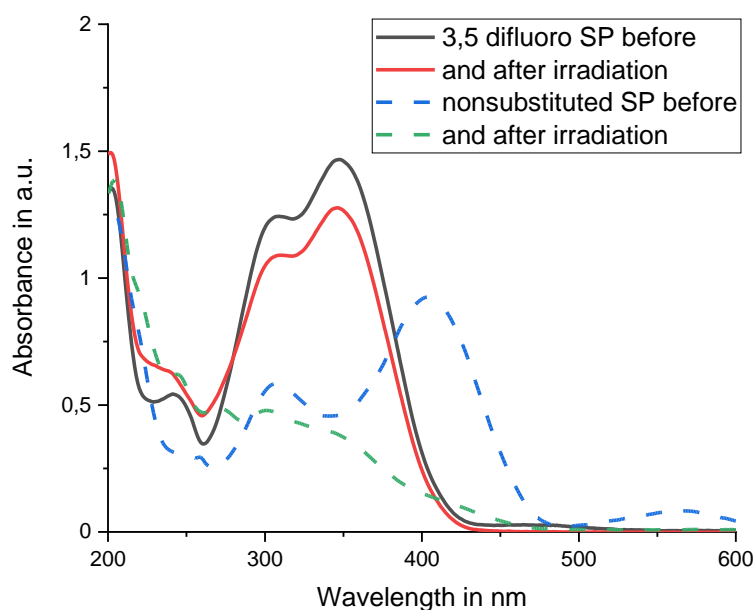


Figure 34: UV-spectrum of the bis and non-substituted spiropyran before and after irradiation with UV light of 375 nm wavelength and 15 W. Shown in black is the absorption of the di-fluoro-SP with a concentration of 50 μM before the irradiation and in red after irradiation. Even here, the conversion to the open form is less than 15% while the non-substituted SP convert completely from the non-irradiated closed form (blue dashed) to the open form after irradiation (green dashed) at the same concentration of 50 μM .

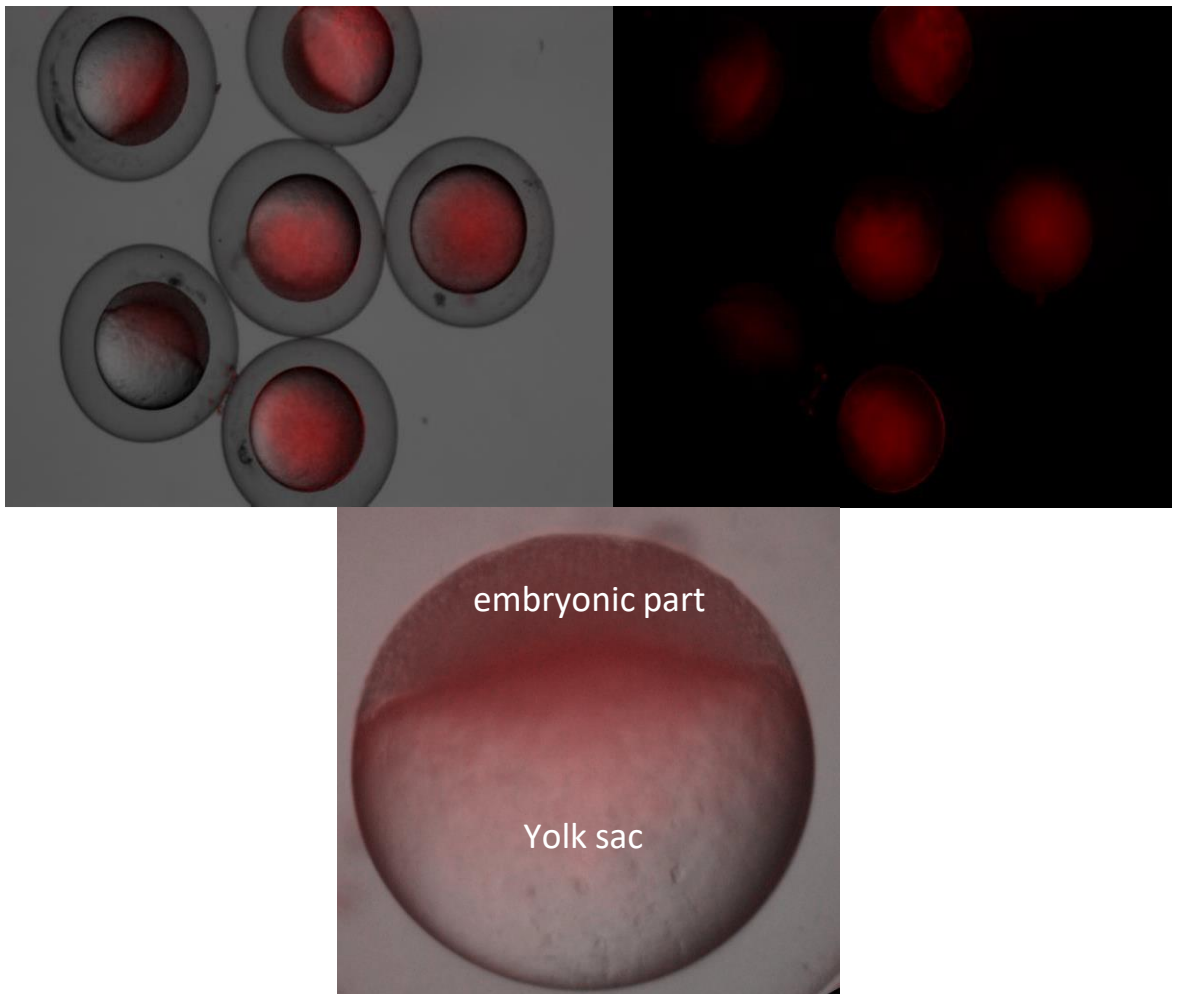


Figure 27: Picture of Zebrafish eggs after the injection of PNA with Cy3 dye in water. The cellular uptake to the embryo was not successful. The PNA stayed in the yolk of the eggs.

As it was shown (figure 27) the PNA stayed in the yolk of the eggs. The PNA did not move to the embryo, respectively was not taken up in the cells. The hatching of the fishes was normal and no significant changes of the tail was observed. This lead to the conclusion to implement the cell-permeable GPNA building blocks for this setup. On top, the photoswitching building block will be implemented to investigate the photoswitching properties *in vivo*.

3.8 (G)PNA oligomers for hybridization experiments against HIV

One of the most challenging diseases of modern times is HIV. If this virus remains undetected, it multiplies with the help of our genetic material and destroys the immune system of the sick person. Researchers from all over the world have been trying to defeat the disease since the mid-1980s. At first there was little or no success, but now the virus can be suppressed with the help of specially developed medication to such an extent, that the disease does not break out or the pathogen cannot be detected by common tests. However, if you stop taking the medication, the virus multiplies again and attacks the immune system.

Like many other viruses, HIV also has a genetic material in the form of RNA, which could be suppressed or blocked by complementary PNA strands, so that important translation processes would no longer take place. The HI virus, however, uses the genetic material of the host to reproduce. In humans, the virus infects the T-helper cells and uses the possibilities there to reproduce its proteins in these cells. There are two structures of the HIV RNA: the 'long distance interaction' (LDI) and the 'branched multiple hairpin' (BMH) structure, which each has its own function in the reproduction cycle of the virus. While in the LDI structure all the necessary proteins are produced to replicate, in the BMH structure the virion is packed and exits the cell to replicate elsewhere. But before this, the 'dimerization initiation site' (DIS) of the BMH structure forms a loop-loop complex with another genomic RNA. In other words: two gRNAs of the HI Virus need to form a complex dimer structure over the DIS before the HI virus can be packed and released from the cell. For this reason, the area around the DIS site is a possible target for the PNA to prevent dimerization of the gRNA and thus stop the virus from multiplying in its entirety.

As has already been said, a complete cure for HIV is not yet possible for everyone. The drugs help, but the virus apparently hides somewhere where they cannot work. For this reason, C. Schwechheimer synthesized cyano dyes in our cooperation, which are said to have a so-called 'light up' effect. This means that as soon as the dye is in a PNA/RNA hybrid, the fluorescent intensity increases significantly. In addition to the expected blockage of proliferation, this could be a medical tool to locate infected cells and produce new, more specific drugs. For this issue we designed for different PNA strands bearing one Dye-PNA building block at the 4th, 5th, 6th or 7th (BT 403, 404, 405, 406) position in the C' to N' direction of a 10mer. Every strand was flanked with two *D*-Lysines at both sides of every chain to increase the water solubility for hybridisation tests. The complementarity was given by 9 of 10 blocks to target the DIS of the HI virus. For the work with RNA it was necessary to provide RNase-free solvents, as well as salt and buffer Solution.

(G)PNA OLIGOMERS FOR HYBRIDIZATION EXPERIMENTS AGAINST HIV

The exact approach is stated under 5.12. All the following experiments were hold under these conditions if not stated otherwise.

To investigate the 'light up' effect, the strands were given together in equal measure with a complementary, commercially purchased RNA 12mer. The single strands were measured in the same concentration as the later double strands in order to obtain comparable fluorescence spectra. After the hybridisation with the complementary RNA the single strand as well as the double strand, respectively, were measured with a FluoroMax 4 with an activation wavelength of 437 nm. Data were collected between 452 and 800 nm with a slit of 1 nm. Except for the strand BT 404 all other showed an increase of the intensity (figure 27), while the strongest increase was detectable at the samples BT 405 and BT 406.

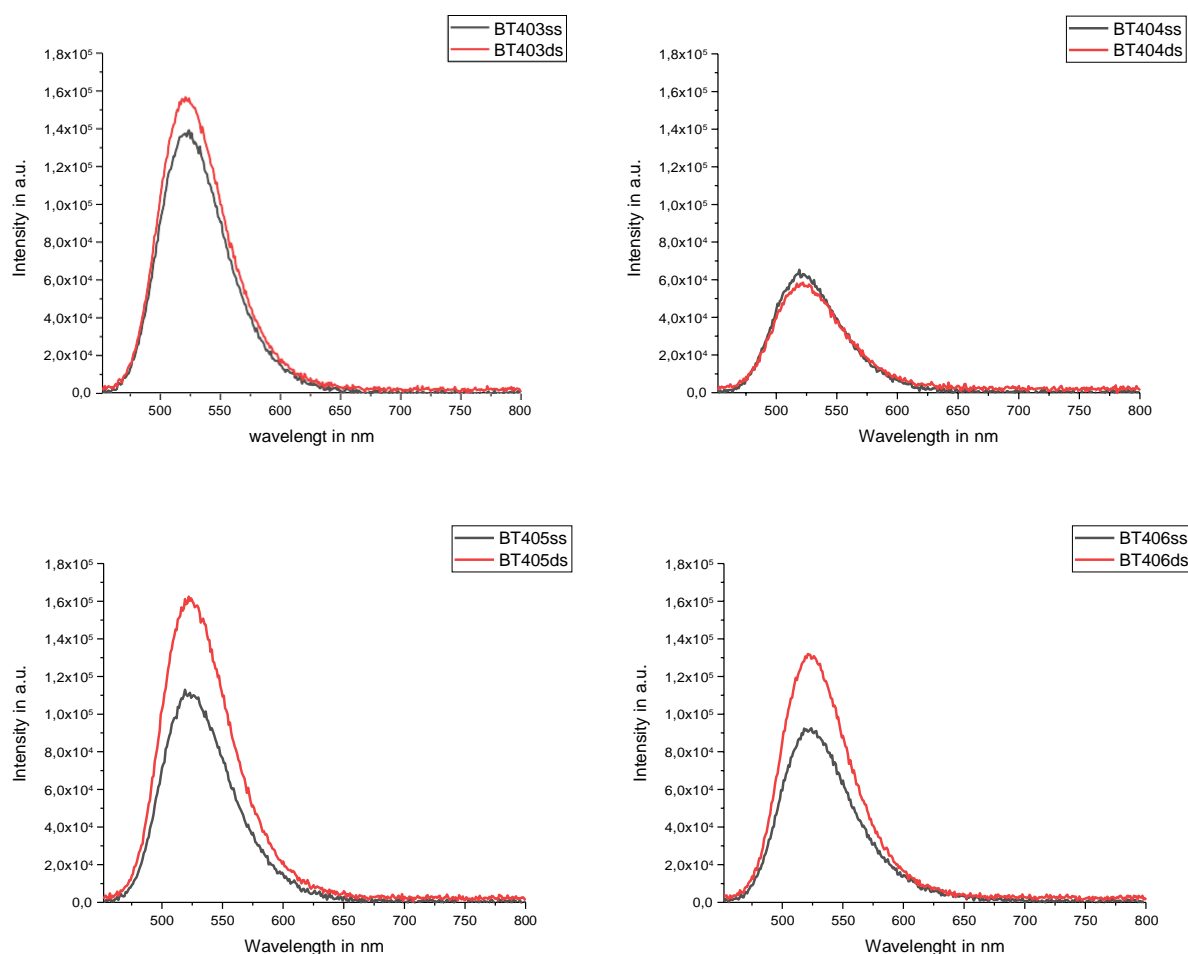


Figure 27: Results of the fluorescent measurements of the PNA strands 403 -406 as a single strand (ss, black) and as a double strand (ds, red) after the hybridisation with the complement ary commercially purchased RNA. Except for the strand 404 the intensity increased while the dye is inside the duplex.

Unfortunately, no significant increase could be observed in any of the strands. After inspection of the UV-Vis spectra (data not shown here) it is clear that it could not be a pipetting error. Therefore, it must be concluded that the dye used is not suitable for this application. To check these results, a

(G)PNA OLIGOMERS FOR HYBRIDIZATION EXPERIMENTS AGAINST HIV

total scrambled PNA without a fluorescent building block was synthesized and measured the same way as the other strands (BT540). To complete the measurement, the quantum yields of the single strands were also compared with the double strands. The results are shown in table 2.

Table 2: measured quantum yields of the single and double strands, respectively. Each sample was measured 10 times and the mean value was determined. Finally, the last line indicates by how much % the double strand behaves in comparison to the single strand.

BT403ss	BT404ss	BT405ss	BT406ss	BT403ds	BT404ds	BT405ds	BT406ds
0,206	0,116	0,208	0,132	0,204	0,093	0,245	0,149
0,207	0,120	0,207	0,130	0,204	0,094	0,241	0,148
0,205	0,116	0,203	0,132	0,202	0,094	0,242	0,152
0,206	0,115	0,205	0,133	0,202	0,094	0,241	0,146
0,204	0,114	0,207	0,130	0,203	0,094	0,243	0,149
0,206	0,118	0,206	0,131	0,203	0,093	0,243	0,148
0,204	0,117	0,203	0,131	0,201	0,095	0,240	0,150
0,204	0,115	0,205	0,132	0,201	0,093	0,242	0,146
0,204	0,116	0,204	0,131	0,201	0,095	0,240	0,145
0,202	0,115	0,203	0,131	0,201	0,096	0,239	0,148
0,205	0,116	0,205	0,131	0,202	0,094	0,242	0,148
n.a	n.a	n.a	n.a	-0,3%	-2,2%	3,7%	1,7%

Just like the fluorescence measurement before, there is no significant difference in the quantum yield. BT403 and BT404 have a lower quantum yield, whereas BT405 and 406 have an increased quantum yield. To prove that the strands hybridized correctly at all, the melting points of the strands were determined. The sample of each double strand was heated 3 times from 10 °C to 90 °C and cooled down again. The data were recorded in half °C steps with a heating rate of 0.7 °C/min. To determine the inflection point of the melting curve the Boltzmann Fit was used. Here the melting points were in the expected range of 37-46 °C and are stated in table 3. Therefore it can be said that the hybridization was successful.

Table 3: measurements of the melting points of the respective PNA/RNA double strands. In red marked numbers are shown but due to failure in the measurements they are not trustworthy.

melting points of PNA/RNA ds without ribonucleic cleaver					
BT403	BT404	BT405	BT406	BT473	BT540
37.7	40.0	40.7	42.9	45.8	n.a.
35.6	40.4	41.1	45.0	46.1	n.a.
37.7	40.8	40.8	44.7	39.7	n.a.

As fluorescence measurements and quantum yield determination have shown, the strands BT405 and BT406 are the two best options to re-synthesize this sequence not only because of the high melting point but also because of the best photophysical properties. In this case, every third unit

(G)PNA OLIGOMERS FOR HYBRIDIZATION EXPERIMENTS AGAINST HIV

of the re-synthesized oligomer was replaced with a cationic GPNA monomer, which should help to improve hybridization and prevent agglomeration in water as far as possible. The two strands BT472 and BT473 were synthesized the same way as described in the experimental part. After cleaving it was recognized that there was no specific absorbance at 432 nm at the strand 472, which was discarded then. The BT 473 line was measured in the same way as the other lines, but due to an as yet unknown error the concentration could not be determined or could only be determined very imprecisely, so that no statement can be made about the properties. For completeness, the melting point was also measured, which would also fit well into the explanation of a strong hybridization. For the sake of completeness, it is listed in the melting point table, but will not be considered in the following.

According to Göbel et al.[112] the further idea was to synthesize a so-called cutter molecule which can be coupled N-terminal to the PNA. This cutter molecule cuts RNA strands as soon as an artificial RNA equipped with this molecule hybridizes with an RNA to be cut. Therefore all the above mentioned strands were synthesized with an additional hexyl linker and the aforementioned cutter molecule at the N-Terminus. To test the cleavage capacity of the 10-unit-long PNA, a 20- nt-long RNA was ordered, which fits complementarily to the PNA strands at positions 1-10 and which does not have more than 2 matching base pairs in one piece with the strand BT540, so that it should not hybridize with the RNA. Thus 10 strands (5 with cutter (+), 5 without) were hybridized with the RNA and tested as described above. Compared to the other results, there were no significant differences, so that a detailed description was omitted.

In order to test whether the molecules cut the desired RNA target, MALDI was first used to search for plausible fragments that could have arisen when the strand was separated. These could also be found in the samples BT404+, BT405+ and BT406+, although of course this statement says nothing about the quantity or the effectiveness. To further verify these results, gel electrophoresis was used to make the separation products visible. For this purpose, two agarose gels with 20 pockets each were cast. The strands BT403-406 were tested in single and double strand as well as with the cutter and without the RNA single strand as reference. The gel consisted of 4% agar and was tested at two voltages (100 V/120 V) whereas the 120 V lead to a blurred picture. Ethidium bromide was used as a coloring agent. The pictures in figure showed the results.

(G)PNA OLIGOMERS FOR HYBRIDIZATION EXPERIMENTS AGAINST HIV

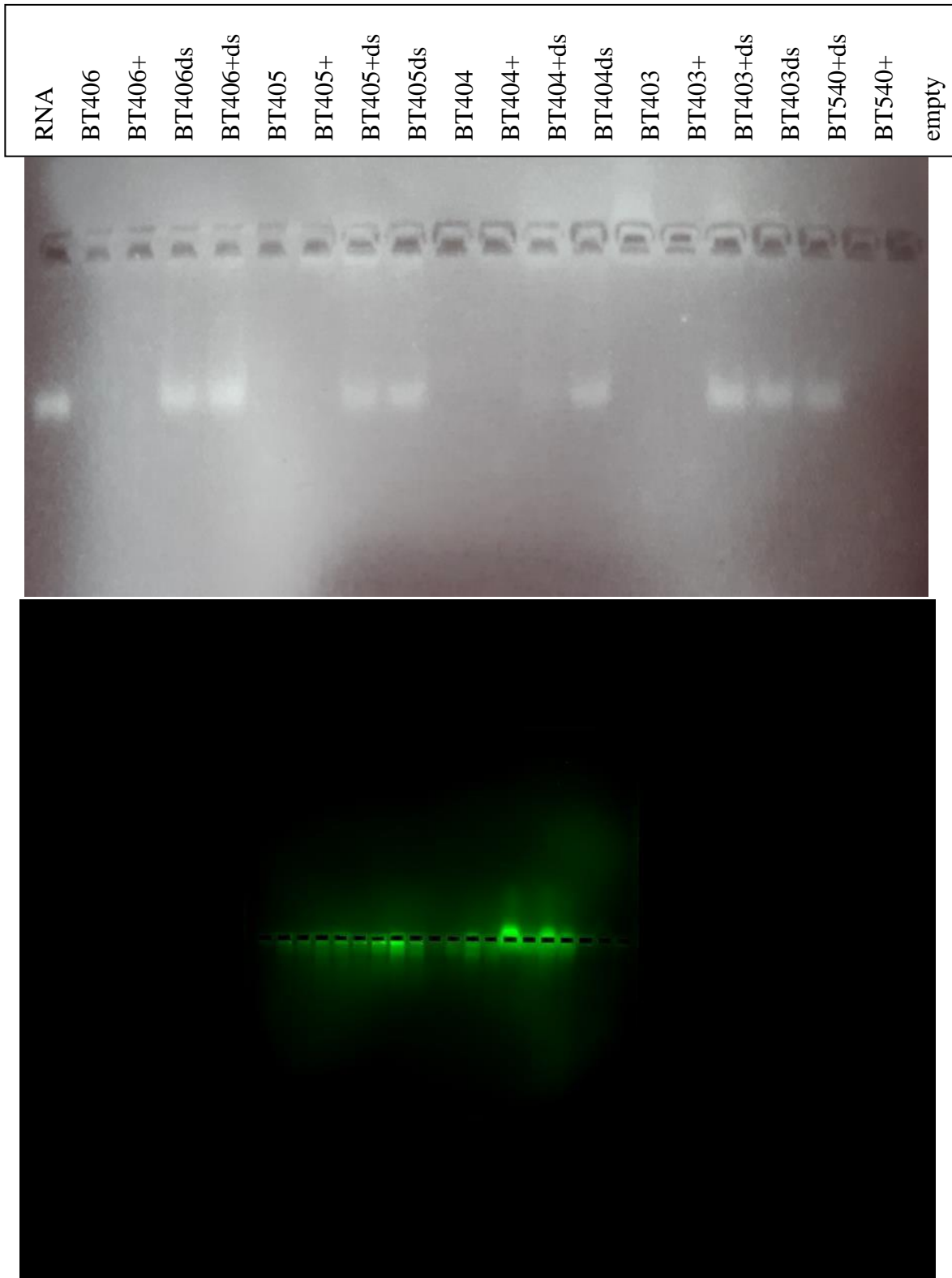


Figure 28: Gel electrophoresis experiment at 100 V with a 4% agarose gel after 30 min. In image A, which was taken under UV light, it can be seen that in every sample containing RNA, a band at the level of 20mer RNA is visible. In image B, +/-20nm was excited with 470 nm and thus makes the dye in the PNA visible.

(G)PNA OLIGOMERS FOR HYBRIDIZATION EXPERIMENTS AGAINST HIV

As can be seen in figure 28, it is not possible to make a clear statement whether the experiment was successful or not. There are some aspects which need to be re-investigated. Firstly, the concentrations of the samples are not the same, which results in a more or less clear visibility. The RNA is approximately the same in all samples and no conclusions can be drawn from the shape of the bands. Therefore, the question arises whether one can actually see cleavage products or whether the hybrid dissolves or the RNA itself cleaves under the conditions of gel electrophoresis. Furthermore, it is quite possible that the strands (~6000 Da and ~3000 Da) cannot be split at all, because the gel was poured not thick enough for such a small difference. Furthermore, it is in the range of possible that the buffer used in the GEP was not RNase free, so that decomposition has already started in the pockets. This would also explain the RNA band in the PNA without the cutter. If you look at picture B) in figure 28 you can see something else. All single strands of the PNA do not run far out of the pockets and if they do, they tend to the negative pole. This can be explained by the positive charge at the dye and at the 4 lysine groups, which are always or temporarily positively charged. But if we now look at the staining of the hybrids (with sufficient concentration) the PNA strands run in the same direction as the RNA. This leads to the conclusion that the hybrids do not dehybridize. Further the RNA band must be a cleaving product which would result in the theory that the two strands cannot differ on the gel. No matter from which side you look at it, no clear conclusions can be drawn, so that in the end only the results of the MALDI ToF show an indication.

To get a valid result, there are some parameters that can be changed. On the one hand, the RNA is quite short and should be replaced by one where you can clearly see the difference (e.g. 100 k total length and 50 k cleavage product). Another option would be to take complementary DNA, since the cutter can also cut it. This would ensure stability in the GEP.

4 Conclusion and outlook

4.1. Synthesis of γ -GPNA

The synthesis of γ GPNA turned out to be a very challenging task, which unfortunately could not be completed in the course of this work. Although many well-known syntheses in the literature have been applied to natural L-arginine, yields were often non-existent or yields were clearly too low to be pursued further. The favoured reaction path from free amino acid (α amine Fmoc and ϵ guanidin Pbf protected) via alcohol to bromide and then via a Finkelstein like reaction to the azide were quite promising. However, the reduction to amine again caused some issues. We suspect that the amine was sufficiently basic in an intermolecular reaction to deprotect the Fmoc protecting group. This could also be shown by NMR spectroscopy and mass spectrometry. Nevertheless, it is right and important to continue working on a better synthesis route, as the L-arginine is clearly a cheaper starting product. Perhaps it would be sufficient if instead of Fmoc the Alloc protecting group on the alpha amine of the amino acid were installed as starting material. This can also be deprotected alkaline, but in a much more basic range with potassium *tert*-butanolate, which would also be compatible with solid-phase synthesis.

4.2. Novel fluorinated Spiropyranes

The synthesis of novel fluorinated spiropyran were challenging and unfortunately in the end not suitable for our bio applications. Instead of a red shift in the absorption spectra we got a shift to the UV range. Never the less the tested spiropyran is to a certain point stable. It does not switch easy to the open state like the non fluorinated spiropyran. Therefore it might be useful in single molecule excitation where a weak switching and a weak fluorescence is sometimes good.

4.3. Azobenzene Derivatives

Azobenzene are and remain one of the most important photoswitches in photopharmacology. Even if the Vásquez et al. have shown that fluorinated AB unfortunately has no great effect on the melting temperature of PNA / RNA hybrids, it is still worthwhile to continue researching. One possibility is the chlorinated ABs, which could be synthesized in the course of this work in monomer form, but a coupling with the PNA backbone has not yet been carried out without any doubt. Nonetheless, further good successes were achieved with cationic and ortho sp² hybridized ABs, so that further work can be done here.

4.4. PNA/GPNA

Many publications are already about PNA or its analogous, and many will follow. Not only the results shown in this work, but also a lot of other work have contributed to the fact that effective antisense medications will soon be considered for clinical studies based on this class. Even if the dye used in this work has not been successful, some have already been researched that could be used here instead. The fight against HIV will always be an issue and with this approach we have taken, it could lead to success. Unfortunately, the results were not meaningful enough to achieve a clearly positive result, but new tests can be implemented in the near future and are promising.

5. Experimental part

5.1. Origin of compounds, chemicals and data

5.1.1 Solvents and reagents

Reagents and substrates were purchased (SIGMA-ALDRICH, METABION, CHEMPUR, ALFA AESAR Fischer Scientific, TCI, ASM, BEPHARM or synthesized in the course of this work. Technical grade solvents were distilled prior to use. HPLC grade solvents were used as delivered without any purification. Absolute solvents (toluene, acetonitrile, dichloromethane, diethyl ether or tetrahydrofuran) were dried with the SPS5 System of MBRAUN.

5.1.2 Thin layer chromatography (TLC)

Analytical thin layer chromatography was carried out using silica coated aluminium plates (silica 60, F₂₅₄, layer thickness: 0.25 mm) with fluorescence indicator by MERCK. The spots were detected by fluorescence quenching of UV-light at $\lambda = 254$ nm or subsequent staining with potassium permanganate solution (1.00 g potassium permanganate, 2.00 g AcOH, 5.00 g sodium bicarbonate in 100 mL water). For amino acids the Seebach stain (2.5% phosphomolybdic acid, 1.0% cerium(IV) sulfate tetrahydrate, 6.0% conc. sulfuric acid, 90.5% water) was used. Amines were detected with a ninhydrin stain (0.2% ninhydrin in 0.1% AcOH in EtOH). Alcohols were detected with KMnO₄-solution (1.5 g of KMnO₄, 10 g K₂CO₃ and 10 mL 10% NaOH in 200 mL of water).

5.1.3 High performance liquid chromatography (HPLC)

The standard solvents for HPLC measurements are HPLC grade acetonitrile with 0.1% TFA and bi-distilled water with 0.1% TFA. Diverse gradients were used to purify some of the compounds. The gradients as well as the flow rates of the HPLC setups are stated with the respective procedure of these molecules.

Analytic HPLC was measured with the 1200 Series from AGILENT TECHNOLOGIES using a YMC C18-column JH08S04-2546WT with 250 mm length \times 4.8 mm diameter and a column bead of 4 μ m diameter. Same system was used for a semi preparative setup equipped with a fraction collector, to purify on a small scale (PNA and GPNA). Preparative HPLC separation was

performed with a PURIFLASH[®] 4125 from INTERCHIM, equipped with InterSoft V5.1.08 software and a UV diode array detector. The stationary phase was a VDSpher column with C18-M-SE, 250 mm length \times 20 mm diameter with a column bead of 10 μ m diameter from VDSOPTILA.

5.1.4 Column chromatography

Crude products were purified according to literature procedure by column chromatography *via* flash-chromatography.[113, 114] Silica gel 60 (0.063 \times 0.200 mm, 70–230 mesh ASTM) (MERCK) or Celite[®] (FLUKA) and sea sand (calcined, washed with hydrochloric acid, RIEDEL-DE HAËN) were used as stationary phase. Column dimensions were chosen according to the amount of the crude products. The flow was regulated with a pressure valve with an overpressure of approximately 300-500 mbar.

5.1.5 Nuclear magnetic resonance (NMR) spectroscopy

Following devices were used for recording the NMR spectra:

¹H NMR: BRUKER 300 (300 MHz), BRUKER AVANCE 400 (400 MHz), BRUKER ASCEND 500 (500 MHz); ¹³C NMR: BRUKER 300 (75 MHz), AVANCE 400 (101 MHz), ASCEND 500 (126 MHz); ¹⁹F NMR: AVANCE 400 (377 MHz). The following solvents from EURISOTOP were used: chloroform-*d*₁, DMSO-*d*₆, methanol-*d*₄ and D₂O. Chemical shifts δ were expressed in parts per million (ppm) and referenced to chloroform-*d*₁ (¹H: δ =7.26 ppm, ¹³C: δ =77.16 ppm), DMSO-*d*₆ (¹H: δ =2.50 ppm, ¹³C: δ =39.52 ppm) and D₂O (¹H: δ =4.79 ppm), methanol-*d*₄ (¹H: δ =3.31 ppm, ¹³C: δ =49.00 ppm). The signal structure is named in the shot forms as follows: s=single t, d=doublet, t=triplet, q=quartet, quin=quintet, bs=broad singlet, m=multiplet, dd=double of doublet, dt=doublet of triplets. The spectra were analysed according to the first order. All coupling constants are absolute values and expressed in Hertz (Hz).

5.1.6 UV-Vis spectroscopy

The UV-Vis spectra were measured with the Lambda 750 from PERKINELMER at 20 °C, slit=2 nm. The volume was prepared with pipet4u[®] performance pipets 100-1000 μ L with an accuracy of 2%- 0.6%, a 10-100 μ L with an accuracy of 2%-0.8% as well as a 2-20 μ L with an accuracy of 2%- 0.8%.

ORIGIN OF COMPOUNDS, CHEMICALS AND DATA

For the measurement of synthesized PNA strands and purchased RNA strands a NanoDrop™ 1000 spectrophotometer from THERMO SCIENTIFIC was used to determine the concentration of aqueous solutions of the nucleic acids.

5.1.7 Solid phase synthesis

For solid phase peptide synthesis (SPPS) rink resin was used if not stated otherwise, following the Fmoc-protocoll. For coupling HBTU, DIPEA, 2,6-lutidine and the corresponding acid in *N*-Methyl-2-pyrrolidone were applied if not stated otherwise. After coupling free amines were capped with a solution of 450 µL acetic acid anhydride and 650 µL 2,6-lutidine in 10 mL DMF for 5 min. The Fmoc-protecting group was removed with a 20% solution of piperidine in DMF for 5 min. Cleaving of the full strand from the resin was done by 100% TFA and repeated two to four times to ensure full cleavage of the strands.

5.1.8 Lyophilization

Substances purified by HPLC were dried by lyophilization. Before freezing the solvents, the major amount of acetonitrile was evaporated under reduced pressure. The used device was a CHRIST LDC-1 ALPHA 2-4 system equipped with a vacuum pump.

5.1.9 Mass spectrometry (EI, FAB, MALDI)

Mass spectra were recorded on a FINNIGAN MAT 95 mass spectrometer using electron ionization mass spectrometry (EI-MS) or fast atom bombardment-mass spectrometry (FAB-MS) for small molecules. For FAB measurements *m*-nitrobenzyl alcohol (3-NBA) was used as the matrix. MALDI-TOF experiments were carried out for large (>2000 Da) molecules using a Shimadzu Biotech Axima Confidence 2.9.3.2011.0624 device.

5.1.10. Analytical balance

For determination of small amounts (< mg) a Satorius iso 9001 microbalance was used.

5.1.11. Preparativ work

Table 4 cooling mixtures

Solvent:	Method:
-0 °C	Ice / water
-10 °C	Ice / water / sodium chloride
-20 °C	Methanol / dry ice
-42 °C	Stirred mixture of ACN / dry ice
-78 °C	Stirred mixture of acetone or isopropanol / dry ice

Solvents were removed at preferably low temperatures (<50 °C) under reduced pressure with a rotary evaporator. Solvent mixtures were measured separately before mixing. If not stated otherwise, solutions of inorganic salts are aqueous, saturated solutions.

5.1.12. RNase free working conditios

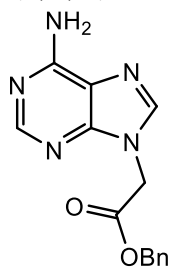
For the work with RNA every instrument or tube was at least heated to 80 °C overnight in an oven. Bi dest. water was treated with DEPC (1/200 Volume) and stirred for 2 h at 100 °C. Stirring was continued over night at room temperature. This water was used to set up an 4 M NaCl solution and a NaH₂CO₃/Na₂HCO₃ buffer solution with the pH value of 7. For preparation always 62.5 µL of the NaCl solution and 100 µL of the buffer solution was added to each sample. After adding the amount of PNA or PNA/RNA the mixture was filled up with RNase free water until the whole sample contained 1 mL of a liquid solution. The concentration of PNA and RNA was determined as stated in 5.1.6. All surfaces of the working place was cleaned with absolute ethanol. Nothing was touched beside with ethanol cleaned gloves.

5.2 Synthesis of literature known procedures

This chapter contains a complete list of all molecules which are already known in literature. The procedures were carried out by Johannes Karcher (k), Philipp Geng (g), Hülya Ucar (u), Stefano Secci (se), Juliana Pfeifer (p), Jens Werstein (w), students (s) of the organic advanced practical internship of the KIT in the course of their bachelor/master training or by myself (b). Every procedure was performed with my knowledge and under my supervision. Deviations or improvements of the literature procedures are stated in *italic*. These compounds were analysed by NMR-spectroscopy (^1H , ^{13}C) to prove their purity.

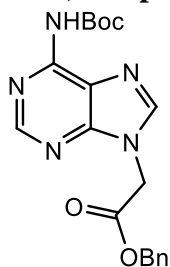
5.2.1 Synthesis of the modified nucleobases

Benzyl 2-(6-amino-9H-purin-9-yl)acetate (b, s, u)



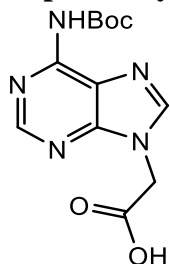
Adenine (5.00 g, 37.0 mmol, 1.00 equiv.) was suspended in DMF (90 mL). NaH (60% in mineral oil, 1.78 g, 44.4 mmol, 1.20 equiv.) was added in two portions in 15 min intervals. After 1 h, an additional 60 mL of DMF was added and the solution was allowed to stir for further 2 h. Subsequently, the solution was cooled in an ice-bath for 30 min. Next, benzyl 2-bromoacetate (6.50 mL, 40.7 mmol, 1.10 equiv.) was added dropwise and the mixture was stirred overnight while warming up to room temperature. DMF was removed under reduced pressure. Water (45 mL) was added to the residue and the mixture was stirred for 1 h. The precipitate was filtered off, washed with water (4x120 mL) and dried *in vacuo*. *The filtrate was diluted with another 200 mL of water and the precipitate was treated the same way.* If NMR analysis showed impurities, the crude product was recrystallized in ethanol (50 mL). The hot solvent was filtered off; the remaining solid was washed with cold ethanol (2x30 mL) and dried *in vacuo*. After cooling the mother liquor to 5 °C overnight, an additional batch of the product crystallized, which was collected by filtration, washed with cold ethanol (2 x 15 mL), and dried *in vacuo*. The title compound was obtained as a light brown solid (7.35 g, 70%).

The spectroscopic data is in agreement with literature.[60]

Benzyl 2-(6-((*tert*-butoxycarbonyl)amino)-9*H*-purin-9-yl)acetate (b, p, s, u)

To benzyl adenine-9-acetate (11.3 g, 39.8 mmol, 1.00 equiv.) in DMF (80 mL) was added carbonyldiimidazole (19.4 g, 120 mmol, 3.00 equiv.) and the mixture was slowly heated to 105 °C and stirred for 2 h. The temperature was reduced to 95 °C and *tert*-butanol (8.84 g, 120 mmol, 3.00 equiv.) was added. The heat source was removed and the solution was allowed to stir overnight while cooling to room temperature. Water (200 mL) was added and the reaction mixture was stirred vigorously for 1 h to obtain precipitates which were filtered off, washed with water (4 x 200 mL) and dried *in vacuo*. The crude product was purified by column chromatography (acetone/DCM, 10:90 to 20:80). The title compound was obtained as a white solid (4.55 g, 30%).

The spectroscopic data is in agreement with literature.[115]

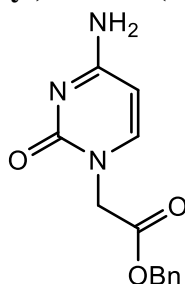
2-(6-((*tert*-Butoxycarbonyl)amino)-9*H*-purin-9-yl)acetic acid (b, s, u)

Benzyl 2-(6-((*tert*-butoxycarbonyl)amino)-9*H*-purin-9-yl)acetate (4.55 g, 11.7 mmol, 1.00 equiv.) and 5 wt-% Pd/C (600 mg) were placed in flask under argon atmosphere. EtOH (100 mL) was added and the mixture was stirred at room temperature and under atmospheric hydrogen pressure until total substrate consumption. Afterwards, the hydrogen was removed *in vacuo*. The reaction mixture was filtered through celite, rinsed with EtOH (3 x 150 mL) and the solvent was removed under reduced pressure. The title compound was obtained as a white solid (3.22 g 94%).

The spectroscopic data is in agreement with literature.[105]

SYNTHESIS OF LITERATURE KNOWN PROCEDURES

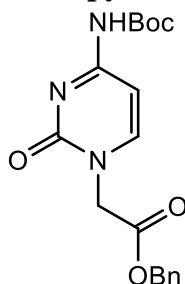
Benzyl 2-(4-amino-2-oxopyrimidin-1(2H)-yl)acetate (b, s)



To cytosine (5.00 g, 45.0 mmol, 1.00 equiv.) in 45 mL of DMF was added potassium *tert*-butoxide (5.80 g, 51.8 mmol, 1.15 equiv.) and the reaction mixture was heated to 100 °C for 2 h. Then, the reaction mixture was cooled to 0 °C, benzyl 2-bromoacetate (8.00 mL, 50.3 mmol, 1.12 equiv.) was added dropwise over a period of 20 min while maintaining the temperature of 0 °C. The mixture was allowed to warm up to room temperature while stirring for 12 h. The reaction mixture was quenched with acetic acid (3.10 mL, 54.0 mmol, 1.20 equiv.) and the solvents were removed under reduced pressure. The residue was suspended in 100 mL of water and stirred for 2 h. The precipitates were filtered off, washed with water (4 x 100 mL) and dried *in vacuo*. The title compound was obtained as a of-white solid (10.6 g, 92%).

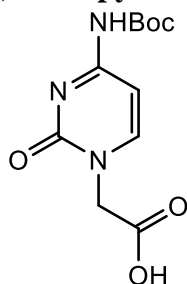
The spectroscopic data is in agreement with literature.[115]

Benzyl 2-(4-((*tert*-butoxycarbonyl)amino)-2-oxopyrimidin-1(2H)-yl)acetate (b, s)



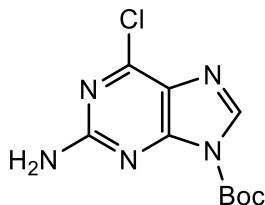
To a stirred solution of benzyl 2-(4-amino-2-oxopyrimidin-1(2H)-yl)acetate (7.50 g, 28.9 mmol, 1.00 equiv.) in DMF (90 mL) was added carbonyldiimidazole (7.50 g, 46.2 mmol, 1.60 equiv.) at 23 °C. After 2 h, *tert*-butanol (10.7 g, 144 mmol, 5.00 equiv.) was added and the mixture was heated to 80 °C. After, 2 h the heat source was removed and the mixture was stirred for 12 h at room temperature. The reaction mixture was quenched with 2.5 mL of MeOH and the solvents were removed under reduced pressure. The resulting oil was dissolved in 50 mL of EtOH and precipitated with 100 mL of water. The precipitate was filtered off, washed with water (3 x 100 mL) and dried *in vacuo*. The title compound was obtained as a white solid (4.79 g, 94%).

The spectroscopic data is in agreement with literature.[115]

2-(4-((*tert*-Butoxycarbonyl)amino)-2-oxopyrimidin-1(2*H*)-yl)acetic acid (b, s)

Benzyl 2-(4-((*tert*-butoxycarbonyl)amino)-2-oxopyrimidin-1(2*H*)-yl)acetate (4.79 g, 13.3 mmol, 1.00 equiv.) was suspended in MeCN (40 mL) and water (15 mL). A solution of LiOH (1.27 g, 53.2 mmol, 4.00 equiv.) in water (10 mL) was added at 23 °C. According to TLC, the substrate was consumed after 5-10 min. Subsequently, the solution was acidified with 1 M HCl to pH = 3 – 4, and stirred for 16 h. The precipitate was filtered off, washed with water (3 x 75 mL) and dried *in vacuo*. The title compound was obtained as a white solid (1.85 g, 52%).

The spectroscopic data is in agreement with literature.[115]

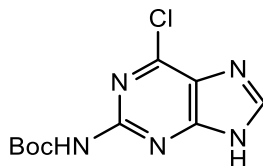
***tert*-Butyl 2-amino-6-chloro-9*H*-purine-9-carboxylate (b, g, p, se, s)**

A rapidly stirred solution of 2-amino-6-chloropurine (8.50 g, 50.0 mmol, 1.00 equiv.) and di-*tert*-butyl dicarbonate (11.0 g, 50.0 mmol, 1.00 equiv.) in anhydrous DMSO (50 mL) was briefly cooled in ice-water bath under an argon atmosphere. After 5 min, the ice-water bath was removed and 4-(dimethylamino)-pyridine (305 mg, 0.25 mmol, 0.05 equiv.) was added to the reaction mixture. The septum was immediately equipped with a venting needle to allow free evolution of the gaseous by-products. After stirring for 30 min at room temperature, TLC indicated full consumption of the starting material. The reaction mixture was diluted with water (200 mL) and extracted with EtOAc (4 x 50 mL). The combined organic phases were washed with water (4 x 60 mL), dried over Na₂SO₄ and the solvent was removed under reduced pressure. The title compound was obtained as a white solid (10.1 g, 75%).

The spectroscopic data is in agreement with literature.[116]

SYNTHESIS OF LITERATURE KNOWN PROCEDURES

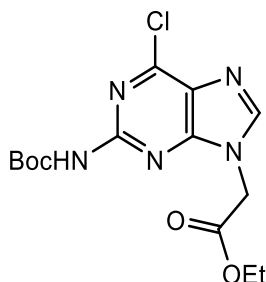
tert-Butyl (6-chloro-9*H*-purin-2-yl)carbamate (b, g, p, st, s)



To a stirred solution of *tert*-butyl 2-amino-6-chloro-9*H*-purine-9-carboxylate (8.10 g, 30.0 mmol, 1.00 equiv.) in anhydrous THF (125 mL) was carefully added NaH (2.70 g of the 60% dispersion in mineral oil; 67.0 mmol, 2.25 equiv.) in one portion under argon atmosphere. After 2 h, the Boc-transfer reaction was complete indicated with TLC. The reaction mixture was cooled to 0 °C and carefully quenched with brine. The solvent was removed under reduced pressure and the residue was washed with NaHCO₃-solution. The mixture was extracted with EtOAc and the combined organic phases were dried over Na₂SO₄ and concentrated under reduced pressure. If the crude product was impure, it was purified by column chromatography (DCM/MeOH/NH₄OH, 92:7:1). The title compound was obtained as a white powder (7.70 g, 95%).

The spectroscopic data is in agreement with literature.[116]

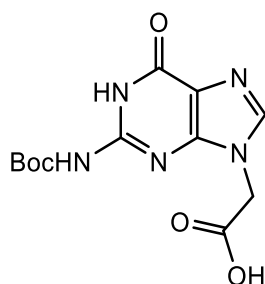
Ethyl 2-(2-((*tert*-butoxycarbonyl)amino)-6-chloro-9*H*-purin-9-yl)acetate (b, g, se, s)



To a solution of *tert*-butyl (6-chloro-9*H*-purin-2-yl)carbamate (7.55 g, 28.0 mmol, 1.00 equiv.) in anhydrous THF (150 mL) was added ethyl 2-hydroxyacetate (2.85 mL, 3.14 g 30.1 mmol, 1.10 equiv.) and triphenylphosphine (7.90 g, 30.1 mmol, 1.10 equiv.) under argon atmosphere. To the stirring solution, diisopropylazodicarboxylate (5.50 mL, 5.67 g 28.0 mmol, 1.00 equiv.) was added dropwise over 2 min. According to TLC, the reaction was complete after 15 min and the solvent was removed under reduced pressure. The residue was by column chromatography (CH₂/EtOAc, 1:2). The title compound was obtained as a white powder (8.26 g, 83%).

The spectroscopic data is in agreement with literature.[117]

2-(2-((*tert*-Butoxycarbonyl)amino)-6-oxo-1,6-dihydro-9H-purin-9-yl)acetic acid (b, g, se, s, u)

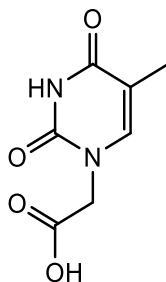


A solution of 3-hydroxypropionitrile (7.50 mL, 7.95 g, 110 mmol, 5.00 equiv.) in dry THF (150 mL) was cooled to $-78\text{ }^{\circ}\text{C}$ and sodium hydride (4.40 g of a 60% suspension in mineral oil, 110 mmol, 5.00 equiv.) was added under argon atmosphere. The reaction mixture was stirred at $-78\text{ }^{\circ}\text{C}$ for 30 min, then at $0\text{ }^{\circ}\text{C}$ for 2.5 h. Afterwards, ethyl 2-(2-((*tert*-butoxycarbonyl)amino)-6-chloro-9H-purin-9-yl)acetate (7.82 g 22.0 mmol, 1.00 equiv.) was added in one portion. The reaction was stirred for 16 h while warming up to room temperature. The solvent was removed under reduced pressure, the residue was suspended in water (100 mL) and the solution was acidified with KHSO_4 to $\text{pH} = 8$. The aqueous phase was washed with EtOAc ($2 \times 25\text{ mL}$) and acidified with KHSO_4 to $\text{pH} = 2$. Any precipitate was filtered off, washed with water ($3 \times 50\text{ mL}$) and dried *in vacuo*. The aqueous phase was extracted with EtOAc ($4 \times 150\text{ mL}$). The combined organic phases were dried over Na_2SO_4 and the solvent was removed under reduced pressure. The residue was triturated with a mixture of diethyl ether and *n*-hexane (1:1, 50 mL) and collected by filtration. The solids were combined. The title compound was obtained as a colorless powder (3.54 g, 52%).

The spectroscopic data is in agreement with literature.[118]

SYNTHESIS OF LITERATURE KNOWN PROCEDURES

2-(5-Methyl-2,4-dioxo-3,4-dihydropyrimidin-1(2H)-yl)acetic acid (b, s)

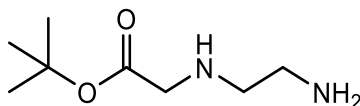


Thymine (7.56 g, 60.0 mmol, 1.00 equiv.) was dissolved in a solution of KOH (13.5 g, 240 mmol, 4.00 equiv.) in 40 mL of water. The solution was heated to 40 °C, and a solution of bromoacetic acid (12.5 g, 90.0 mmol, 1.50 equiv.) in 20 mL of water was added dropwise over 45 min. After the addition, the reaction mixture was stirred for another 30 min. The mixture was allowed to cool to room temperature and the solution was acidified with concentrated HCl to pH = 5.5. The solution was cooled to 5 °C for 2 h. Any precipitate was removed by filtration. The remaining solution was acidified with concentrated HCl to pH = 2, and cooled to -18 °C overnight. The resulting precipitate was isolated by filtration, washed with water and dried *in vacuo*. The title compound was obtained as a colorless solid (8.80 g, 80%).

The spectroscopic data is in agreement with literature.[119]

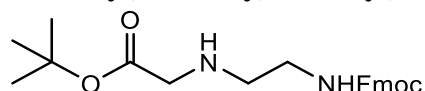
5.2.2 Synthesis of PNA and GPNA monomers

tert-Butyl (2-aminoethyl)glycinate (b, p, s, u)



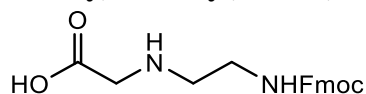
A solution of *tert*-butyl bromoacetate (10.0 mL, 13.1 g, 68.1 mmol, 1.00 equiv.) in DCM (260 mL) was added dropwise over 5 h to a vigorously stirred solution of ethanediamine (22.7 mL, 20.4 g, 341 mmol, 5.00 equiv.) in DCM (260 mL) at -5 °C. The reaction mixture was stirred at room temperature for 16 h. Subsequently, the mixture was washed with water (3 x 120 mL) and the aqueous phase was extracted with DCM (120 mL). The combined organic phases were dried over Na₂SO₄ and the solvent was removed under reduced pressure. The title compound was obtained as a pale-yellow solid (9.49 g, 80%). Some di-protected species are detectable in the NMR, but due to degradation reasons the product was used without further purification.

The spectroscopic data is in agreement with literature.[120]

***tert*-Butyl (2-(((9*H*-fluoren-9-yl)methoxy)carbonyl)amino)ethyl)glycinate (b, p, s, u)**

A solution of 9-fluorenylmethyl *N*-succinimidyl carbonate (17.5 g, 51.8 mmol, 0.95 equiv.) in DCM (200 mL) was added dropwise over 3 h to a stirred solution of *tert*-butyl (2-aminoethyl)glycinate (9.49 g, 54.5 mmol, 1.00 equiv.) and DIPEA (7.04 g, 9.49 mL, 54.5 mmol, 1.00 equiv.) in DCM (200 mL) and stirring was continued at room temperature for 16 h. The mixture was washed with 1 M HCl (5 x 75 mL) and brine (75 mL). A saturated NaHCO₃-solution was added to the organic phase until no gas evolution was observed. The organic phase was dried over Na₂SO₄ and the solvent was removed under reduced pressure. The title compound was obtained as a white amorphous solid (18.2 g, 80%).

The spectroscopic data is in agreement with literature.[120]

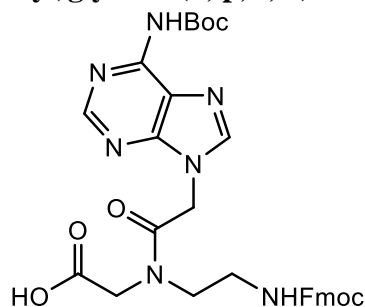
(2-(((9*H*-Fluoren-9-yl)methoxy)carbonyl)amino)ethyl)glycine (b, p, s, u)

Trifluoroacetic acid (100 mL, 149 g, 1.31 mol 30.0 equiv.) was added dropwise over a period of 90 min to a stirred solution of *tert*-butyl (2-(((9*H*-fluoren-9-yl)methoxy)carbonyl)amino)ethyl)glycinate (17.3 g, 43.6 mmol 1.00 equiv.) in DCM (100 mL) at -5 °C. After 20 min, the solution was allowed to warm to room temperature and stirring was continued for an additional 5 h. The reaction mixture was dried under reduced pressure and TFA was completely removed by co-evaporation with toluene. *The sticky brown residue was dissolved in DCM and added dropwise into vigorously stirring diethylether (800 ml). The precipitate was filtered off and dried in vacuo. The liquid phase was concentrated under reduced pressure and the procedure was repeated, affording more of the precipitate.* The title compound was obtained as a white solid (8.90 g, 60%).

The spectroscopic data is in agreement with literature.[120]

SYNTHESIS OF LITERATURE KNOWN PROCEDURES

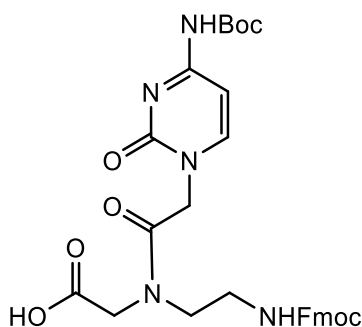
***N*-2-(((9*H*-Fluoren-9-yl)methoxy)carbonyl)amino)ethyl)-*N*-(2-(4-((*tert*-butoxycarbonyl)amino)-9*H*-purin-9-yl)acetyl)glycine (b, p, s, u)**



TSTU (1.46 g, 4.84 mmol 1.10 equiv.) and DIPEA (1.00 mL, 742 mg, 5.73 mmol, 1.30 equiv.) were added to a solution of 2-(6-((*tert*-butoxycarbonyl)amino)-9*H*-purin-9-yl)acetic acid (1.29 g, 4.41 mmol, 1.00 equiv.) in 20 mL dry DMF. After 20 min of stirring at room temperature (2-(((9*H*-fluoren-9-yl)methoxy)carbonyl)amino)ethyl)glycine (1.50 g, 4.42 mmol, 1.00 equiv.) was added followed by DIPEA (1.00 mL, 5.73 mmol, 1.30 equiv.) and the reaction mixture was stirred for another 1 h. The mixture was diluted with water and acidified with 1 M HCl until no more crude product precipitated. Stirring was continued for 15 min. The precipitate was filtered off, washed with water (4 × 15 mL) and dried *in vacuo*. The aqueous phase was extracted with DCM (3 × 50 mL), the combined organic phases were washed with brine, dried over Na₂SO₄ and the solvent was removed under reduced pressure. The combined solids were purified by column chromatography, (MeOH/Acetone, 0:1 to 1:3). The title compound was obtained as a yellow-w hite powder (1.02 g, 38%).

The spectroscopic data is in agreement with literature.[115]

***N*-2-(((9*H*-Fluoren-9-yl)methoxy)carbonyl)amino)ethyl)-*N*-(2-(4-((*tert*-butoxycarbonyl)amino)-2-oxopyrimidin-1(2*H*)-yl)acetyl)glycine (b, s, u)**

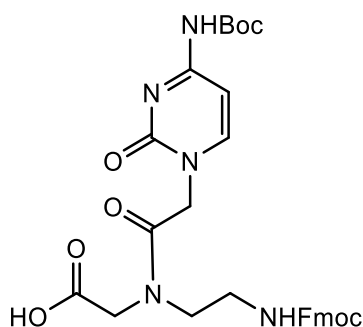


TSTU (1.46 g, 4.84 mmol 1.10 equiv.) and DIPEA (1.00 mL, 742 mg, 5.73 mmol 1.30 equiv.) were added to a solution of 2-(4-((*tert*-butoxycarbonyl)amino)-2-oxopyrimidin-1(2*H*)-yl)acetic acid (1.19 g, 4.41 mmol, 1.00 equiv.) in 20 mL dry DMF. After 20 min stirring at room temperature, (2-(((9*H*-fluoren-9-yl)methoxy)carbonyl)amino)ethylglycine (1.50 g, 4.42 mmol, 1.00 equiv.) was added followed by DIPEA (1.00 mL, 5.73 mmol, 1.30 equiv.) and the reaction mixture was stirred for another 1 h at room temperature. The mixture was diluted with water and acidified with 1 M HCl until no more crude product precipitate. Stirring was continued for 15 min. The precipitate was filtered off, washed with water (4 × 15 mL) and dried under high vacuum. The aqueous phase was extracted with DCM (3 × 50 mL), the combined organic layers were washed with brine, dried over Na₂SO₄ and the solvent was evaporated under reduced pressure. The combined solids were purified by column chromatography (MeOH/Acetone, 0:1 to 1:3). The title compound was obtained as a yellow-white powder (1.14 g, 44%).

The spectroscopic data is in agreement with literature.[115]

SYNTHESIS OF LITERATURE KNOWN PROCEDURES

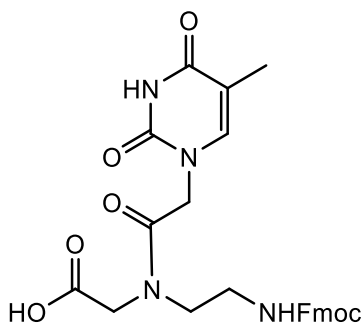
N-2-(((9H-Fluoren-9-yl)methoxy)carbonyl)amino)ethyl)-*N*-(2-(2-((*tert*-butoxycarbonyl)amino)-6-oxo-5,6-dihydro-9H-purin-9-yl)acetyl)glycine (b, s, u)



TSTU (1.46 g, 4.84 mmol 1.10 equiv.) and DIPEA (1.00 mL, 742 mg, 5.73 mmol 1.30 equiv.) were added to a solution of 2-(2-((*tert*-butoxycarbonyl)amino)-6-oxo-1,6-dihydro-9H-purin-9-yl)acetic acid (1.36 g, 4.41 mmol, 1.00 equiv.) in 20 mL dry DMF. After 20 min of stirring at room temperature, (2-(((9H-fluoren-9-yl)methoxy)carbonyl)amino)ethyl)glycine (1.50 g, 4.42 mmol, 1.00 equiv.) was added followed by DIPEA (1.00 mL, 5.73 mmol, 1.30 equiv.) and the reaction mixture was stirred for another 1 h. The mixture was diluted with water and acidified with 1 M HCl until no more crude product precipitated. Stirring was continued for 15 min. The precipitate was filtered off, washed with water (4 × 15 mL) and dried *in vacuo*. The aqueous phase was extracted with DCM (3 × 50 mL), the combined organic phases were washed with brine, dried over Na₂SO₄ and the solvent was removed under reduced pressure. The combined solids were purified by column chromatography (MeOH/Acetone, 0:1 to 1:3). The title compound was obtained as a yellow-white powder (1.21 g, 43%).

The spectroscopic data is in agreement with literature.[115]

***N*-(2-(((9*H*-Fluoren-9-yl)methoxy)carbonyl)amino)ethyl)-*N*-(2-(5-methyl-2,4-dioxo-3,4-dihydropyrimidin-1(2*H*)-yl)acetyl)glycine (b, s, u)**

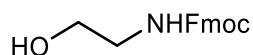


TSTU (1.46 g, 4.84 mmol 1.10 equiv.) and DIPEA (1.00 mL, 742 mg, 5.73 mmol 1.30 equiv.) were added to a solution of 2-(5-methyl-2,4-dioxo-3,4-dihydropyrimidin-1(2*H*)-yl)acetic acid (813 mg, 4.41 mmol, 1.00 equiv.) in 20 mL dry DMF. After 20 min stirring at room temperature, (2-(((9*H*-fluoren-9-yl)methoxy)carbonyl)amino)ethylglycine (1.50 g, 4.42 mmol, 1.00 equiv.) was added followed by DIPEA (1.00 mL, 5.73 mmol, 1.30 equiv.) and the reaction mixture was stirred for another 1 h. The mixture was diluted with water and acidified with 1 M HCl until no more crude product precipitated. Stirring was continued for 15 min. The precipitate was filtered off, washed with water (4 × 15 mL) and dried *in vacuo*. The aqueous phase was extracted with DCM (3 × 50 mL), the combined organic phases were washed with brine, dried over Na₂SO₄ and the solvent was removed under reduced pressure. The combined solids were purified by column chromatography (MeOH/Acetone, 0:1 to 1:3). The title compound was obtained as a yellow-white powder (963 mg, 44%).

The spectroscopic data is in agreement with literature.[115]

SYNTHESIS OF LITERATURE KNOWN PROCEDURES

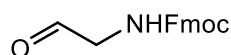
(9*H*-Fluoren-9-yl)methyl (2-hydroxyethyl)carbamate (b, g, p, s)



A solution of 9-fluorenylmethyl *N*-succinimidyl carbonate (16.1 g, 47.5 mmol, 1.00 equiv.) in DCM (200 mL) was added dropwise over 3 h to a stirred solution of 2-aminoethan-1-ol (3.02 mL, 3.05 g, 50.0 mmol 1.05 equiv.) and DIPEA (8.50 mL, 6.31 g, 50.0 mmol, 1.05 equiv.) in DCM (200 mL) and the solution was stirred at room temperature for 16 h. The reaction mixture was washed with 1 M HCl (5 x 75 mL) and brine (75 mL), dried over Na₂SO₄ and the solvent was removed under reduced pressure. The title compound was obtained as a white solid (12.8 g, 95%).

The spectroscopic data is in agreement with literature.[121]

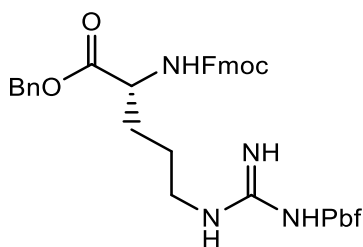
(9*H*-Fluoren-9-yl)methyl (2-oxoethyl)carbamate (b, g, p, s)



A solution of DCM (250 mL) and oxalyl chloride (2.57 mL, 3.83 g, 30.0 mmol, 1.50 equiv.) was placed in a 1 L 3-neck round-bottom flask equipped with a thermometer and a pressure-equalizing dropping funnel containing DMSO (4.26 mL, 4.69 g, 60.0 mmol, 3.00 equiv.) dissolved in DCM (40 mL). The mixture was cooled to -78 °C and the DMSO was added to the stirring oxalyl chloride solution at -50 to -60 °C. The reaction mixture was stirred for 2 min and a solution of (9*H*-fluoren-9-yl)methyl (2-hydroxyethyl)carbamate (5.67 g, 20.0 mmol, 1.00 equiv) in DCM(300 mL) was added over 10 min. Stirring was continued for an additional 15 min. Triethylamine (11.1 mL, 8.06 g, 80.0 mmol, 4.00 equiv.) was added and stirring was continued for another 15 min. The reaction mixture was allowed to warm to room temperature, water (100 mL) was added and the aqueous phase was extracted with DCM (100 mL). The combined organic phases were washed with saturated brine (100 mL) and dried over Na₂SO₄. The crude product was purified by column chromatography (EtOAc/CH₂Cl₂, 2:1). The title compound was obtained as a light yellow solid (4.50 g, 80%).

The spectroscopic data is in agreement with literature.[122]

Benzyl *N*²-(((9*H*-fluoren-9-yl)methoxy)carbonyl)-*N*^ω-((2,2,4,6,7-pentamethyl-2,3-dihydrobenzofuran-5-yl)sulfonyl)-*D*-argininate (b, g, u)

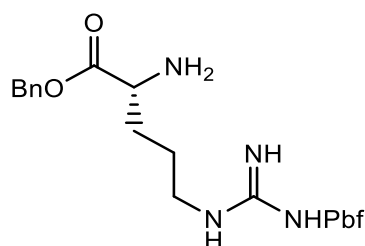


*N*²-(((9*H*-fluoren-9-yl)methoxy)carbonyl)-*N*^ω-((2,2,4,6,7-pentamethyl-2,3-dihydrobenzofuran-5-yl)sulfonyl)-*D*-arginine (10.0 g, 15.4 mmol, 1.00 equiv.) and HBTU (6.45 g, 17.0 mmol, 1.10 equiv.) were placed in a 250 mL round bottom flask under argon atmosphere. DMF (40 mL) was added and the solution was cooled to 0 °C before adding DIPEA (2.80 mL, 2.08 g, 1.10 equiv.). The reaction mixture was stirred for 15 min and benzyl alcohol (2.40 mL, 23.0 mmol, 1.50 equiv.) and DIPEA (3.80 mL, 2.82 g, 23.0 mmol, 1.50 equiv.) were added. The solution was stirred for 16 h while warming up to room temperature. The solvents were removed under reduced pressure and the crude product was purified by column chromatography (EtOAc/CH₂Cl₂, 3:7 to 1:0). The title compound was obtained as a white solid (10.8 g, 95%).

The spectroscopic data is in agreement with literature.[123]

SYNTHESIS OF LITERATURE KNOWN PROCEDURES

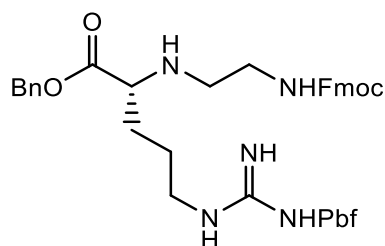
Benzyl N^{ω} -((2,2,4,6,7-pentamethyl-2,3-dihydrobenzofuran-5-yl)sulfonyl)- D -argininate (**b, g, u**)



To a stirring solution of benzyl N^2 -(((9H-fluoren-9-yl)methoxy)carbonyl)- N^{ω} -((2,2,4,6,7-pentamethyl-2,3-dihydrobenzofuran-5-yl)sulfonyl)- D -argininate (10.7 g, 14.5 mmol, 1.00 equiv.) in 40 mL DMF was added 10 mL piperidine (20% v/v). The reaction mixture was stirred for 1 h. Subsequently, the solvent was removed under reduced pressure. The crude product was purified by column chromatography (EtOAc/CH₂Cl₂, 1:1, then DCM/MeOH, 19:1). The title compound was obtained as a yellow foam (5.67 g, 76%).

The spectroscopic data is in agreement with literature.[124]

Benzyl N^2 -(2-(((9H-fluoren-9-yl)methoxy)carbonyl)amino)ethyl)- N^{ω} -((2,2,4,6,7-pentamethyl-2,3-dihydrobenzofuran-5-yl)sulfonyl)- D -argininate (**b, g, u**)



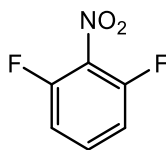
Benzyl N^{ω} -((2,2,4,6,7-pentamethyl-2,3-dihydrobenzofuran-5-yl)sulfonyl)- D -argininate (5.55 g, 10.7 mmol, 1.00 equiv.) was dissolved in dry MeOH (40 mL). To the reaction mixture 1 g Na₂SO₄ was added at 0 °C. (9H-Fluoren-9-yl)methyl (2-oxoethyl)carbamate (3.61 g, 12.8 mmol, 1.20 equiv.) was added and stirring was continued for 1.5 h. Sodium cyanoborohydride (804 mg, 12.8 mmol, 1.20 equiv.) was added followed by glacial acetic acid (732 μ L, 12.8 mmol, 1.20 equiv.). The reaction mixture was allowed to warm up to room temperature and stirring was continued for 6 h. The mixture was filtered, the solvents were evaporated and after purification by column chromatography (EtOAc/CH₂Cl₂, 1:1 to 1:0). The title compound was obtained as a white

solid. According to HPLC separation 2.47 g (3.16 mmol, 29%) of the desired benzyl ester and 820 mg (1.16 mmol, 11%) of the methyl ester were isolated.

The spectroscopic data is in agreement with literature.[124]

5.2.3 Synthesis of modified Azobenzenes

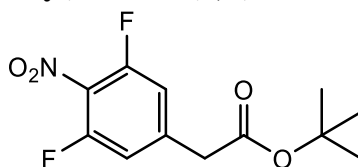
1,3-difluoro-2-nitrobenzene (b, s)



A solution of 2,6-difluoroaniline (10.8 mL, 12.9 g, 100 mmol, 1.00 equiv.) in glacial acetic acid (50 mL) was added slowly to a stirred suspension of sodium perborate tetrahydrate (76.9 g, 500 mmol, 5.00 equiv.) in glacial acetic acid (250 mL) at 80 °C. After 1 h, the cooled reaction mixture was poured on water (200 mL) and extracted with diethyl ether (4 × 150 mL). The combined organic phases were washed with a Na₂CO₃-solution (4 × 50 mL), dried over Na₂SO₄ and concentrated under reduced pressure. The residue was purified by column chromatography (CH/THF, 9:1) and the product was washed with *n*-hexane and dried *in vacuo*. The title compound was obtained as light yellow solid (9.04 g, 57%).

The spectroscopic data is in agreement with literature.[125]

tert-Butyl 2-(3,5-difluoro-4-nitrophenyl)acetate (b, s)



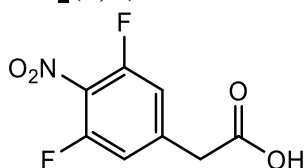
A solution of 1,3-difluoro-2-nitrobenzene (9.04 g, 56.6 mmol, 1.00 equiv.) and *tert*-butyl chloroacetate (14.5 g, 96.2 mmol, 1.70 equiv.) in anhydrous DMF (100 mL) was added dropwise at -42 °C over 1 h to a suspension of potassium *tert*-butoxide (22.2 g, 198 mmol, 3.50 equiv.) in anhydrous DMF (100 mL) under argon atmosphere. The reaction mixture was stirred at -42 °C for 1.5 h, then quenched with 2 M HCl (80 mL), warmed up to room temperature and extracted with cyclohexane (4 × 200 mL). The combined organic phases were washed with water (3 × 200 mL), brine (200 mL), dried over Na₂SO₄ and the solvent was removed under reduced pressure.

SYNTHESIS OF LITERATURE KNOWN PROCEDURES

The residue was purified by column chromatography (EtOAc/CH₂Cl₂, 1:9). The title compound was obtained as a yellow oil (14.0 g, 90%).

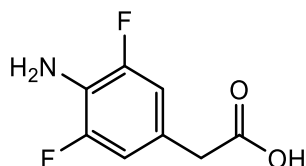
The spectroscopic data is in agreement with literature.[126]

2-(3,5-Difluoro-4-nitrophenyl)acetic acid (b, s)



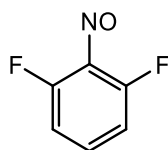
Trifluoroacetic acid (30 mL) was added dropwise over 90 min at 0 °C to a solution of *tert*-butyl 2-(3,5-difluoro-4-nitrophenyl)acetate (11.2 g, 41.0 mmol, 1.00 equiv.) in DCM (60 mL). Upon completion of the addition, the reaction mixture was allowed to warm to room temperature and stirred for 3 h. Then toluene (50 mL) was added to the reaction mixture and the solvent was removed under reduced pressure to leave a sticky brown solid. Purification by column chromatography (MeOH/DCM, 1:19) and recrystallization with a mixture of toluene and cyclohexane (1:1, 55 mL). The title compound was obtained as a yellow solid (2.33 g, 26%).

The spectroscopic data is in agreement with literature.[126]

2-(4-Amino-3,5-difluorophenyl)acetic acid (b, s)

2-(3,5-Difluoro-4-nitrophenyl)acetic acid (2.30 g 10.6 mmol, 1.00 equiv.) and 5% Pd/C catalyst (400 mg) were placed in a flask under argon atmosphere. The argon was removed *in vacuo* and hydrogen was introduced into the flask. The suspension stirred vigorously for 2 h at room temperature. After the exchange of hydrogen with argon, the crude product was filtered over Celite and washed with EtOH (3 × 50 mL), the solvent was removed under reduced pressure and the residue was dried *in vacuo*. The title compound was obtained as a light yellow solid (1.92 g, 98%).

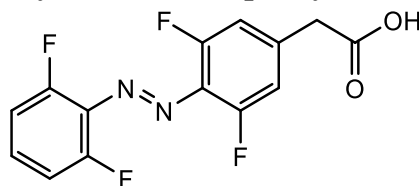
The spectroscopic data is in agreement with literature.[126]

1,3-Difluoro-2-nitrosobenzene (b, s)

Oxone® (7.19 g, 23.4 mmol, 2.00 equiv.) dissolved in water (140 mL) and was added to a solution of 2,6-difluoroaniline (1.51 g, 11.7 mmol, 1.00 equiv.) in DCM (50 mL). The solution was stirred at room temperature for 4 h. Subsequently, the phases were separated and the organic phase was washed with water (3 × 100 mL), dried over Na₂SO₄ and the solvent was removed under reduced pressure. The title compound was obtained as a brown solid (1.55 g 93%). The crude product was instantly used for the next reaction.

SYNTHESIS OF LITERATURE KNOWN PROCEDURES

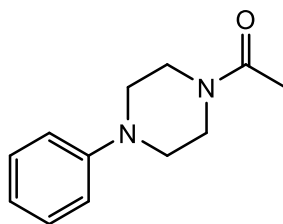
(E)-2-(4-((2,6-Difluorophenyl)diazenyl)-3,5-difluorophenyl)acetic acid (b, s)



The crude 1,3-difluoro-2-nitrosobenzene (1.55 g, 10.8 mmol, 1.04 equiv.) was suspended in a mixture of glacial acetic acid, toluene and TFA (6:6:1, 79 mL) and 2-(4-amino-3,5-difluorophenyl)acetic acid (1.92 g, 10.4 mmol, 1.00 equiv.) was added. The resulting mixture was stirred for 3 d in the dark at room temperature. The solution was diluted with water, and extracted with EtOAc. The organic phase was dried over Na₂SO₄ and the solvent was removed under reduced pressure. Residual nitrosobenzene was removed by co-evaporation with toluene (2 × 50 mL). The resulting mixture was purified by column chromatography (MeOH/DCM, 1:19). The title compound was obtained as an orange-red solid (1.45 g, 45%).

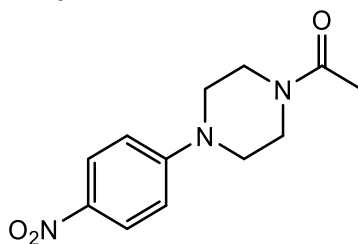
The spectroscopic data is in agreement with literature.[126]

1-(4-Phenylpiperazin-1-yl)ethan-1-one (b)



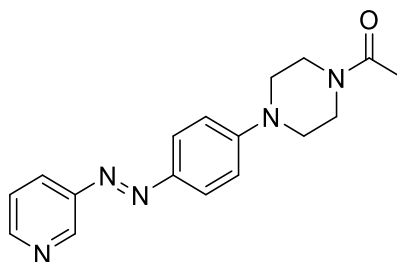
1-Phenylpiperazine (2.00 g, 12.3 mmol, 1.00 equiv.) was stirred in acetic anhydride (10 mL) for 1 h at 0 °C and another 3 h at room temperature. The reaction mixture was quenched by addition of water (5 mL). The solvent was removed by lyophilisation. The title compound was obtained as a light pink solid (2.52 g, quant.).

The spectroscopic data is in agreement with literature.[126]

1-(4-(4-Nitrophenyl)piperazin-1-yl)ethan-1-one (b)

1-(4-Nitrophenyl)piperazine (2.00 g, 9.66 mmol, 1.00 equiv). was stirred in acid anhydride (10 mL) for 1 h at 0 °C and another 3 h at room temperature. The reaction mixture was quenched by addition of water (5 mL). The solvent was removed by lyophilisation. The title compound was obtained as a yellow solid (2.40 g, quant.).

The spectroscopic data is in agreement with literature.[127]

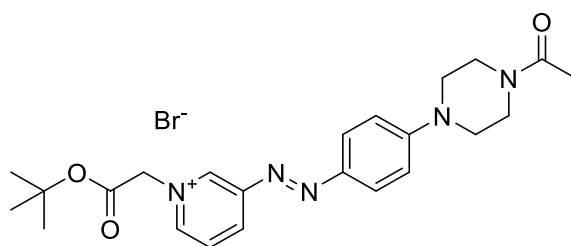
(E)-1-(4-(4-(Pyridin-3-yl)diazenyl)phenyl)piperazin-1-yl)ethan-1-one (b)

A solution of sodium nitrite (244 mg, 3.53 mmol, 1.20 equiv.) in water (10 mL) and MeOH (4 mL) was added to a solution of 1-(4-phenylpiperazin-1-yl)ethan-1-one (600 mg, 2.94 mmol, 1.00 equiv.) in MeOH (2 mL). Subsequently, the mixture was added dropwise to a solution of 3-aminopyridine (332 mg, 3.53 mmol, 1.20 equiv.) in concentrated HCl (1.7 mL) and water (10 mL) at 0 °C. Stirring was continued for 2 h. After neutralisation with NaHCO₃-solution, the aqueous phase was extracted with EtOAc (3 × 10 mL). The organic phase was dried over Na₂SO₄ and the solvent was removed under reduced pressure. The crude product was purified by column chromatography (MeOH/EtOAc, 1:9). The title compound was obtained as an orange solid (546 mg, 60%).

The spectroscopic data is in agreement with literature.[126]

SYNTHESIS OF LITERATURE KNOWN PROCEDURES

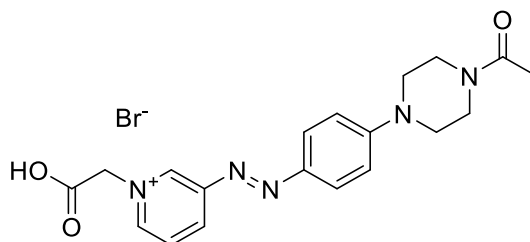
(E)-3-((4-(4-Acetylpiperazin-1-yl)phenyl)diazenyl)-1-(2-(tert-butoxy)-2-oxoethyl)pyridin-1-ium bromide (b)



(E)-1-(4-(4-(Pyridin-3-yl)diazenyl)phenyl)piperazin-1-ylethan-1-one (450 mg, 1.46 mmol, 1.00 equiv.) was dissolved in DMF (15 mL). *tert*-Butyl-bromoacetate (567 mg, 2.92 mmol, 2.00 equiv.) was added and the mixture was stirred at room temperature for 16 h. The solvent was removed under reduced pressure and the residue was dissolved in a minimum amount of MeOH and poured into the ten-fold volume of diethyl ether. The precipitating crystals were collected by filtration and dried *in vacuo*. The title compound was obtained as an orange-red solid (515 mg, 70%).

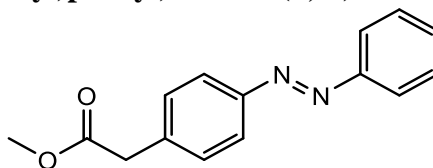
The spectroscopic data is in agreement with literature.[126]

(E)-3-((4-(4-Acetylpiperazin-1-yl)phenyl)diazenyl)-1-(carboxymethyl)pyridin-1-ium bromide (b)



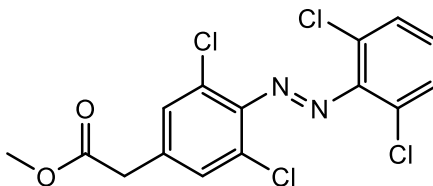
To a solution of (E)-3-((4-(4-acetylpiperazin-1-yl)phenyl)diazenyl)-1-(2-(*tert*-butoxy)-2-oxoethyl)pyridin-1-ium bromide (300 mg, 0.595 mmol, 1.00 equiv.) in DCM (10 mL) was added TFA (10 mL) dropwise over a period of 10 min. After 3 h, toluene (20 mL) was added and the solvent was removed under reduced pressure. The remaining solid was dissolved in a minimum amount of MeOH and poured into the ten-fold volume of diethyl ether. The precipitating crystals were collected by filtration and the product was dried *in vacuo*. The title compound was obtained as a red solid (240 mg, 90%).

The spectroscopic data is in agreement with literature.[126]

Methyl-(*E*)-2-(4-(phenyldiazenyl)phenyl)acetate (b, k)

Methyl-2-(4-aminophenyl)acetate (5,00 g, 30.3 mmol, 1.00 equiv.) and nitrosobenzene (4.21 g, 39.3 mmol, 1.30 equiv.) were dissolved in glacial acetic acid (50 mL) and the mixture was stirred for 3 d in an aluminium foil wrapped round bottom flask. The crude mixture was filtered through celite and rinsed with DCM. The solvents were removed under reduced pressure and the crude was purified by column chromatography (DCM). The title compound was obtained as an orange solid (7.26 g, 94%).

The spectroscopic data is in agreement with literature.[126]

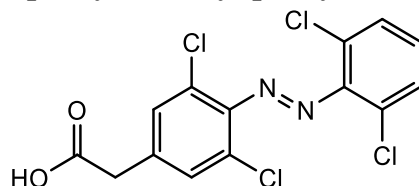
Methyl-(*E*)-2-(3,5-dichloro-4-((2,6-dichlorophenyl)diazenyl)phenyl)acetate (b, k)

Methyl-(*E*)-2-(4-(phenyldiazenyl)phenyl)acetate (3.00 g, 11.8 mmol, 1.00 equiv.), *N*-chlorosuccinimide (7.87 g, 59.0 mmol, 5.00 equiv.) and palladium(II) acetate (132 mg, 0.590 mmol, 0.05 equiv.) were placed in a 50 mL crimp vial under argon atmosphere. Degassed glacial acetic acid (40 mL) was added and the reaction mixture was stirred overnight at 140 °C. The mixture was cooled down the room temperature, filtered over a small silica pad (4 cm high, 5 cm diameter) and rinsed with DCM. The solvents were removed under reduced pressure and the residue was purified by column chromatography (DCM/CH₂Cl₂, 2:3). The title compound was obtained as a red solid (483 mg, 10%).

The spectroscopic data is in agreement with literature.[126]

SYNTHESIS OF LITERATURE KNOWN PROCEDURES

(*E*)-2-(3,5-Dichloro-4-((2,6-dichlorophenyl)diazenyl)phenyl)acetic acid (b)

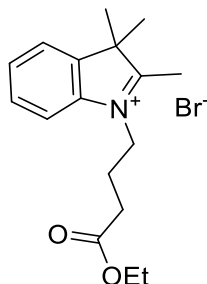


To a solution of methyl-(*E*)-2-(3,5-dichloro-4-((2,6-dichlorophenyl)diazenyl)phenyl)acetate (650 mg, 1.66 mmol, 1.00 equiv.) in acetonitrile (8 mL) was added lithium hydroxide (159 mg, 6.63 mmol, 4.00 equiv.) in water (2 mL). After 2 h, the solvent was removed under reduced pressure and the crude product was purified in two portions *via* preparative HPLC (water+0.1% TFA/Acetonitrile+0.1% TFA 60:40 to 0:100 in 35 min). The solvent was removed by lyophilisation. The title compound was obtained as a red solid (588 mg, 94%).

The spectroscopic data is in agreement with literature.[126]

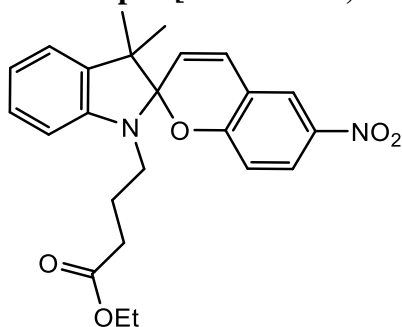
5.2.4 Synthesis of Nitro-Spyropranes

1-(4-Ethoxy-4-oxobutyl)-2,3,3-trimethyl-3*H*-indol-1-ium bromide (se, w)



2,3,3-Trimethyl-3*H*- indole (2.02 g, 12.6 mmol, 1.00 equiv.) and ethyl-4-bromobutanoate (5.42 mL, 7.37 g, 37.8 mmol, 3.00 equiv.) were dissolved in dry acetonitrile (30 mL) and stirred for 48 h at 82 °C. Subsequently, the reaction mixture was cooled to room temperature and the solvent was removed under reduced pressure. The residue was dissolved in MeOH and precipitated the ten-fold volume of diethyl ether. The title compound was obtained as a light pink solid (2.67 g, 60%).

The spectroscopic data is in agreement with literature.[23]

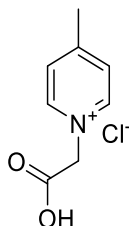
Ethyl 4-(3',3'-dimethyl-6-nitrospiro[chromene-2,2'-indolin]-1'-yl)butanoate (se, w)

To a solution of 2-hydroxy-5-nitrobenzaldehyde (438 mg, 2.62 mmol, 1.00 equiv.) in dry EtOH (20 mL) a solution of 1-(4-ethoxy-4-oxobutyl)-2,3,3-trimethyl-3*H*-indol-1-ium bromide (927 mg, 2.62 mmol, 1.00 equiv.) in EtOH (8 mL) was added slowly over a period of 1 h. The reaction mixture was heated to 80 °C and stirring was continued for 24 h. The solvent was evaporated under reduced pressure and the residue was purified by recrystallization in acetonitrile. After filtration and drying in *vacuo*. The title compound was obtained as a yellow-brown solid (343 mg, 31%).

The spectroscopic data is in agreement with literature.[23]

5.2.5 Synthesis of cyano-dyes

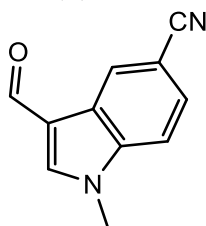
1-(Carboxymethyl)-4-methylpyridin-1-ium chloride (b)



4-Methylpyridine (1.00 mL, 957 mg, 10.0 mmol, 1.00 equiv.) and chloro acetic acid (1.04 g, 11.0 mmol, 1.10 equiv.) were placed in a flask and the mixture was stirred for 16 h at 100 °C. After cooling to room temperature, the mixture was poured into methanol (10 mL) and precipitated in the ten-fold amount of a mixture of diethyl ether and cyclohexane (1:1). The solid was filtered off, washed with diethyl ether (3 × 10 mL) and dried *in vacuo*. The title product was obtained as white solid (1.28 g, 68%).

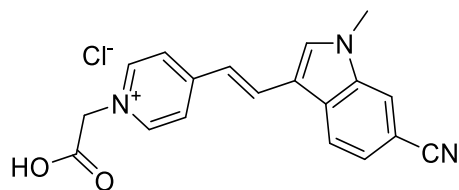
The spectroscopic data is in agreement with literature.[128]

3-Formyl-1-methyl-1H-indole-5-carbonitrile (b)



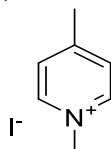
3-Formyl-1H-indol-5-carbonitrile (511 mg, 3.00 mmol, 1.00 equiv.) and potassium carbonate (456 mg, 3.30 mmol, 1.10 equiv.) were suspended in DMF (3 mL). Dimethyl carbonate (1.01 mL, 12.0 mL, 4.00 equiv.) was added and the suspension was stirred for 19 h at 130 °C. After cooling to room temperature, the mixture was poured onto ice-water (50 mL). The aqueous phase was extracted with EtOAc (3 × 50 mL). The combined organic phases were washed with water and dried over Na₂SO₄. The solvents were removed under reduced pressure. The title compound was obtained as an off white solid (503 mg, 91%).

The spectroscopic data is in agreement with literature.[128]

(E)-1-(Carboxymethyl)-4-(2-(6-cyano-1-methyl-1H-indol-3-yl)vinyl)pyridin-1-ium chloride (b)

1-(Carboxymethyl)-4-methylpyridin-1-ium chloride (375 mg, 2.00 mmol, 1.00 equiv.) and 3-formyl-1-methyl-1*H*-indole-5-carbonitrile (368 mg, 2.00 mmol, 1.00 equiv.) were dissolved in chloroform (15 mL). Piperidine (593 μ L, 511 mg, 6.00 mmol, 3.00 equiv.) was added and the mixture was stirred for 16 h at room temperature. The solvent was removed under reduced pressure and the residue was dissolved in acetonitrile (4 mL) and water (1 mL) and purified *via* HPLC (water+0.1% TFA/acetonitrile+0.1% TFA 95:5 to 5:95, 45 min). The title compound was obtained as an orange solid (489 mg, 69%).

The spectroscopic data is in agreement with literature.[128]

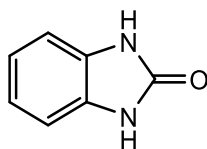
1,4-Dimethylpyridin-1-ium iodide (b)

4-Methylpyridine (1.00 mL, 10.0 mmol, 1.00 equiv.) was dissolved in DMF (5 mL) and methyl iodide (1.87 mL, 4.26 g, 30.0 mmol, 3.00 equiv.) was added dropwise. The mixture was stirred for 16 h at 50 $^{\circ}$ C. After cooling to room temperature, the crude product was precipitated in the five-fold volume of diethyl ether. The solid was filtered off, washed with diethyl ether (3 \times 10 mL) and dried *in vacuo*. The title compound was obtained as a brownish solid (2.18 g, 93%).

The spectroscopic data is in agreement with literature.[128]

5.2.6 Synthesis of Ribonucleic cleaver

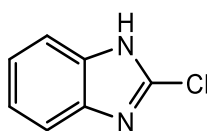
1,3-Dihydro-2H-benzo[d]imidazol-2-one (b)



Benzene-1,2-diamine (1.70 g, 15.7 mmol, 1.00 equiv.) and urea (2.83 g, 47.1 mmol, 3.00 equiv.) were dissolved in DMF (10 mL) and stirred for 4 h at 120 °C. The solvent was removed under reduced pressure. The crude product was precipitated in water (200 mL), filtered off, washed with water (3 × 50 mL) and dried *in vacuo*. The title compound was obtained as an off white solid (1.92 g, 92%).

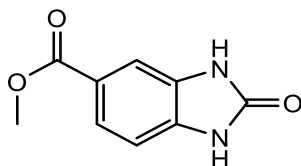
The spectroscopic data is in agreement with literature.[112]

2-Methyl-1H-benzo[d]imidazole (b)



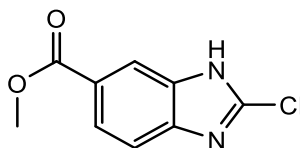
A solution of 1,3-dihydro-2H-benzo[d]imidazol-2-one (980 mg, 7.31 mmol, 1.00 equiv.) in POCl₃ (10 mL) was stirred for 8 h at 100 °C. The solvent was removed under reduced pressure. The residue was dissolved in water (10 mL) and the solution was neutralized with NaHCO₃ solution and extracted with DCM. The organic phase was dried over Na₂SO₄ and the solvent was removed under reduced pressure. The title compound was obtained as light brown solid (730 mg, 65%).

The spectroscopic data is in agreement with literature.[112]

Methyl 2-oxo-2,3-dihydro-1H-benzo[d]imidazole-5-carboxylate (b)

A solution of methyl 3,4-diaminobenzoate (700 mg, 4.21 mmol, 1.00 equiv.) and urea (759 mg, 12.6 mmol, 3.00 equiv.) in DMF (5 mL) was stirred for 4 h at 120 °C. The solvent was removed under reduced pressure. The crude product was precipitated in water (100 mL), filtered off, washed with water (3 × 50 mL) and dried *in vacuo*. The title compound was obtained as a brown solid (563 mg, 70%).

The spectroscopic data is in agreement with literature.[112]

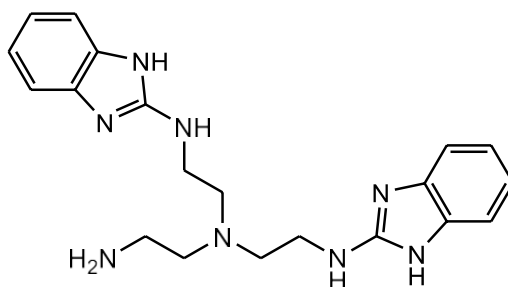
Methyl 2-chloro-1H-benzo[d]imidazole-6-carboxylate (b)

A solution of methyl 2-oxo-2,3-dihydro-1H-benzo[d]imidazole-5-carboxylate (470 mg, 2.45 mmol, 1.00 equiv.) in POCl₃ (5 mL) was stirred for 8 h at 100 °C. The solvent was removed under reduced pressure. The residue was dissolved in water (10 mL) and the solution was neutralized with NaHCO₃ solution and extracted with DCM. The organic phase was dried over Na₂SO₄ and the solvent was removed under reduced pressure. The title compound was obtained as a brown solid (263 mg, 51%).

The spectroscopic data is in agreement with literature.[112]

SYNTHESIS OF LITERATURE KNOWN PROCEDURES

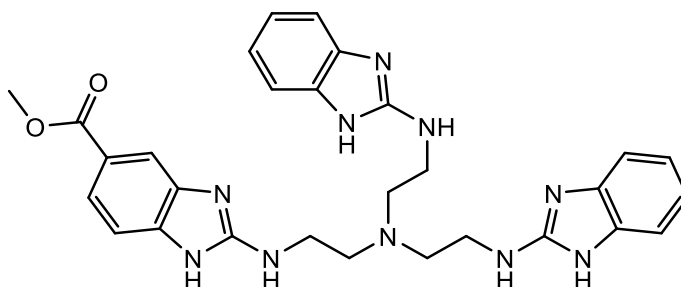
*N*¹-(2-((1*H*-Benzo[*d*]imidazol-2-yl)amino)ethyl)-*N*¹-(2-aminoethyl)-*N*²-(1*H*-benzo[*d*]imidazol-2-yl)ethane-1,2-diamine (b)



A suspension of TREN (598 μ L, 585 mg, 4.00 mmol, 1.00 equiv), 2-chloro benzimidazole (916 mg, 6.00 mmol, 1.50 equiv) and DIPEA (1.04 mL, 771 mg, 6.00 mmol, 1.50equiv) was heated to reflux for 4 h. The solvent was removed under reduced pressure, the solid residue was adsorbed to silica and purified via column chromatography (DCM/MeOH 10:1, 2 % $\text{NH}_3(\text{aq})$) \rightarrow DCM/MeOH 2:1, 2 % $\text{NH}_3(\text{aq})$) to obtain the product as a yellow foam (270 mg, 18%).

The spectroscopic data is in agreement with literature.[112]

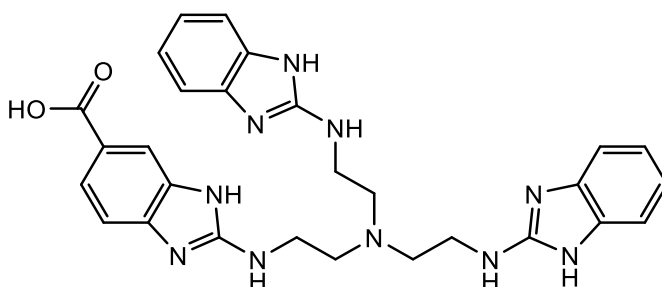
Methyl 2-((2-(bis(2-((1*H*-benzo[*d*]imidazol-2-yl)amino)ethyl)amino)ethyl)amino)-1 *H*-benzo[*d*]imidazole-6-carboxylate (b)



A suspension of *N*¹-(2-((1*H*-Benzo[*d*]imidazol-2-yl)amino)ethyl)-*N*¹-(2-aminoethyl)-*N*²-(1*H*-benzo[*d*]imidazol-2-yl)ethane-1,2-diamine (379 mg, 1.00 mmol, 1.00 equiv), 2-chloro benzimidazole methyl carboxylate (315 mg, 1.50 mmol, 1.50 equiv) and DIPEA (351 μ L, 261 mg, 1.50 mmol, 1.50 equiv) in *n*BuOH (2 mL) was heated to reflux for 8 h. The solvent was evaporated under reduced pressure and the residue was purified via column chromatography (DCM/MeOH 15:1, 2 % $\text{NH}_3(\text{aq})$) \rightarrow DCM/MeOH 10:1, 2 % $\text{NH}_3(\text{aq})$) to obtain a beige solid (400 mg mixture of methyl and butyl carboxylate).

The spectroscopic data is in agreement with literature.[112]

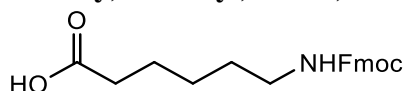
2-((2-(Bis(2-((1*H*-benzo[*d*]imidazol-2-yl)amino)ethyl)amino)ethyl)amino)-2,3-dihydro-1*H*-indene-5-carboxylic acid (b)



A suspension of Methyl/Butyl2-((2-(bis(2-((1*H*-benzo[*d*]imidazol-2-yl)amino)ethyl)amino)ethyl)amino)-1*H*-benzo[*d*]imidazole-6-carboxylate (400 mg) in 6 M hydrochloric acid (6 mL) was heated to reflux for 6 h. The solvent was removed under reduced pressure and the residue was dried in *vacuo* to obtain a light brown solid. The crude product could be used in the conjugation experiments without further purification (366 mg, 68 % for two steps).

The spectroscopic data is in agreement with literature.[112]

6-(((9*H*-Fluoren-9-yl)methoxy)carbonyl)amino)hexanoic acid



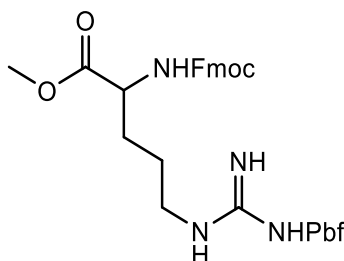
To a solution of 6-aminohexanoic acid (1.31 g, 10.0 mmol, 1.00 equiv.) in DCM (20 mL) was added (9*H*-fluoren-9-yl)methyl (2,5-dioxopyrrolidin-1-yl) carbonate (3.37 g, 10.0 mmol, 1.00 equiv.) followed by DIPEA (1.74 mL, 1.29 g, 10.0 mmol, 1.00 equiv.). The mixture was stirred for 16 h, washed with NH₄Cl solution and dried over Na₂SO₄. The solvent was removed under reduced pressure. The title compound was obtained as a white solid (3.51 g, quant.).

The spectroscopic data is in agreement with literature.[112]

5.3 New products

5.3.1 Synthesis of α -GPNA

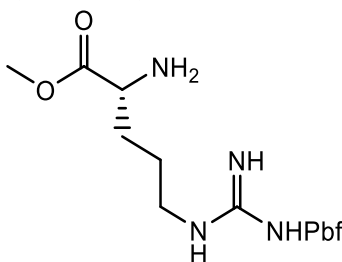
Methyl-*N*²-(((9H-fluoren-9-yl)methoxy)carbonyl)-*N*^ω-((2,2,4,6,7-pentamethyl-2,3-dihydrobenzofuran-5-yl)sulfonyl)argininate (b, g)



*N*²-(((9H-Fluoren-9-yl)methoxy)carbonyl)-*N*^ω-((2,2,4,6,7-pentamethyl-2,3-dihydrobenzofuran-5-yl)-sulfonyl)-D-arginine (10.0 g, 15,4 mmol, 1.00 equiv.) and HBTU (6.45 g, 17,0 mmol, 1,10 equiv.) in a 250 mL round bottom flask under argon. DMF (40 mL) was added and the solution was cooled down to 0 °C before adding DIPEA (2.80 mL, 2.08 g, 17.0 mmol, 1.10 equiv.). The reaction mixture was stirred for 15 min and dry MeOH (2.40 mL, 23.0 mmol, 1.50 equiv.) was added followed by further DIPEA (3.80 mL, 2.82 g, 23,0 mmol, 1.50 equiv.). Stirring was continued for 16 h while warming up to room temperature. The solvent was removed under reduced pressure and the crude product was purified by column chromatography (EtOAc/CH₂Cl₂, 3:7 to 1:0). The title compound was obtained as a white solid (10.2 g, quant.)

¹H NMR (CDCl₃-*d*₁, 400 MHz, 25 °C): δ = 11.06 (s, 1H), 9.67–8.82 (m, 1H), 7.77 (dt, J = 7.3, 3.3 Hz, 2H), 7.56 (dd, J = 15.0, 7.5 Hz, 2H), 7.40 (td, J = 7.3, 2.4 Hz, 2H), 7.26 (s, 2H), 5.92–5.73 (m, 1H), 4.39 (s, 1H), 4.29 (s, 1H), 4.20 (d, J = 7.0 Hz, 1H), 3.76 (d, J = 4.7 Hz, 3H), 3.45 (s, 1H), 3.19 (s, 1H), 2.93 (s, 2H), 2.49 (s, 3H), 2.44 (s, 3H), 2.08 (s, 3H), 1.94–1.80 (m, 1H), 1.69 (d, J = 12.9 Hz, 3H), 1.45 (d, J = 4.7 Hz, 6H) ppm.

¹³C NMR (CDCl₃-*d*₁, 100 MHz, 25 °C): δ = 72.2, 161.4, 157.3, 153.4, 143.5, 143.3, 141.3, 140.8, 135.0, 127.9, 127.2, 126.2, 126.0, 125.0, 120.2, 118.9, 87.7, 67.6, 52.9, 47.0, 42.8, 28.5, 24.0, 19.2, 17.5, 12.4 ppm.

Methyl-*N*^ω-((2,2,4,6,7-pentamethyl-2,3-dihydrobenzofuran-5-yl)sulfonyl)-*D*-argininate (b, g)

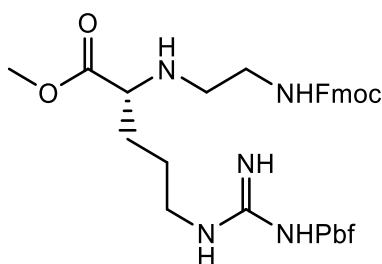
To a stirring solution of methyl-*N*²-(((9H-fluoren-9-yl)methoxy)carbonyl)-*N*^ω-((2,2,4,6,7-pentamethyl-2,3-dihydrobenzofuran-5-yl)sulfonyl)-*D*-argininate (10.2 g, 15.4 mmol, 1.00 equiv.) in 40 mL DMF was added 10 mL piperidine (20% v/v). The reaction mixture was stirred for 1 h. Subsequently, the solvent was removed under reduced pressure. The residue was purified by column chromatography (EtOAc/CH₂Cl₂, 1:1, then DCM/MeOH, 19:1). The title compound was obtained as a yellow foam (6.10 g, 90%).

¹H NMR (CDCl₃-*d*₁, 400 MHz, 25 °C): δ = 8.28 (bs, 4H), 7.50 (s, 2H), 5.13 (dd, J = 12.1, 4.2 Hz, 2H), 4.13 (d, J = 6.4 Hz, 1H), 3.17 (s, 2H), 2.92 (s, 2H), 2.44 (s, 3H), 2.40 (s, 3H), 2.05 (s, 3H), 1.98 (s, 2H), 1.81-1.50 (bm, 2H), 1.45 (s, 6H) ppm.

¹³C NMR (CDCl₃-*d*₁, 100 MHz, 25 °C): δ = 169.3, 162.9, 162.5, 162.1, 134.2, 128.8, 128.7, 128.5, 114.7, 87.5, 77.3, 68.6, 52.7, 42.9, 41.0, 28.5, 27.2, 19.1, 17.4, 12.4 ppm.

NEW PRODUCTS

Methyl-*N*²-(2-(((9*H*-fluoren-9-yl)methoxy)carbonyl)amino)ethyl)-*N*^ω-((2,2,4,6,7-pentamethyl-2,3-dihydrobenzofuran-5-yl)sulfonyl)-*D*-argininate (**b**, **g**, **u**)

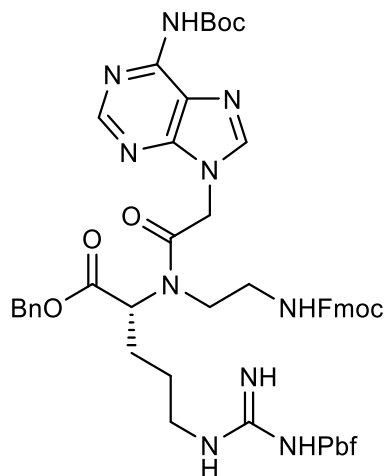


Benzyl *N*^ω-((2,2,4,6,7-pentamethyl-2,3-dihydrobenzofuran-5-yl)sulfonyl)-*D*-argininate (2.90 g, 6.58 mmol, 1.00 equiv.) was dissolved in dry MeOH (40 mL). Na₂SO₄ (1 g) was added to the reaction mixture. (9*H*-fluoren-9-yl)methyl (2-oxoethyl)carbamate (1.85 g, 6.58 mmol, 1.00 equiv.) was added at -5 °C and stirring was continued for 1.5 h. Sodium cyanoborohydride (496 mg, 7.90 mmol, 1.20 equiv.) was added followed by glacial acetic acid (452 μL, 475 mg, 7.90 mmol, 1.20 equiv.). The reaction mixture was allowed to warm up to room temperature and stirring was continued for 6 h. The mixture was filtered, the solvent was removed under reduced pressure. The residue was purified by column chromatography (EtOAc/CH₂Cl₂, 1:1 to 1:0). The title compound was obtained as a white solid (2.93 g, 63%).

¹H NMR (CDCl₃-*d*₁, 400 MHz, 25 °C): δ = 9.47 (s, 1H), 9.11 (s, 4H), 7.74 (dd, *J* = 11.5, 7.6 Hz, 2H), 7.54 (d, *J* = 7.6 Hz, 2H), 7.44-7.31 (m, 2H), 7.31-7.19 (m, 4H), 6.29 (s, 1H), 4.63-4.35 (m, 1H), 4.31 (d, *J* = 7.3 Hz, 2H), 4.14 (t, *J* = 7.2 Hz, 1H), 3.99 (s, 1H), 3.76 (s, 3H), 3.53 (s, 2H), 3.25 (s, 3H), 2.94 (d, *J* = 5.7 Hz, 3H), 2.48 (s, 3H), 2.43 (s, 3H), 2.07 (s, 4H), 1.45 (s, 6H) ppm.

¹³C NMR (CDCl₃-*d*₁, 100 MHz, 25 °C): δ = 168.4, 162.0, 161.6, 158.2, 143.6, 141.3, 141.2, 134.9, 128.9, 128.7, 128.3, 127.8, 127.1, 125.1, 120.0, 87.6, 67.7, 59.7, 53.7, 46.9, 42.9, 37.8, 28.5, 26.5, 19.1, 17.4, 12.4 ppm.

Benzyl *N*²-(2-((((9*H*-fluoren-9-yl)methoxy)carbonyl)amino)ethyl)-*N*^ω-(2-(6-((*tert*-butoxycarbonyl)amino)-9*H*-purin-9-yl)acetyl)-*N*^ω-(2,2,4,6,7-pentamethyl-2,3-dihydrobenzofuran-5-yl)sulfonyl)argininate (b)



To a stirring solution of benzyl *N*²-(2-((((9*H*-fluoren-9-yl)methoxy)carbonyl)amino)ethyl)-*N*^ω-(2,2,4,6,7-pentamethyl-2,3-dihydrobenzofuran-5-yl)sulfonyl)-*D*-argininate (150 mg, 192 μmol, 1.00 equiv.) and 2-(6-((*tert*-butoxycarbonyl)amino)-9*H*-purin-9-yl)acetic acid (169 mg, 576 μmol, 3.00 equiv.) in dry acetonitrile (4 mL) diisopropylmethanediimine (89.0 μL, 71.7 mg, 576 μmol, 3.00 equiv.) was added. The mixture was stirred for 16 h at room temperature and subsequently quenched with water (1 mL), filtered, purified *via* HPLC (water+0.1% TFA/acetonitrile+0.1% TFA 60:40 to 0:100, 35 min) and lyophilized. The title compound was obtained as a white solid (28 mg, 63%).

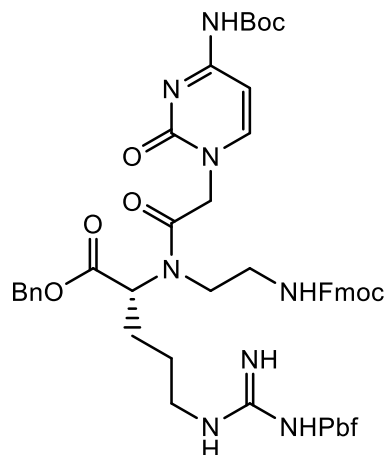
¹H NMR (CDCl₃-*d*₁, 400 MHz, 25 °C): δ = 10.63(s, 4H), 8.64 (s, 1H), 8.44 (s, 1H), 7.76 – 7.62 (m, 2H), 7.59 – 7.48 (m, 2H), 7.42 – 7.31 (m, 2H), 7.30 – 7.19 (m, 7H), 5.87 (s, 1H), 5.30 – 5.18 (m, 2H), 5.05 (s, 2H), 4.45 (d, J = 6.2 Hz, 2H), 4.17 (t, J = 7.0 Hz, 1H), 4.04 (s, 1H), 3.75 (s, 1H), 3.61 – 3.14 (m, 4H), 2.95 (s, 3H), 2.49 (s, 3H), 2.43 (s, 3H), 2.08 (s, 3H), 1.97 (s, 2H), 1.66 (s, 2H), 1.55 (s, 9H), 1.47 (s, 6H) ppm.

¹³C NMR (CDCl₃-*d*₁, 100 MHz, 25 °C): δ = 165.6, 161.9, 161.6, 157.1, 143.8, 143.6, 128.7, 128.6, 128.2, 127.7, 127.1, 125.0, 119.9, 117.3, 114.4, 85.2, 67.6, 47.1, 42.9, 28.5, 27.8, 19.2, 12.4 ppm.

HRMS (FAB) Calc. for C₅₅H₆₅N₁₀O₁₁S₁: 1057.4608 m/z [M+H], found: 1057.4606 m/z (Δ = 0.2 ppm).

NEW PRODUCTS

Benzyl *N*²-(2-(((9*H*-fluoren-9-yl)methoxy)carbonyl)amino)ethyl)-*N*²-(2-(6-((*tert*-butoxycarbonyl)amino)-9*H*-purin-9-yl)acetyl)-*N*^ω-((2,2,4,6,7-pentamethyl-2,3-dihydrobenzofuran-5-yl)sulfonyl)argininate (b)



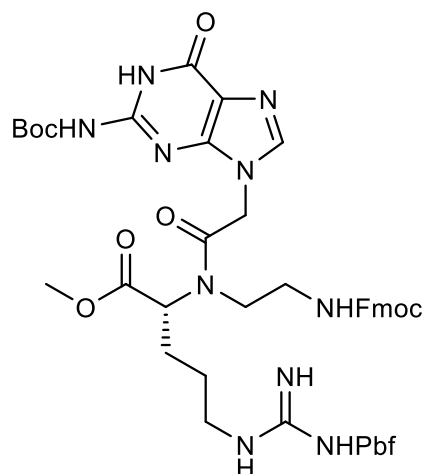
To a stirring solution of benzyl *N*²-(2-(((9*H*-fluoren-9-yl)methoxy)carbonyl)amino)ethyl)-*N*^ω-((2,2,4,6,7-pentamethyl-2,3-dihydrobenzofuran-5-yl)sulfonyl)-*D*-argininate (150 mg, 192 μmol, 1.00 equiv.) and 2-(4-((*tert*-butoxycarbonyl)amino)-2-oxopyrimidin-1(2*H*)-yl)acetic acid (155 mg, 576 μmol, 3.00 equiv.) in dry acetonitrile (4 mL) diisopropylmethanediimine (89.0 μL, 71.7 mg, 576 μmol, 3.00 equiv.) was added. The mixture was stirred for 16 h at room temperature and subsequently quenched with water (1 mL), filtered, purified *via* HPLC (water+0.1% TFA/acetonitrile+0.1% TFA 60:40 to 0:100, 35 min) and lyophilized. The title compound was obtained as a white solid (155 mg, 78%).

¹H NMR (CDCl₃-*d*₁, 400 MHz, 25 °C): δ = 9.30 (s, 1H), 7.85–7.66 (m, 2H), 7.62–7.49 (m, 2H), 7.48–7.37 (m, 2H), 7.36–7.27 (m, 7H), 7.16 (s, 1H), 5.73 (s, 1H), 5.12 (q, J = 12.0 Hz, 2H), 4.81 (d, J = 14.8 Hz, 2H), 4.47 (d, J = 7.4 Hz, 2H), 4.34 (t, J = 9.2 Hz, 2H), 4.19 (t, J = 6.6 Hz, 2H), 3.79 (s, 3H), 3.47 (s, 1H), 3.25 (s, 5H), 2.97 (s, 3H), 2.52 (s, 3H), 2.46 (s, 3H), 2.07 (d, J = 8.9 Hz, 5H), 1.53 (s, 9H), 1.47 (s, 6H) ppm.

¹³C NMR (CDCl₃-*d*₁, 100 MHz, 25 °C): δ = 170.0, 166.7, 161.5, 161.1, 156.7, 152.5, 150.9, 144.0, 141.3, 140.3, 135.0, 128.8, 128.7, 128.3, 127.9, 127.4, 127.2, 126.2, 125.2, 124.9, 120.1, 119.1, 117.1, 114.3, 95.9, 87.8, 67.7, 66.9, 51.4, 47.0, 42.9, 42.0, 39.5, 28.6, 28.5, 27.9, 25.4, 24.1, 19.3, 17.3, 12.5 ppm.

HRMS (FAB) Calc. for C₅₄H₆₅N₈O₁₁S: 1033.4495 m/z [M+H], found: 1033.4494 m/z (Δ = 0.1 ppm).

Methyl N^2 -(2-((((9*H*-fluoren-9-yl)methoxy)carbonyl)amino)ethyl)- N^2 -(2-(6-((*tert*-butoxycarbonyl)amino)-4-oxo-4,5-dihydro-1*H*-imidazo[4,5-*c*]pyridin-1-yl)acetyl)- N^{ω} -((2,2,4,6,7-pentamethyl-2,3-dihydrobenzofuran-5-yl)sulfonyl)argininate (**b**)



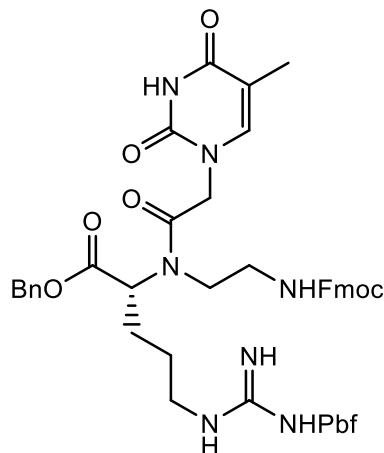
To a stirring solution of methyl N^2 -(2-((((9*H*-fluoren-9-yl)methoxy)carbonyl)amino)ethyl)- N^{ω} -((2,2,4,6,7-pentamethyl-2,3-dihydrobenzofuran-5-yl)sulfonyl)-*D*-argininate (50.0 mg, 71.0 μ mol, 1.00 equiv.) and 2-(6-((*tert*-butoxycarbonyl)amino)-9*H*-purin-9-yl)acetic acid (62.5 mg, 213 μ mol, 3.00 equiv.) in dry acetonitrile (4 mL) diisopropylmethanediimine (33.2 μ L, 26.8 mg, 213 μ mol, 3.00 equiv.) was added. The mixture was stirred for 16 h at room temperature and subsequently quenched with water (1 mL), filtered, purified *via* HPLC (water+0.1% TFA/acetonitrile+0.1% TFA 60:40 to 0:100, 35 min) and lyophilized. The title compound was obtained as a white solid (41 mg, 59%).

$^1\text{H NMR}$ (CDCl_3 -*d*₁, 400 MHz, 25 °C): δ = 9.23–8.59 (m, 2H), 7.82–7.57 (m, 2H), 7.57–7.39 (m, 2H), 7.40–7.06 (m, 6H), 6.96 (t, *J* = 7.5 Hz, 1H), 5.60 (s, 1H), 5.26–4.93 (m, 1H), 4.94–4.75 (m, 1H), 4.72–4.61 (m, 1H), 4.37 (s, 2H), 4.21–3.99 (m, 2H), 3.76–3.63 (m, 2H), 3.53 (s, 2H), 3.46 (s, 2H), 3.20 (s, 2H), 3.05–2.65 (m, 5H), 2.52–2.26 (m, 6H), 2.10–1.97 (m, 3H), 1.94 (s, 1H), 1.49 (s, 6H), 1.45 (s, 9H).

$^{13}\text{C NMR}$ (CDCl_3 -*d*₁, 100 MHz, 25 °C): δ = 171.0, 161.4, 161.1, 160.8, 160.4, 156.9, 153.4, 153.0, 152.6, 150.8, 148.2, 143.7, 143.5, 141.6, 141.2, 140.6, 134.9, 128.0, 127.8, 127.4, 127.1, 126.0, 125.0, 124.3, 119.8, 119.0, 116.9, 114.1, 111.0, 87.7, 85.1, 52.8, 47.3, 42.8, 28.5, 27.9, 27.7, 19.1, 17.4, 12.4, 1.9 ppm.

NEW PRODUCTS

Benzyl N^2 -(2-(((9*H*-fluoren-9-yl)methoxy)carbonyl)amino)ethyl)- N^{ω} -(2-(5-methyl-2,4-dioxo-3,4-dihydropyrimidin-1(2*H*)-yl)acetyl)- N^{ω} -((2,2,4,6,7-pentamethyl-2,3-dihydrobenzofuran-5-yl)sulfonyl)argininate (b)



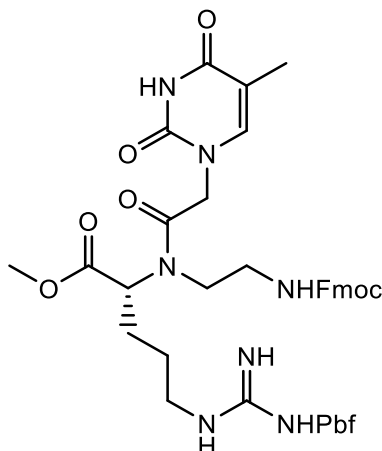
To a stirring solution of benzyl N^2 -(2-(((9*H*-fluoren-9-yl)methoxy)carbonyl)amino)ethyl)- N^{ω} -((2,2,4,6,7-pentamethyl-2,3-dihydrobenzofuran-5-yl)sulfonyl)-*D*-argininate (150 mg, 192 μ mol, 1.00 equiv.) and 2-(5-methyl-2,4-dioxo-3,4-dihydropyrimidin-1(2*H*)-yl)acetic acid (106 mg, 576 μ mol, 3.00 equiv.) in dry acetonitrile (4 mL) diisopropylmethanediimine (89.0 μ L, 71.7 mg, 576 μ mol, 3.00 equiv.) was added. The mixture was stirred for 16 h at room temperature and subsequently quenched with water (1 mL), filtered, purified *via* HPLC (water+0.1% TFA/acetonitrile+0.1% TFA 60:40 to 0:100, 35 min) and lyophilized. The title compound was obtained as a white solid (149 mg, 82%).

$^1\text{H NMR}$ (CDCl_3 - d_1 , 400 MHz, 25 $^\circ\text{C}$): δ = 9.89 (s, 3H), 9.05 (s, 1H), 7.82–7.70 (m, 2H), 7.60–7.51 (m, 2H), 7.44–7.17 (m, 9H), 6.91–6.69 (m, 1H), 5.78 (s, 1H), 5.30–5.01 (m, 2H), 4.60 (d, J = 16.5 Hz, 1H), 4.47–4.31 (m, 2H), 4.27–3.89 (m, 2H), 3.70 (d, J = 12.1 Hz, 1H), 3.51–3.06 (m, 5H), 2.93 (s, 3H), 2.47 (s, 3H), 2.42 (s, 3H), 2.07 (s, 5H), 1.81 (s, 3H), 1.64 (s, 2H), 1.45 (s, 6H) ppm.

$^{13}\text{C NMR}$ (CDCl_3 - d_1 , 100 MHz, 25 $^\circ\text{C}$): δ = 170.1, 165.2, 161.9, 161.5, 161.1, 157.0, 153.2, 151.5, 143.7, 143.5, 142.1, 141.3, 140.8, 135.0, 128.8, 128.8, 128.7, 128.3, 127.9, 127.2, 126.0, 125.1, 120.1, 118.9, 87.7, 67.7, 67.0, 47.1, 42.8, 41.8, 39.6, 28.5, 25.5, 24.8, 19.2, 17.5, 12.4, 12.1 ppm.

HRMS (FAB) Calc. for $\text{C}_{54}\text{H}_{58}\text{N}_7\text{O}_5\text{S}_1$: 948.4118 m/z $[\text{M}+\text{H}]^+$, found: 948.4118 m/z (Δ = 0.1 ppm).

Methyl *N*²-(2-((((9*H*-fluoren-9-yl)methoxy)carbonyl)amino)ethyl)-*N*²-(2-(5-methyl-2,4-dioxo-3,4-dihydropyrimidin-1(2*H*)-yl)acetyl)-*N*^ω-((2,2,4,6,7-pentamethyl-2,3-dihydrobenzofuran-5-yl)sulfonyl)argininate (b)



To a stirring solution of methyl *N*²-(2-((((9*H*-fluoren-9-yl)methoxy)carbonyl)amino)ethyl)-*N*^ω-((2,2,4,6,7-pentamethyl-2,3-dihydrobenzofuran-5-yl)sulfonyl)-D-argininate (50.0 mg, 71.0 μmol, 1.00 equiv) and 2-(5-methyl-2,4-dioxo-3,4-dihydropyrimidin-1(2*H*)-yl)acetic acid (62.5 mg, 213 μmol, 3.00 equiv) in dry acetonitrile (4 mL) diisopropylmethanediimine (33.2 μL, 26.8 mg, 213 μmol, 3.00 equiv) was added. The mixture was stirred for 16 h at room temperature and subsequently quenched with water (1 mL), filtered, purified with HPLC (water+0.1% TFA/acetonitrile+0.1% TFA 60:40 to 0:100, 35 min) and lyophilized. The title compound was obtained as a white solid (36.0 mg, 53%).

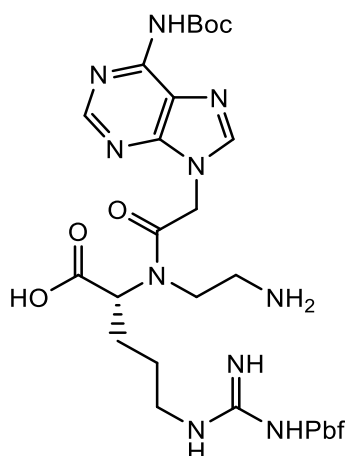
¹H NMR (CDCl₃-*d*₁, 400 MHz, 25 °C): δ = 9.50 (s, 3H), 9.12 (s, 1H), 7.90 – 7.72 (m, 2H), 7.64 – 7.51 (m, 2H), 7.46 – 7.20 (m, 4H), 6.89 (s, 1H), 6.06 (s, 1H), 4.79 – 4.38 (m, 3H), 4.27 – 4.03 (m, 3H), 3.89 – 3.65 (m, 3H), 3.23 (m, 5H), 2.96 (s, 3H), 2.50 (s, 3H), 2.45 (s, 3H), 2.10 (s, 3H), 2.06– 1.96 (m, 2H), 1.84 (d, J = 16.7 Hz, 3H), 1.67 (s, 2H), 1.48 (s, 6H) ppm.

¹³C NMR (CDCl₃-*d*₁, 100 MHz, 25 °C): δ = 170.9, 165.2, 161.5, 161.1, 157.0, 153.2, 143.7, 143.6, 142.1, 141.3, 127.9, 127.2, 126.0, 125.1, 120.0, 118.9, 87.7, 67.1, 52.8, 47.1, 42.8, 39.5, 28.5, 19.2, 17.5, 12.4, 12.1 ppm.

HRMS (FAB) Calc. for C₄₄H₅₄N₇O₁₀S₁: 872.3652 m/z [M+H]⁺, found: 872.3653 m/z (Δ = 0.1 ppm).

NEW PRODUCTS

*N*²-(2-Aminoethyl)-*N*²-(2-(6-((*tert*-butoxycarbonyl)amino)-9*H*-purin-9-yl)acetyl)-*N*^ω-((2,2,4,6,7-pentamethyl-2,3-dihydrobenzofuran-5-yl)sulfonyl)arginine (b)



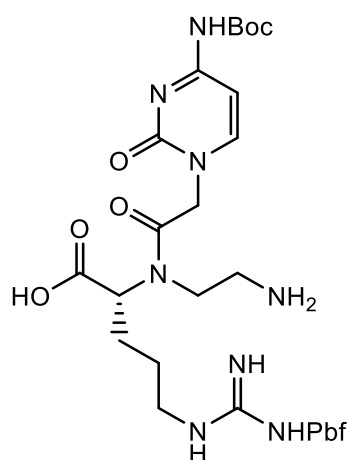
a) To a solution of benzyl *N*²-(2-(((9*H*-fluoren-9-yl)methoxy)carbonyl)amino)ethyl)-*N*²-(2-(6-((*tert*-butoxycarbonyl)amino)-9*H*-purin-9-yl)acetyl)-*N*^ω-((2,2,4,6,7-pentamethyl-2,3-dihydrobenzofuran-5-yl)sulfonyl)argininate (128 mg, 121 μmol, 1.00 equiv.) in acetonitrile (3 mL) was added a solution of lithium hydroxide (11.6 mg, 484 μmol, 4.00 equiv.) in water (1 mL). The reaction mixture was stirred for 2 h, filtered and purified *via* HPLC (water+0.1% TFA/acetonitrile+0.1% TFA 95:5 to 5:95, 45 min).

b) The same procedure was performed simultaneously with 36 mg of the methyl ester. The title compound was obtained from the combined product fractions as a white solid (44.0 mg, 82%).

¹H NMR (MeOD-*d*₄, 400 MHz, 25 °C): δ = 7.99–7.68 (m, 2H), 7.19–6.97 (m, 2H), 4.52 (s, 2H), 4.16–3.90 (m, 2H), 3.63–3.37 (m, 3H), 3.21 (p, J = 1.7 Hz, 2H), 3.20–3.06 (m, 4H), 2.90 (s, 2H), 2.47 (s, 3H), 2.41 (s, 3H), 1.98 (s, 3H), 1.92–1.78 (m, 2H) 1.64–1.49 (m, 3H) 1.44 (s, 9H), 1.35 (s, 6H) ppm.

¹³C NMR (MeOD-*d*₄, 100 MHz, 25 °C): δ = 169.6, 169.3, 167.7, 163.7, 160.4, 160.0, 156.1, 151.8, 150.7, 124.9, 117.5, 114.6, 95.5, 86.5, 82.5, 59.1, 52.3, 46.2, 42.5, 27.3, 26.9, 18.2, 18.2, 17.0, 11.1 ppm.

*N*²-(2-aminoethyl)-*N*²-(2-(4-((*tert*-butoxycarbonyl)amino)-2-oxopyrimidin-1(2*H*)-yl)acetyl)-*N*^ω-((2,2,4,6,7-pentamethyl-2,3-dihydrobenzofuran-5-yl)sulfonyl)arginine (b)



a) To a solution of benzyl benzyl *N*²-(2-(((9*H*-fluoren-9-yl)methoxy)carbonyl)amino)ethyl)-*N*²-(2-(6-((*tert*-butoxycarbonyl)amino)-9*H*-purin-9-yl)acetyl)-*N*^ω-((2,2,4,6,7-pentamethyl-2,3-dihydrobenzofuran-5-yl)sulfonyl)argininate (155 mg, 150 μmol, 1.00 equiv.) in acetonitrile (3 mL) was added a solution of lithium hydroxide (14.4 mg, 600 μmol, 4.00 equiv.) in water (1 mL). The reaction mixture was stirred for 2 h, filtered and purified *via* HPLC (water+0.1% TFA/acetonitrile+0.1% TFA 95:5 to 5:95, 45 min).

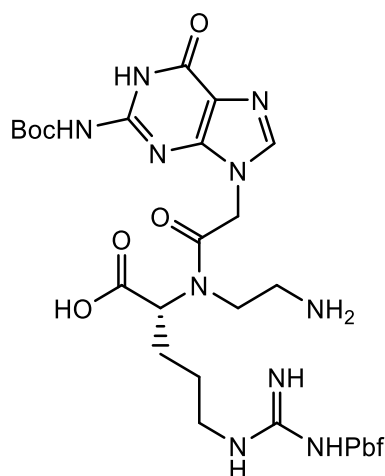
b) The same procedure was performed simultaneously with 36.0 mg of the methyl ester. The title compound was obtained from the combined product fractions as a white solid (44.0 mg, 34%).

¹H NMR (MeOD-*d*₄, 400 MHz, 25 °C): δ = 8.67–8.44 (m, 1H), 8.37–8.12 (m, 1H), 5.51–5.20 (m, 2H), 5.11 (s, 1H), 4.09–3.93 (m, 1H), 3.65–3.45 (m, 2H), 3.40–3.03 (m, 6H), 2.89 (s, 2H), 2.46 (s, 3H), 2.39 (s, 3H), 1.97 (s, 2H), 1.92 (s, 2H), 1.53 (s, 9H), 1.37–1.31 (m, 7H) ppm.

¹³C NMR MeOD-*d*₄, 100 MHz, 25 °C): δ = 172.3, 169.7, 168.8, 168.0, 166.6, 161.3, 161.0, 160.6, 152.0, 151.7, 149.3, 148.3, 148.2, 147.6, 146.3, 146.1, 124.9, 117.7, 117.2, 114.8, 86.5, 84.0, 59.3, 46.0, 42.5, 36.1, 27.3, 26.9, 26.1, 18.2, 17.0, 11.1 ppm.

NEW PRODUCTS

*N*²-(2-Aminoethyl)-*N*²-(2-(2-((*tert*-butoxycarbonyl)amino)-6-oxo-1,6-dihydro-9*H*-purin-9-yl)acetyl)-*N*^ω-((2,2,4,6,7-pentamethyl-2,3-dihydrobenzofuran-5-yl)sulfonyl)arginine (b)



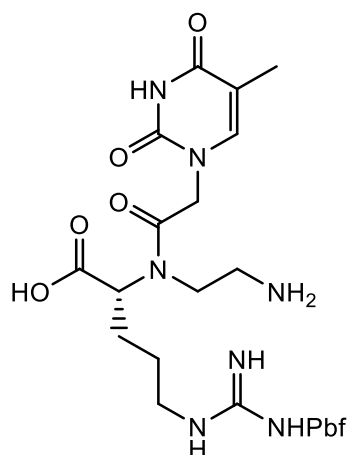
a) To a solution of benzyl *N*²-(2-(((9*H*-fluoren-9-yl)methoxy)carbonyl)amino)ethyl)-*N*²-(2-(6-((*tert*-butoxycarbonyl)amino)-4-oxo-4,5-dihydro-1*H*-imidazo[4,5-*c*]pyridin-1-yl)acetyl)-*N*^ω-((2,2,4,6,7-pentamethyl-2,3-dihydrobenzofuran-5-yl)sulfonyl)argininate (180 mg, 168 μmol, 1.00 equiv.) in acetonitrile (3 mL) was added a solution of lithium hydroxide (16.2 mg, 672 μmol, 4.00 equiv.) in water (1 mL). The reaction mixture was stirred for 2 h, filtered and purified *via* HPLC (water+0.1% TFA/acetonitrile+0.1% TFA 95:5 to 5:95, 45 min).

b) The same procedure was performed simultaneously with 41 mg of the methyl ester. The title compound was obtained from the combined product fractions as a white solid (176 mg, 90%).

¹H NMR (MeOD-*d*₄, 400 MHz, 25 °C): δ = 7.79 (s, 1H), 7.30–7.07 (m, 1H), 5.25–4.95 (m, 2H), 4.14 (dd, *J* = 9.9, 5.3 Hz, 1H), 4.03–3.84 (m, 1H), 3.65 (s, 1H), 3.55–3.35 (m, 1H), 3.22 (p, *J* = 1.6 Hz, 3H), 3.19–3.02 (m, 3H), 3.01–2.91 (m, 3H), 2.85 (s, 3H), 2.46 (s, 3H), 2.39 (s, 3H), 2.15–2.03 (m, 1H), 1.94 (s, 3H), 1.84–1.71 (m, 1H), 1.64–1.49 (m, 2H), 1.46 (s, 9H), 1.33 (s, 6H)ppm.

¹³C NMR (MeOD-*d*₄, 100 MHz, 25 °C): δ = 176.2, 169.3, 162.1, 161.8, 161.5, 161.1, 158.5, 156.8, 156.4, 154.1, 148.2, 141.2, 137.9, 132.9, 132.1, 124.7, 121.2, 118.3, 117.1, 115.4, 112.5, 86.4, 83.3, 44.7, 42.5, 37.9, 27.3, 27.0, 18.2, 17.0, 11.1 ppm.

*N*²-(2-Aminoethyl)-*N*²-(2-(5-methyl-2,4-dioxo-3,4-dihydropyrimidin-1(2*H*)-yl)acetyl)-*N*^ω-((2,2,4,6,7-pentamethyl-2,3-dihydrobenzofuran-5-yl)sulfonyl)arginine (b)



a) To a solution of benzyl *N*²-(2-(((9*H*-fluoren-9-yl)methoxy)carbonyl)amino)ethyl)-*N*²-(2-(5-methyl-2,4-dioxo-3,4-dihydropyrimidin-1(2*H*)-yl)acetyl)-*N*^ω-((2,2,4,6,7-pentamethyl-2,3-dihydrobenzofuran-5-yl)sulfonyl)argininate (149 mg, 157 μmol, 1.00 equiv.) in acetonitrile (3 mL) was added a solution of lithium hydroxide (15.1 mg, 628 μmol, 4.00 equiv.) in water (1 mL). The reaction mixture was stirred for 2 h, filtered and purified *via* HPLC (water+0.1% TFA/acetonitrile+0.1% TFA 95:5 to 5:95, 45 min).

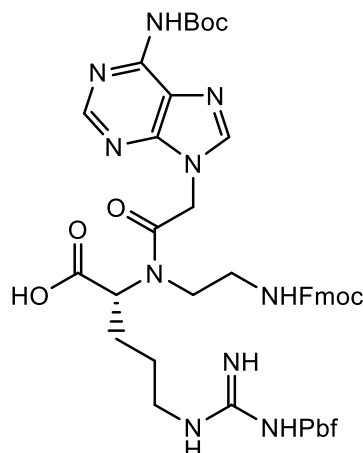
b) The same procedure was performed simultaneously with 36.0 mg of the methyl ester. The title compound was obtained from the combined product fractions as a white solid (93.0 mg, 75%).

¹H NMR (MeOD-*d*₄, 400 MHz, 25 °C): δ = 7.66–6.63 (m, 2H), 4.87 (s, 3H), 4.81 – 4.65 (m, 1H), 4.63–4.46 (m, 1H), 4.37 (s, 1H), 4.22 – 3.76 (m, 1H), 3.67 – 3.41 (m, 2H), 3.25 (p, J = 1.7 Hz, 3H), 3.22–3.06 (m, 3H), 2.93 (s, 2H), 2.50 (s, 3H), 2.44 (s, 3H), 2.01 (s, 3H), 1.80 (s, 3H), 1.64 – 1.50 (m, 2H), 1.38 (s, 6H) ppm.

¹³C NMR (MeOD-*d*₄, 100 MHz, 25 °C): δ = 170.2, 165.5, 151.9, 142.4, 142.3, 142.2, 138.1, 128.0, 126.9, 126.6, 124.8, 124.8, 117.2, 110.0, 109.8, 109.7, 86.5, 86.4, 63.8, 42.5, 38.7, 37.5, 36.0, 27.3, 18.2, 17.0, 11.1, 10.9 ppm.

NEW PRODUCTS

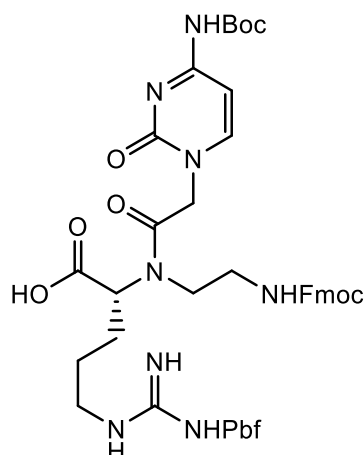
***N*²-(2-(((9*H*-Fluoren-9-yl)methoxy)carbonyl)amino)ethyl)-*N*²-(2-(6-((*tert*-butoxycarbonyl)amino)-9*H*-purin-9-yl)acetyl)-*N*^ω-((2,2,4,6,7-pentamethyl-2,3-dihydrobenzofuran-5-yl)sulfonyl)-*D*-arginine (b)**



To a solution of *N*²-(2-aminoethyl)-*N*²-(2-(6-((*tert*-butoxycarbonyl)amino)-9*H*-purin-9-yl)acetyl)-*N*^ω-((2,2,4,6,7-pentamethyl-2,3-dihydrobenzofuran-5-yl)sulfonyl)-*D*-arginine (44.0 mg, 59.1 μmol, 1.00 equiv.) in acetonitrile (1 mL) was added (9*H*-fluoren-9-yl)methyl (2,5-dioxopyrrolidin-1-yl) carbonate (19.9 mg, 59.1 μmol, 1.00 equiv.) followed by DIPEA (15.4 μL, 88.7 μmol, 1.50 equiv.). The solution was stirred for 16 h. Subsequently, the crude mixture was diluted with water (2 mL) and acetonitrile (2 mL), purified *via* HPLC (water+0.1% TFA/acetonitrile+0.1% TFA 95/5 to 5/95, 40 min) and lyophilized. The title compound was obtained as a white solid (45.0 mg, 79%).

The analytical data is in agreement with the literature.[124]

***N*²-(2-(((9*H*-Fluoren-9-yl)methoxy)carbonyl)amino)ethyl)-*N*²-(2-(4-((*tert*-butoxycarbonyl)amino)-2-oxopyrimidin-1(2*H*)-yl)acetyl)-*N*^ω-((2,2,4,6,7-pentamethyl-2,3-dihydrobenzofuran-5-yl)sulfonyl)-*D*-arginine (b).**

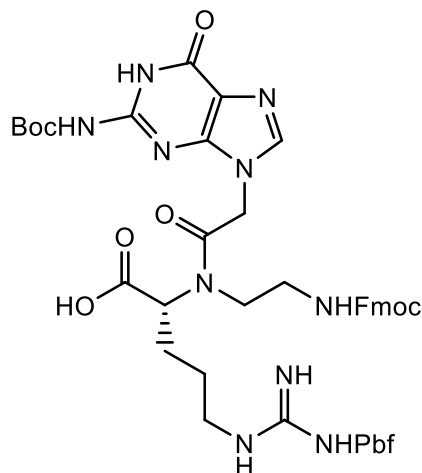


To a solution of *N*²-(2-aminoethyl)-*N*²-(2-(4-((*tert*-butoxycarbonyl)amino)-2-oxopyrimidin-1(2*H*)-yl)acetyl)-*N*^ω-((2,2,4,6,7-pentamethyl-2,3-dihydrobenzofuran-5-yl)sulfonyl)-*D*-arginine (44.0 mg, 61.1 μmol, 1.00 equiv.) in acetonitrile (1 mL) was added (9*H*-fluoren-9-yl)methyl (2,5-dioxopyrrolidin-1-yl) carbonate (20.6 mg, 61.1 μmol, 1.00 equiv.) followed by DIPEA (15.9 μL, 91.7 μmol, 1.50 equiv.). The solution was stirred for 16 h. The crude mixture was diluted with water (2 mL) and acetonitrile (2 mL), purified *via* HPLC (water+0.1% TFA/acetonitrile+0.1% TFA 95/5 to 5/95, 40 min) and lyophilized. The title compound was obtained as a white solid (34.0 mg, 59%).

The analytical data is in agreement with the literature.[124]

NEW PRODUCTS

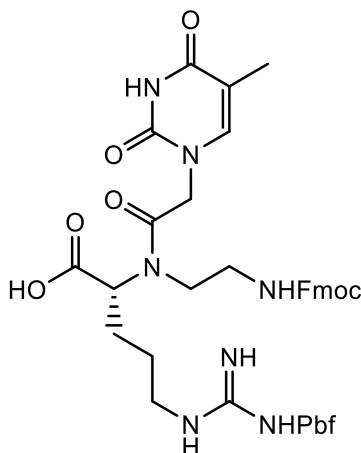
***N*²-(2-(((9*H*-Fluoren-9-yl)methoxy)carbonyl)amino)ethyl)-*N*²-(2-(2-((*tert*-butoxycarbonyl)amino)-6-oxo-1,6-dihydro-9*H*-purin-9-yl)acetyl)-*N*^ω-((2,2,4,6,7-pentamethyl-2,3-dihydrobenzofuran-5-yl)sulfonyl)-*D*-arginine (b)**



To a solution of *N*²-(2-aminoethyl)-*N*²-(2-(2-((*tert*-butoxycarbonyl)amino)-6-oxo-1,6-dihydro-9*H*-purin-9-yl)acetyl)-*N*^ω-((2,2,4,6,7-pentamethyl-2,3-dihydrobenzofuran-5-yl)sulfonyl)-*D*-arginine (186 mg, 244 μmol, 1.00 equiv.) in acetonitrile (1 mL) was added (9*H*-fluoren-9-yl)methyl (2,5-dioxopyrrolidin-1-yl) carbonate (82.4 mg, 244 μmol, 1.00 equiv.) followed by DIPEA (63.6 μL, 366 μmol, 1.50 equiv.). The solution was stirred for 16 h. The crude mixture was diluted with water (2 mL) and acetonitrile (2 mL), purified *via* HPLC (water+0.1% TFA/acetonitrile+0.1% TFA 95/5 to 5/95, 40 min) and lyophilized. The title compound was obtained as white solid (96.0 mg, 40%).

The analytical data is in agreement with the literature.[124]

***N*²-(2-(((9*H*-Fluoren-9-yl)methoxy)carbonyl)amino)ethyl)-*N*²-(2-(5-methyl-2,4-dioxo-3,4-dihydropyrimidin-1(2*H*)-yl)acetyl)-*N*^ω-((2,2,4,6,7-pentamethyl-2,3-dihydrobenzofuran-5-yl)sulfonyl)-*D*-arginine (b)**

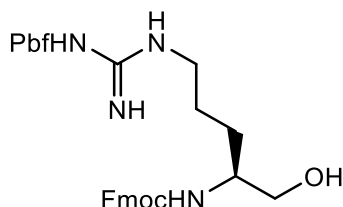


To a solution of *N*²-(2-aminoethyl)-*N*²-(2-(5-methyl-2,4-dioxo-3,4-dihydropyrimidin-1(2*H*)-yl)acetyl)-*N*^ω-((2,2,4,6,7-pentamethyl-2,3-dihydrobenzofuran-5-yl)sulfonyl)-*D*-arginine (93.0 mg, 146 μmol, 1.00 equiv.) in acetonitrile (1 mL) was added (9*H*-fluoren-9-yl)methyl (2,5-dioxopyrrolidin-1-yl) carbonate (49.4 mg, 146 μmol, 1.00 equiv.) followed by DIPEA (38.1 μL, 219 μmol, 1.50 equiv.). The solution was stirred for 16 h. The crude mixture was diluted with water (2 mL) and acetonitrile (2 mL), purified *via* HPLC (water+0.1% TFA/acetonitrile+0.1% TFA 95/5 to 5/95, 40 min) and lyophilized. The title compound was obtained as white solid (96.0 mg, 40%).

The analytical data is in agreement with the literature.[124]

5.3.2 Synthesis of γ -GPNA

(9*H*-Fluoren-9-yl)methyl (*S*)-(1-hydroxy-5-(3-((2,2,4,6,7-pentamethyl-2,3-dihydrobenzofuran-5-yl)sulfonyl)guanidino)pentan-2-yl)carbamate (**b**, **g**, **se**, **w**)



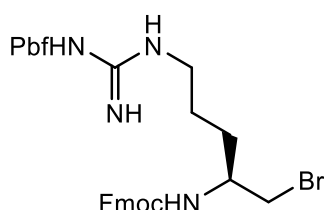
A solution of *N*²-(((9*H*-fluoren-9-yl)methoxy)carbonyl)-*N*^ω-((2,2,4,6,7-pentamethyl-2,3-dihydrobenzofuran-5-yl)sulfonyl)-*L*-arginine (6.00 g, 9.27 mmol, 1.00 equiv.) in 1,2-dimethoxyethane (60 mL) was cooled down to -5°C . *N*-methylmorpholine (1.12 mL, 10.2 mmol, 1.10 equiv.) and *iso*-butyl chloroformate (1.32 mL, 10.2 mmol, 1.10 equiv.) were added successively. After 1 min, a solution of NaBH_4 (1.22 g, 32.4 mmol, 3.50 equiv.) in water (60 mL) was added to the reaction mixture followed by an additional portion of water (500 mL). After 5 min, the aqueous phase was extracted with DCM (4×100 mL). The combined organic phases were washed with 1 M HCl (200 mL), brine (200 mL) and water (200 mL) and dried over Na_2SO_4 . The solvents were removed under reduced pressure and the crude product was purified by column chromatography (DCM/MeOH, 9:1). The title compound was obtained as white solid (4.71 g, 80%).

¹H NMR (DMSO-*d*₆, 400 MHz, 25 °C): δ = 7.89 (d, *J* = 7.4 Hz, 2H), 7.70 (d, *J* = 7.4 Hz, 2H), 7.41 (t, *J* = 7.4 Hz, 2H), 7.32 (t, *J* = 7.4 Hz, 2H), 7.03 (d, *J* = 8.4 Hz, 1H), 6.69 (s, 1H), 6.40 (s, 1H), 5.76 (s, 1H), 4.65 (t, *J* = 5.3 Hz, 1H), 4.37–4.16 (m, 3H), 3.91–3.62 (m, 1H), 3.55–3.35 (m, 2H), 3.24 (s, 1H), 3.07–2.98 (m, 3H), 2.94 (s, 2H), 2.59 (s, 1H), 2.43 (s, 3H), 2.00 (s, 3H), 1.72–1.06 (m, 10H) ppm.

¹³C NMR (DMSO-*d*₆, 100 MHz, 25 °C): δ = 158.8, 156.6, 143.4, 141.2, 140.2, 138.2, 138.0, 132.7, 132.2, 128.8, 127.1, 125.2, 124.7, 121.0, 119.8, 117.6, 107.8, 86.4, 66.9, 62.1, 59.2, 55.4, 47.2, 46.4, 43.2, 28.6, 19.3, 18.0, 12.5 ppm.

HRMS (FAB) Calc. for $\text{C}_{34}\text{H}_{42}\text{N}_4\text{O}_6\text{S}$: 634.2825 *m/z* [*M*+*H*]⁺, found: 635.2903 *m/z*.

(9*H*-Fluoren-9-yl)methyl (S)-(1-bromo-5-(3-((2,2,4,6,7-pentamethyl-2,3-dihydrobenzofuran-5-yl)sulfonyl)guanidino)pentan-2-yl)carbamate (b, g, se, w)



(9*H*-Fluoren-9-yl)methyl (S)-(1-hydroxy-5-(3-((2,2,4,6,7-pentamethyl-2,3-dihydrobenzofuran-5-yl)sulfonyl)guanidino)pentan-2-yl)carbamate (3.61 g, 5.69 mmol, 1.00 equiv.), carbontetrabromide (2.28 g, 6.82 mmol, 1.50 equiv.) and triphenylphosphine (1.79 g, 6.82 mmol, 1.50 equiv.) were dissolved in dry DCM (70 mL) and the mixture was stirred for 16 h. The solvent was removed under reduced pressure and the crude product was purified by column chromatography (EtOAc/CH/MeOH, 4:1:0 to 9:0:1). The title compound was obtained as a white solid (2.42 g, 61%).

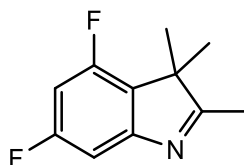
¹H NMR (DMSO-*d*₆, 400 MHz, 25 °C): δ = 7.89 (d, *J* = 7.5 Hz, 2H), 7.69 (dd, *J* = 7.6, 2.8 Hz, 2H), 7.41 (t, *J* = 7.3 Hz, 2H), 7.31 (td, *J* = 7.4, 1.2 Hz, 2H), 6.68 (s, 1H), 6.40 (s, 1H), 5.76 (d, *J* = 3.4 Hz, 1H), 4.62 (s, 1H), 4.41–4.30 (m, 2H), 4.23 (d, *J* = 6.8 Hz, 1H), 3.87–3.66 (m, 1H), 3.52–3.37 (m, 2H), 3.02 (d, *J* = 5.1 Hz, 2H), 2.94 (s, 2H), 2.58 (s, 3H), 2.42 (s, 3H), 2.00 (s, 3H), 1.39 (s, 10H) ppm.

¹³C NMR (DMSO-*d*₆, 100 MHz, 25 °C): δ = 157.9, 156.5, 156.3, 144.3, 141.2, 137.7, 134.7, 131.9, 128.1, 127.5, 125.7, 124.8, 120.6, 116.7, 86.7, 65.7, 61.5, 58.8, 52.2, 47.3, 43.0, 38.0, 30.2, 28.7, 21.2, 19.5, 18.1, 14.6, 12.8 ppm.

HRMS (FAB) Calc. for C₃₄H₄₁BrN₄O₅S: 696,1981 m/z [M+H]⁺, found: 697.2059 m/z.

5.3.3 Synthesis of Novel Spiropyranes

4,6-Difluoro-2,3,3-trimethyl-3H-indole (se, w, b)

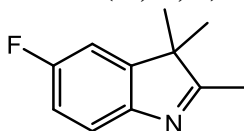


(3,5-Difluorophenyl)hydrazine hydrochloride (3.00 g, 16.6 mmol, 1.00 equiv.) and 3-methylbutan-2-on (2.64 mL, 24.9 mmol, 1.50 equiv.) were dissolved in glacial acetic acid (11 mL) and refluxed for 16 h. The solvents were removed under reduced pressure. The residue was dissolved in DCM (50 mL), washed with NaHCO₃-solution, dried over Na₂SO₄ and the solvent was removed under reduced pressure. The crude product was purified by column chromatography (EtOAc/CH₂Cl₂, 1:4). The title compound was obtained as an orange brown solid (2.03 g, 63%).

¹H NMR (DMSO-*d*₆, 400 MHz, 25 °C): δ = 7.06 (dd, J = 8.4, 2.1 Hz, 1H), 6.61 (td, J = 9.4, 2.1 Hz, 1H), 2.27 (s, 3H), 1.41 (s, 6H) ppm.

¹³C NMR (DMSO-*d*₆, 100 MHz, 25 °C): δ = 191.1, 174.8, 163.0 (dd, J = 245.5, 11.7 Hz), 159.1 (d, J = 14.3 Hz), 157.0–156.1 (m), 126.1 (d, J = 19.5 Hz), 104.1 (dd, J = 24.1, 4.2 Hz), 101.6–99.5 (m), 54.35 (d, J = 3.5 Hz), 21.5, 15.0 ppm.

¹⁹F NMR (CDCl₃-*d*₁, 377 MHz, 25 °C): δ = -111.5, -120.9 ppm.

5-Fluoro-2,3,3-trimethyl-3H-indole (se, w, b)

(4-Fluorophenyl)hydrazine hydrochloride (6.50 g, 40.0 mmol, 1.00 equiv.), 3-methyl-butan-2-one (8.51 mL, 80.0 mmol, 2.00 equiv.) and concentrated sulfuric acid (2.13 mL, 40.0 mmol, 1.00 equiv.) were dissolved in ethanol (60 mL) and stirred for 24 h at 80 °C. The solvent was removed under reduced pressure. The residue was dissolved in DCM (20 mL), washed with NaHCO₃-solution and dried over Na₂SO₄. The solvent was removed under reduced pressure and the crude product was purified by column chromatography (CH:EtOAc, 4:1). The title compound was obtained as brown crystals (5.05 g, 71%).

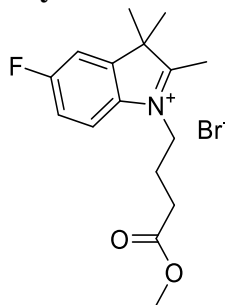
¹H NMR (DMSO-*d*₆, 400 MHz, 25 °C): δ = 7.49-7.36 (m, 1H), 7.03-6.89 (m, 2H), 2.23 (s, 3H), 1.27 (s, 6H) ppm.

¹³C NMR (DMSO-*d*₆, 100 MHz, 25 °C): δ = 187.7 (d, J = 3.6 Hz), 162.4, 160.0, 149.6 (d, J = 2.2 Hz), 147.6 (d, J = 8.6 Hz), 120.5 (d, J = 9.0 Hz), 114.1 (d, J = 23.8 Hz), 109.1 (d, J = 24.1 Hz), 54.1 (d, J = 2.2 Hz), 23.0, 15.4 ppm.

¹⁹F NMR (CDCl₃-*d*₁, 377 MHz, 25 °C): δ = -117.7 ppm.

NEW PRODUCTS

5-Fluoro-1-(4-methoxy-4-oxobutyl)-2,3,3-trimethyl-3*H*-indol-1-ium bromide (se, w, b)

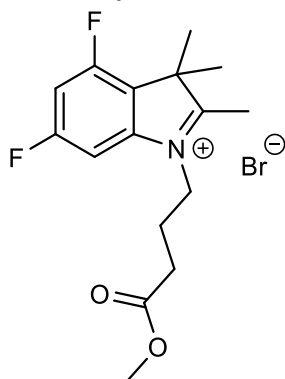


5-Fluoro-2,3,3-trimethyl-3*H*- indole (5.05 g, 28.5 mmol, 1.00 equiv.) and methyl-4-bromobutyrate (10.8 mL, 85.5 mmol, 3.00 equiv.) were dissolved in anhydrous acetonitrile (100 mL) and stirred for 4 d at 90 °C. The solvent was removed under reduced pressure. The residue was washed with MTBE (4 × 50 mL), dissolved in a minimal amount of methanol and precipitated with diethyl ether. The title compound was obtained as a violett solid (9.47 g, 93%).

¹H NMR (DMSO-*d*₆, 400 MHz, 25 °C): δ = 8.09 (dd, *J* = 8.9, 4.1 Hz, 1H), 7.93 – 7.77 (m, 1H), 7.62 – 7.38 (m, 1H), 4.48 (t, *J* = 7.7 Hz, 2H), 2.84 (s, 3H), 2.50 (s, 2H, overlaps with DMSO), 2.21 – 1.87 (m, 2H), 1.55 (s, 6H).

¹³C NMR (DMSO-*d*₆, 100 MHz, 25 °C): δ = 197.4 (d, *J* = 3.1 Hz), 174.2, 163.07 (d, *J* = 247.1 Hz), 144.9 (dd, *J* = 34.3, 10.0 Hz), 138.9, 138.0, 118.1 – 116.1 (m), 112.0 (dd, *J* = 26.1, 21.7 Hz), 54.9, 47.7, 35.5, 30.8, 22.9, 22.3, 22.0, 14.64 ppm.

¹⁹F NMR (CDCl₃-*d*₁, 377 MHz, 25 °C): δ = -111.8 ppm.

4,6-difluoro-1-(4-methoxy-4-oxobutyl)-2,3,3-trimethyl-3H-indol-1-ium bromide (se, w, b)

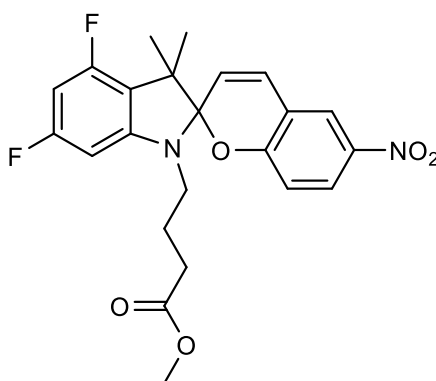
4,6-difluoro-2,3,3-trimethyl-3H-indole (140 mg, 0.717 mmol, 1.00 equiv.) and methyl-4-bromobutyrate (272 μ L, 2.15 mmol, 3.00 equiv.) were dissolved in anhydrous acetonitrile (3 mL) and stirred for 4 d at 90 $^{\circ}$ C. The solvent was removed under reduced pressure. The residue was washed with MTBE (4×5 mL), dissolved in a minimal amount of methanol and precipitated with diethyl ether. The title compound was obtained as light pink solid (172 mg, 64%).

As stated in the text reproduction could not be made so far.

$^1\text{H NMR}$ (CDCl_3 - d_1 , 300 MHz, 25 $^{\circ}$ C): δ = 7.84 (d, J = 7.5 Hz, 1H), 6.93 (t, J = 9.1 Hz, 1H), 4.82 (t, J = 7.8 Hz, 2H), 3.62 (s, 3H), 3.18 (s, 2H), 2.93 (s, 1H), 2.71 (s, 2H), 2.21 (s, 2H), 1.72 (s, 6H) ppm.

NEW PRODUCTS

methyl 4-(4',6'-difluoro-3',3'-dimethyl-6-nitrospiro[chromene-2,2'-indolin]-1'-yl)butanoate (w,b)

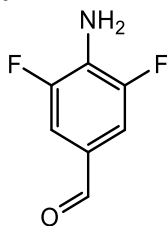


To a solution of 5 nitrosalicylaldehyde (66.6 mg, 0.40 mmol, 1.00 equiv) in anhydrous ethanol (3 mL) a solution of 4,6-difluoro-1-(4-methoxy-4-oxobutyl)-2,3,3-trimethyl-3H-indol-1-ium bromide (150 mg, 0.40 mmol, 1.00 equiv) in anhydrous ethanol (2 mL) was added slowly over a period of 20 min. After the addition was complete the mixture was set to reflux for 24 h. The solvent were evaporated to dryness and the crude was purified with column chromatograp hy (EtOAc:MeOH 1:0→20:80) to yield a red solid (10 mg, 6%).

¹H NMR (DMSO-*d*₆, 400 MHz, 25 °C): δ = 8.24 (d, *J* = 2.8 Hz, 1H), 8.03 (dt, *J* = 9.0, 2.1 Hz, 1H), 7.26 (dd, *J* = 10.4, 7.0 Hz, 1H), 6.96 (t, *J* = 9.2 Hz, 1H), 6.62–6.38 (m, 2H), 5.99 (d, *J* = 10.4 Hz, 1H), 3.54 (d, *J* = 1.6 Hz, 2H), 3.17 (d, *J* = 1.6 Hz, 4H), 2.70 (d, *J* = 1.6 Hz, 2H), 1.91 (d, *J* = 1.6 Hz, 1H), 1.34–1.22 (m, 3H), 1.20–1.13 (m, 3H) ppm.

5.3.4 Synthesis of Azobenzenes

4-Amino-3,5-difluorobenzaldehyde (b)



To a solution of 2,6-difluoroaniline (514 mg, 4.00 mmol, 1.00 equiv.) in DMSO (10 mL) was added CuCl₂ (1.34 g, 10.0 mmol, 2.50 equiv.) and concentrated HCl (2.50 mL). The mixture was stirred for 16 h at 130 °C. The reaction mixture was poured onto ice-water (200 mL), neutralized with NaOH and filtered. The aqueous phase was extracted with DCM (4 × 100 mL). The combined organic phases were washed with brine (100 mL), dried over Na₂SO₄ and the solvents were removed under reduced pressure. The title compound was obtained as a light yellow (627 mg, quant.).

¹H NMR (DMSO-*d*₆, 400 MHz, 25 °C): δ = 9.65 (t, J = 2.0 Hz, 1H), 7.45 (dd, J = 6.2, 3.2 Hz, 2H), 6.45 (s, 2H) ppm.

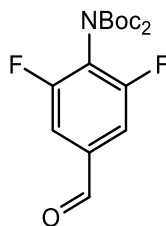
¹³C NMR (DMSO-*d*₆, 100 MHz, 25 °C): δ = 189.7 (t, J = 2.9 Hz), 150.5, 133.1 (t, J = 16.7 Hz), 122.8 (t, J = 6.46 Hz), 112.9 (dd, J = 13.7, 6.5 Hz) ppm.

¹⁹F NMR (CDCl₃-*d*₁, 377 MHz, 25 °C): δ = -131.4 ppm.

HRMS (EI⁺): *m/z* calc. for C₇H₅N₁O₁F₂: 157.0340 Da [M]⁺, found: 157.0339 Da (Δ = 0.1 ppm).

NEW PRODUCTS

Di-*tert*-butyl (2,6-difluoro-4-formylphenyl)dicarbamate

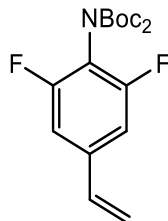


4-Amino-3,5-difluorobenzaldehyde (500 mg, 3.00 mmol, 1.00 equiv.) was dissolved in acetonitrile (10 mL). Di-*tert*-butyl dicarbonate (2.00 g, 9.00 mmol, 3.00 equiv.) and DMAP (18.3 mg, 0.15 mmol, 0.05 equiv.) were added and the mixture was stirred for 16 h. The solvent was removed under reduced pressure and the residue was purified by column chromatography(DCM). The title compound was obtained as a light yellow solid (337 mg, 31%).

$^1\text{H NMR}$ (CDCl_3 - d_1 , 400 MHz, 25 °C): δ = 9.94 (t, J = 1.7 Hz, 1H), 7.47 (dd, J = 7.0 Hz, 2H), 1.43 (s, 18H) ppm.

$^{13}\text{C NMR}$ ($\text{DMSO-}d_6$, 100 MHz, 25 °C): δ = 188.9, 158.6 (dd, J = 251.5, 3.6 Hz), 149.3, 136.6, 112.1 (d, J = 24.3 Hz), 84.2, 27.7 ppm.

HRMS (EI+): m/z calc. for $\text{C}_{17}\text{H}_{22}\text{N}_1\text{O}_5\text{F}_2$: 358.1465 Da [M], found: 358.1466 Da (Δ = 0.1 ppm).

Di-*tert*-butyl (2,6-difluoro-4-ethylenphenyl)dicarbamate

Di-*tert*-butyl (2,6-difluoro-4-formylphenyl)dicarbamate (166 mg, 464 μ mol, 1.00 equiv.) was dissolved in DCM (10 mL). Methyl triphenylphosphonium bromide (332 mg, 928 μ mol, 2.00 equiv.) and DBU (156 μ L, 1.02 mmol, 2.20 equiv.) were added and the mixture was stirred for 6 h at 40 $^{\circ}$ C. The solvent was removed under reduced pressure and the residue was purified by column chromatography (DCM). The title compound was obtained as a yellowish oil (44.0 mg, 27%).

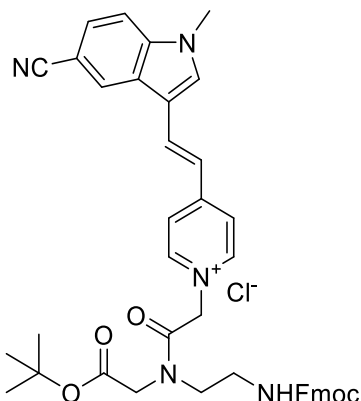
$^1\text{H NMR}$ (CDCl_3 - d_1 , 400 MHz, 25 $^{\circ}$ C): δ = 6.96 (d, J = 8.5 Hz, 1H), 6.61 (dd, J = 17.4, 10.8 Hz, 1H), 5.76 (d, J = 17.5 Hz, 1H), 5.38 (d, J = 10.8 Hz, 1H) 1.42 (s, 18H) ppm.

$^{13}\text{C NMR}$ (CDCl_3 - d_1 , 100 MHz, 25 $^{\circ}$ C): δ = 158.2 (dd, J = 250.5, 5.1 Hz) 150.0, 139.1 (t, J = 9.2 Hz), 134.7, 116.8, 108.9 (dd, J = 18.5, 6.4 Hz), 83.5, 27.7 ppm.

$^{19}\text{F NMR}$ (CDCl_3 - d_1 , 377 MHz, 25 $^{\circ}$ C): δ = -119.8 ppm.

5.3.5 Synthesis of Dye-PNA

(E)-1-(2-((2-(((9H-Fluoren-9-yl)methoxy)carbonyl)amino)ethyl)(2-(*tert*-butoxy)-2-oxoethyl)amino)-2-oxoethyl)-4-(2-(5-cyano-1-methyl-1*H*-indol-3-yl)vinyl)pyridin-1-ium chloride (b)

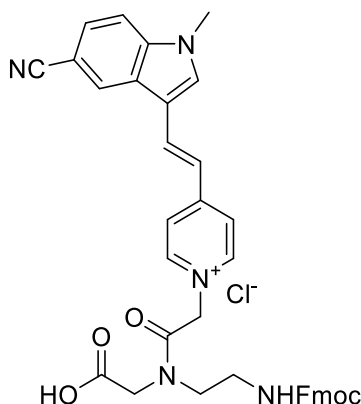


To a solution of (*E*)-1-(carboxymethyl)-4-(2-(6-cyano-1-methyl-1*H*-indol-3-yl)vinyl)pyridin-1-ium chloride (706 mg, 2.00 mmol, 1.00 equiv.) and *tert*-butyl (2-(((9*H*-fluoren-9-yl)methoxy)carbonyl)amino)ethyl)glycinate (791 mg, 2.00 mmol, 1.00 equiv.) in dry DMF (1 mL) was added diisopropylmethanediimine (1.55 mL, 1.00 mmol, 5.00 equiv.). The mixture was stirred for 5 h at room temperature. Afterwards, the mixture was diluted with water (2 mL) and acetonitrile (2 mL), purified *via* HPLC (water+0.1% TFA/acetonitrile+0.1% TFA 95/5 to 5/95, 40 min) and lyophilized. The title compound was obtained as an orange red solid (620 mg, 42%).

¹H NMR (DMSO-*d*₆, 400 MHz, 25 °C): δ = 8.41–8.19 (m, 2H), 7.98–7.64 (m, 6H), 7.63–7.50 (m, 2H), 7.51–7.42 (m, 4H), 7.40–7.19 (m, 4H), 7.14–6.86 (m, 2H), 5.55 (s, 1H), 5.35 (s, 1H), 4.43–4.23 (m, 3H), 4.15 (s, 3H), 3.65–3.50 (m, 2H), 3.40 (s, 2H), 3.35–3.20 (m, 3H), 1.19 (s, 9H) ppm.

¹³C NMR (DMSO-*d*₆, 100 MHz, 25 °C): δ = 171.1, 166.6, 166.0, 161.3, 161.0, 157.6, 155.6, 144.5, 143.8, 141.2, 141.1, 139.8, 136.9, 135.0, 127.5, 126.8, 125.6, 125.4, 125.2, 124.8, 124.7, 124.6, 121.7, 119.8, 119.6, 118.1, 113.6, 111.4, 104.1, 68.1, 66.4, 59.3, 38.6, 38.1, 32.4, 29.7, 21.8, 21.7, 18.0 ppm.

(*E*)-1-(2-((2-(((9*H*-Fluoren-9-yl)methoxy)carbonyl)amino)ethyl)(carboxymethyl)amino)-2-oxoethyl)-4-(2-(5-cyano-1-methyl-1*H*-indol-3-yl)vinyl)pyridine-1-ium chloride (b)



To a solution of (*E*)-1-(2-((2-(((9*H*-fluoren-9-yl)methoxy)carbonyl)amino)ethyl)(2-(*tert*-butoxy)-2-oxoethyl)amino)-2-oxoethyl)-4-(2-(5-cyano-1-methyl-1*H*-indol-3-yl)vinyl)pyridin-1-ium chloride (620 mg, 847 μ mol, 1.00 equiv.) in DCM (5 mL) was added TFA (5 mL). The mixture was stirred for 5 h at room temperature. Toluene (10 mL) was added and the solvents were removed under reduced pressure. The residue was dissolved in acetonitrile (3 mL) and water (1 mL), purified *via* HPLC (water+0.1% TFA/acetonitrile+0.1% TFA 95/5 to 5/95, 40 min) and lyophilized. The title compound was obtained as an orange-red solid (544 mg, 95%).

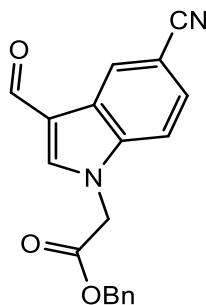
¹H NMR (MeOD-*d*₄, 400 MHz, 25 °C): δ = 8.39–8.17 (m, 2H), 7.95–7.63 (m, 4H), 7.57 (dd, *J* = 15.3, 7.5 Hz, 2H), 7.51–7.40 (m, 4H), 7.39–7.29 (m, 2H), 7.29–7.18 (m, 2H), 7.09–6.88 (m, 1H), 5.55 (s, 1H), 5.35 (s, 1H), 4.46–4.22 (m, 3H), 4.15 (s, 4H), 3.80 (s, 3H), 3.63–3.49 (m, 2H), 3.48–3.36 (m, 2H), 3.33–3.25 (m, 2H) ppm.

¹³C NMR (MeOD-*d*₄, 100 MHz, 25 °C): δ = 171.1, 166.6, 166.1, 161.3, 161.0, 157.6, 155.6, 144.6, 143.9, 143.8, 141.2, 141.1, 139.8, 137.0, 136.9, 135.0, 134.9, 127.5, 126.8, 125.7, 125.4, 125.3, 124.8, 124.7, 121.7, 121.6, 119.8, 119.6, 118.1, 113.6, 111.4, 104.0, 66.4, 59.4, 38.6, 32.4, 21.7, 18.0 ppm.

HRMS (EI⁺): *m/z* calcd for C₃₈H₃₄N₅O₅: 640.2561 Da [M], found: 640.2560 Da (Δ = 0.1 ppm).

NEW PRODUCTS

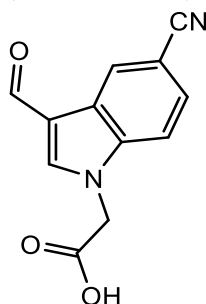
Benzyl 2-(5-cyano-3-formyl-1*H*-indol-1-yl)acetate (b)



To a solution of 3-formyl-1*H*-indole-5-carbonitrile (340 mg, 2.00 mmol, 1.00 equiv.) in dry DMF (3 mL) was added NaH (27.9 mg of the 60% dispersion in mineral oil, 8.00 mmol, 4.00 equiv.) in two portions at 0 °C. The mixture was stirred for 2 h at 0 °C before bromoacetic acid benzyl ester (475 μ L, 3.00 mmol, 1.50 equiv.) was added dropwise over a period of 15 min at 0 °C. Subsequently, the cooling was removed and the mixture was stirred for 16 h. The solvents were removed under reduced pressure. The residue was dissolved in acetonitrile (3 mL) and water (1 mL), purified *via* HPLC (water+0.1% TFA/acetonitrile+0.1% TFA 95/5 to 5/95, 40 min) and lyophilized. The title compound was obtained as a white solid (240 mg, 38%).

¹H NMR (DMSO-*d*₆, 400 MHz, 25 °C): δ = 10.01 (s, 1H), 8.50 (s, 2H), 7.83 (d, *J* = 8.6 Hz, 1H), 7.71 (dd, *J* = 8.6, 1.6 Hz, 1H), 7.45-7.31 (m, 5H), 5.47 (s, 2H), 5.21 (s, 2H) ppm.

¹³C NMR (DMSO-*d*₆, 100 MHz, 25 °C): δ = 185.9, 168.4, 143.8, 139.8, 135.9, 128.9, 128.8, 128.5, 127.2, 126.3, 124.7, 120.2, 118.0, 113.3, 105.5, 67.3, 48.3 ppm.

2-(5-Cyano-3-formyl-1*H*-indol-1-yl)acetic acid (b)

Benzyl 2-(5-cyano-3-formyl-1*H*-indol-1-yl)acetate (240 mg, 75.5 mmol, 1.00 equiv.) was dissolved in acetonitrile (3 mL). A solution of lithium hydroxide (7.25 mg, 302 mmol, 4.00 equiv.) in water (1 mL) and was added to the reaction mixture and stirred for 1 h at room temperature. The solvent was removed under reduced pressure. The residue was purified *via* HPLC (water+0.1% TFA/acetonitrile+0.1% TFA 95/5 to 5/95, 40 min) and lyophilized. The title compound was obtained as a white solid (88.0 mg, 51%).

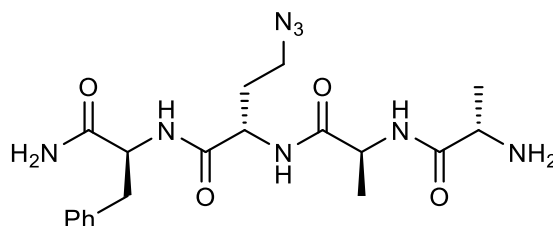
¹H NMR (DMSO-*d*₆, 400 MHz, 25 °C): δ = 9.99 (s, 1H), 7.47 (s, 2H), 7.80 (d, J = 8.6 Hz, 1H), 7.69 (dd, J = 8.6, 1.7 Hz, 1H), 5.26 (s, 2H) ppm.

¹³C NMR (DMSO-*d*₆, 100 MHz, 25 °C): δ = 185.7, 169.8, 143.9, 139.8, 127.1, 126.2, 124.7, 120.2, 117.9, 113.2, 105.3, 48.4 ppm.

5.3.6 Synthesis of PNA-Oligomers and Oligo-Peptides

The following PNA-oligomers were synthesized on the rink resin with a decreased loading of 0.1 mmol/g following the Fmoc-protocol if not stated otherwise. 5.00 equivalents of the *D*-Lysine (*D*-Lys) and PNA-monomers were used relative to the pure resin. Coupling reagents (HBTU, HOBt, DIPEA, 2,6-lutidine) were used in equimolar amounts to the PNA-monomers (5.00 equiv.). For implementing buildingblocks with stereo information at the α -carbon atom (e.g. *D*-Lysine) additionally HOBt (5 equiv.) was implemented to avoid racemization. The single monomers are abbreviated with their respective first letter (A, C, G, T). The guanidine modified GPNA are labelled with '*' (e.g. A*) and dye-bearing building blocks are abbreviated with 'Dye'. For the coupling of the dye-monomers to the growing chain, DIC (5.00 equiv. relative to the monomer) and HOBt (10.0 equiv.) were used as coupling reagents. The same conditions were employed for the coupling of the building block successive the dye-building block.

(*S*)-N-((*S*)-1-amino-1-oxo-3-phenylpropan-2-yl)-2-((*S*)-2-((*S*)-2-aminopropanamido)propanamido)-4-azidobutanamide



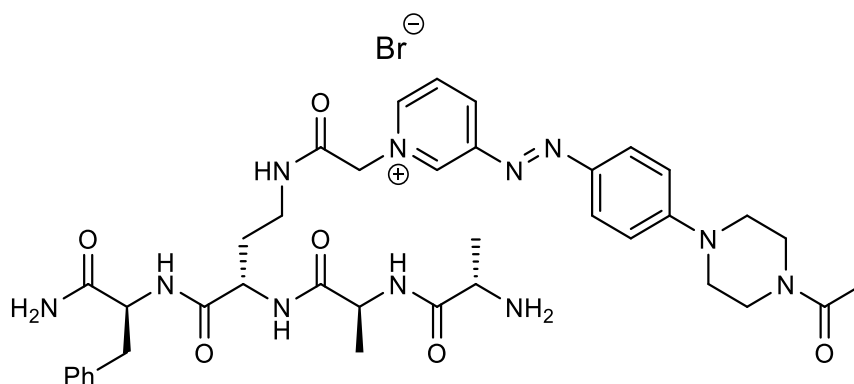
Rink resin (200 mg, 0.04 mmol, 1.00 equiv.) was swollen with CH_2Cl_2 for 1 h, filtered off and treated with 20% piperidine in DMF (5 mL) to remove the N-terminal Fmoc protecting group. After extensive washing with DMF and CH_2Cl_2 , the resin was shook with a coupling mixture comprised of (*S*)-*N*-Fmoc-2-amino-4-azidobutanoic acid (73.3 mg, 0.20 mmol, 5.00 eq.), HBTU (75.9 mg, 0.20 μmol , 5.00 eq.), DIPEA (65 μL , 0.20 μmol , 5.00 eq.) and 2,6-lutidine (65 μL , 0.30 μmol , 7.50 equiv.) in NMP (5 mL) for 2 h. The resin was washed with CH_2Cl_2 and treated with the 'capping mixture' mentioned above (previous procedure) to acetylate the potentially unreacted amino groups. The same procedure (*N*-terminal Fmoc group deprotection, coupling and acetylation) was further performed with Fmoc-Ala-OH (62.3 mg, 0.20 mmol, 5.00 eq.) and Boc-Ala-OH (73.3 mg, 0.20 mmol, 5.00 eq.) (and identical amounts of HBTU, DIPEA and 2,6-lutidine). In order to check the outcome of the synthesis and purity of the product on the solid support, some resin beads were treated with 100 μL of 20% *m*-cresol solution in TFA for 1 h, to cleave the oligopeptide

from the solid support and concomitantly deprotect the N-terminal Boc-group. The polymeric beads were filtered off and the remaining solution was mixed with Et₂O (1 mL) in an Eppendorf tube (1.5 mL), spun down with a centrifuge (5 min, 14,000 rpm) and the resulting pellet was washed with fresh Et₂O (1 mL). It was dissolved in 100 μL of MeCN:H₂O 1:1 and used for MALDI-MS as well as HPLC analysis, which both confirmed the purity and the expected composition of the oligopeptide.

MS (MALDI-TOF): *m/z* calc. for C₁₉H₂₈N₈O₄: 433.2234 Da [M+H], found: 433.2401 Da.

HPLC: water+0.1% TFA/acetonitrile+0.1%TFA 95:5 to 5:95 in 30 min, flow rate: 1.00 mL/min, *t*_{Ret} = 11.6 min.

3-((E)-(4-(4-acetylpiperazin-1-yl)phenyl)diazenyl)-1-(2-(((S)-4-(((S)-1-amino-1-oxo-3-phenylpropan-2-yl)amino)-3-((S)-2-((S)-2-aminopropanamido)propanamido)-4-oxobutyl)amino)-2-oxoethyl)pyridin-1-ium bromide



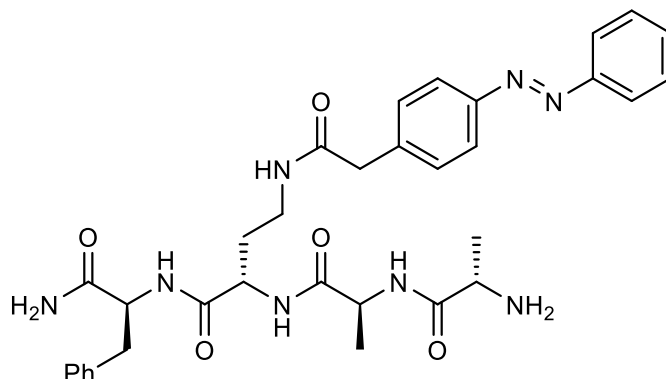
Boc-Ala-Ala-Aha-Phe-Rink resin (120 mg, 0.02 mmol, 1.00 equiv.) was treated with 17% solution of tri-*n*-butylphosphine in a mixture of NMP:THF:water (10:9:1) (3.0 mL) for 4 h to reduce the azide to an amino group. After extensive washing with THF and CH₂Cl₂, the resin was shook with a coupling mixture of the (*E*)-3-((4-(4-acetylpiperazin-1-yl)phenyl)diazenyl)-1-(carboxymethyl)pyridin-1-ium bromide (173 mg, 0.400 mmol, 20.0 equiv.), HOBt (216 mg, 1.60 mmol, 80.0 eq.) and DIC (253 mg, 2.00 μmol, 100 eq.) in NMP (5 mL) overnight and then extensively washed with DMF and CH₂Cl₂. In order to cleave the product from resin and remove the Boc protecting group, the beads were treated with 500 μL of 20% *m*-cresol in TFA for 2 h. The resulting solution was filtered to separate the remaining resin and mixed with 10 mL Et₂O to precipitate the product. The crude product was isolated by spinning the mixture in a 50 mL Falcon tube (20 min centrifugation, 8,000 rpm) and washing the pellet with fresh Et₂O (20 mL). The product was purified *via* preparative HPLC.

HRMS (ESI+): *m/z* calc. for C₃₈H₅₀N₁₁O₆₊: 756.3940 Da [M]₊, 757.3974 Da [41%], found: 756.3976 Da (Δ = 4.8 ppm), 757.3951 Da (Δ = 3.0 ppm).

NEW PRODUCTS

HPLC: water+0.1% TFA/acetonitrile+0.1%TFA 95:5 to 5:95 in 30 min, flow rate: 1.00 mL/min, $t_{\text{ret}} = 5.6$ min.

(S)-N-((S)-1-amino-1-oxo-3-phenylpropan-2-yl)-2-((S)-2-((S)-2-aminopropanamido)propanamido)-4-(2-(4-((E)-phenyldiazenyl)phenyl)acetamido)butanamide



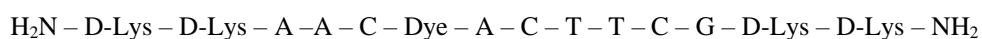
Boc-Ala-Ala-Aha-Phe-Rink resin (120 mg, 0.02 mmol, 1.00 equiv.) was treated with 17% solution of tri-*n*-butylphosphine in a mixture of NMP:THF:water (10:9:1) (3.0 mL) for 4 h to reduce the azide to an amino group. After extensive washing with THF and CH₂Cl₂ the resin was shook with a coupling mixture of the (*E*)-2-(4-(phenyldiazenyl)phenyl)acetic acid (97.0 mg, 0.400 mmol, 20.0 equiv.), HOBt (216 mg, 1.60 mmol, 80.0 eq.) and DIC (253 mg, 2.00 μmol, 100 eq.) in NMP (5 mL) overnight, and then extensively washed with DMF and CH₂Cl₂. In order to cleave the product from resin and remove the Boc protecting group, the beads were treated with 500 μL of 20% *m*-cresol in TFA for 2 h. The resulting solution was filtered to separate the remaining resin and mixed with 10 mL Et₂O to precipitate the product. The crude product was isolated by spinning the mixture in a 50 mL Falcon tube (20 min centrifugation, 8,000 rpm) and washing the pellet with fresh Et₂O (20 mL). The product was purified *via* preparative HPLC.

HRMS (ESI+): *m/z*. calc. For C₃₃H₄₁N₈O₅+: 629.3194 Da [M+H]⁺, found: 629.3196 Da (Δ = 0.3 ppm).

HPLC: water+0.1% TFA:acetonitrile+0.1%TFA 95:5 to 5:95 in 30 min, flow rate: 1.00 mL/min, $t_{\text{ret}} = 6.82$ min (*cis*-conformation); $t_{\text{ret}} = 7.30$ min (*trans*-conformation).

BT 403

4-((*E*)-2-(5-cyano-1-methyl-1*H*-indol-3-yl)vinyl)-1-((44*R*,47*R*)-47,51-diamino-15,33-bis(2-(4-amino-2-oxopyrimidin-1(2*H*)-yl)acetyl)-3-((22*R*,25*R*)-29-amino-6-(2-(4-amino-2-oxopyrimidin-1(2*H*)-yl)acetyl)-12,18-bis(2-(6-amino-9*H*-purin-9-yl)acetyl)-22-(4-aminobutyl)-25-carbamoyl-2,8,14,20,23-pentaoxo-3,6,9,12,15,18,21,24-octaazanonacosyl)-39-(2-(2-amino-6-oxo-1,6-dihydro-9*H*-purin-9-yl)acetyl)-9-(2-(6-amino-9*H*-purin-9-yl)acetyl)-44-(4-aminobutyl)-21,27-bis(2-(5-methyl-2,4-dioxo-3,4-dihydropyrimidin-1(2*H*)-yl)acetyl)-2,7,13,19,25,31,37,43,46-nonaoxo-3,6,9,12,15,18,21,24,27,30,33,36,39,42,45-pentadecaazahenpentacontyl)pyridin-1-ium chloride



25.0 mg of rink resin was used to synthesize BT 403. At the end of the synthesis sequence before deprotection, the resin was split in half. One part was stored in the fridge and the other part was treated with a 20%-solution of piperidine in DMF to remove the Fmoc protecting group. TFA was added to the resin (1 mL) and the mixture was shaken for 1 h. The crude product was precipitated in diethyl ether (10 mL). The resin was treated 3 times with TFA to ensure the full cleavage of the oligo-PNA. The mixture was centrifuged and the liquid phase was removed *via* decantation. The crude product was dissolved in a minimum amount of water (~500 μl) and purified *via* semipreparative HPLC (water+0.1% TFA/acetonitrile+0.1% TFA 95/5 to 5/95, 30 min). 256 μg was obtained as a yellow solid.

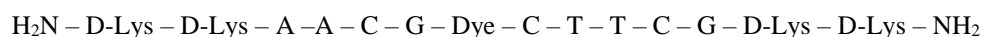
MS (MALDI-TOF): m/z calc. for $\text{C}_{143}\text{H}_{192}\text{N}_{67}\text{O}_{31}$: 3331.5389 Da [M^+], found: 3333.0246 Da.

HPLC: water+0.1% TFA/acetonitrile+0.1% TFA 95:5 to 5:95 in 30 min, flow rate: 1.00 mL/min, $t_{\text{Ret}} = 11.4$ min.

NEW PRODUCTS

BT 404

4-((*E*)-2-(5-cyano-1-methyl-1*H*-indol-3-yl)vinyl)-1-((38*R*,41*R*)-41,45-diamino-3-((28*R*,31*R*)-35-amino-12-(2-(4-amino-2-oxopyrimidin-1(2*H*)-yl)acetyl)-6-(2-(6-amino-4-oxo-4,5-dihydro-1*H*-imidazo[4,5-*c*]pyridin-1-yl)acetyl)-18,24-bis(2-(6-amino-9*H*-purin-9-yl)acetyl)-28-(4-aminobutyl)-31-carbamoyl-2,8,14,20,26,29-hexaoxo-3,6,9,12,15,18,21,24,27,30-decaazapentatriacontyl)-9,27-bis(2-(4-amino-2-oxopyrimidin-1(2*H*)-yl)acetyl)-33-(2-(2-amino-6-oxo-1,6-dihydro-9*H*-purin-9-yl)acetyl)-38-(4-aminobutyl)-15,21-bis(2-(5-methyl-2,4-dioxo-3,4-dihydropyrimidin-1(2*H*)-yl)acetyl)-2,7,13,19,25,31,37,40-octaoxo-3,6,9,12,15,18,21,24,27,30,33,36,39-tridecaazapatetracontyl)pyridin-1-ium chloride



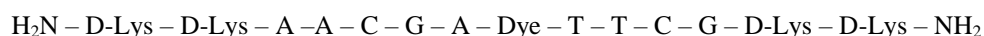
25.0 mg of a rink resin was used to synthesize BT 404. At the end of the synthesis sequence before deprotection, the resin was split in half. One part was stored in the fridge and the other part was treated with a 20%-solution of piperidine in DMF to remove the Fmoc protecting group. TFA was added to the resin (1 mL) and the mixture was shaken for 1 h. The crude product was precipitated in diethyl ether (10 mL). The resin was treated 3 times with TFA to ensure the full cleavage of the oligo-PNA. The mixture was centrifuged and the liquid phase was removed *via* decantation. The crude product was dissolved in a minimum amount of water (~500 μ l) and purified *via* semipreparative HPLC (water+0.1% TFA/acetonitrile+0.1% TFA 95/5 to 5/95, 30 min). 328 μ g was obtained as a yellow solid.

MS (MALDI-TOF): *m/z* calc. for C₁₄₄H₁₉₃N₆₄O₃₃: 3346.5386 Da [M⁺], found: 3340.1529 Da.

HPLC: water+0.1% TFA/acetonitrile+0.1% TFA 95:5 to 5:95 in 30 min, flow rate: 1.00 mL/min, $t_{\text{ret}} = 10.7$ min.

BT 405

1-((37R,40R)-44-amino-21-(2-(4-amino-2-oxopyrimidin-1(2H)-yl)acetyl)-15-(2-(6-amino-4-oxo-4,5-dihydro-1H-imidazo[4,5-c]pyridin-1-yl)acetyl)-9,27,33-tris(2-(6-amino-9H-purin-9-yl)acetyl)-37-(4-aminobutyl)-40-carbamoyl-3-((29R,32R)-32,36-diamino-18-(2-(4-amino-2-oxopyrimidin-1(2H)-yl)acetyl)-24-(2-(2-amino-6-oxo-1,6-dihydro-9H-purin-9-yl)acetyl)-29-(4-aminobutyl)-6,12-bis(2-(5-methyl-2,4-dioxo-3,4-dihydropyrimidin-1(2H)-yl)acetyl)-4,10,16,22,28,31-hexaoxo-3,6,9,12,15,18,21,24,27,30-decaazahexatriacontyl)-2,5,11,17,23,29,35,38-octaoxo-3,6,9,12,15,18,21,24,27,30,33,36,39-tridecaazatetracontyl)-4-((E)-2-(5-cyano-1-methyl-1H-indol-3-yl)vinyl)pyridin-1-ium chloride



25.0 mg of a rink resin was used to synthesize BT 405. At the end of the synthesis sequence before deprotection, the resin was split in half. One part was stored in the fridge and the other part was treated with a 20%-solution of piperidine in DMF to remove the Fmoc protecting group. TFA was added to the resin (1 mL) and the mixture was shaken for 1 h. The crude product was precipitated in diethyl ether (10 mL). The resin was treated 3 times more with TFA to ensure the full cleavage of the oligo-PNA. The mixture was centrifuged and the liquid phase was removed *via* decantation. The crude product was dissolved in a minimum amount of water (~500 μ l) and purified *via* semipreparative HPLC (water+0.1% TFA/acetonitrile+0.1% TFA 95/5 to 5/95, 30 min). 222 μ g was obtained as a yellow solid.

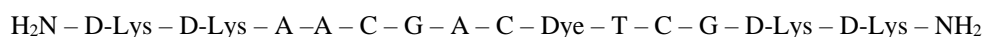
MS (MALDI-TOF): m/z calc. for $\text{C}_{145}\text{H}_{193}\text{N}_{66}\text{O}_{32}$: 3370.5498 Da [M+], found: 3363.1466 Da.

HPLC: water+0.1% TFA/acetonitrile+0.1%TFA 95:5 to 5:95 in 30 min, flow rate: 1.00 mL/min, $t_{\text{Ret}} = 11.1$ min.

NEW PRODUCTS

BT 406

1-((43R,46R)-50-amino-9,27-bis(2-(4-amino-2-oxopyrimidin-1(2H)-yl)acetyl)-21-(2-(6-amino-4-oxo-4,5-dihydro-1H-imidazo[4,5-c]pyridin-1-yl)acetyl)-15,33,39-tris(2-(6-amino-9H-purin-9-yl)acetyl)-43-(4-aminobutyl)-46-carbamoyl-3-((23R,26R)-26,30-diamino-12-(2-(4-amino-2-oxopyrimidin-1(2H)-yl)acetyl)-18-(2-(2-amino-6-oxo-1,6-dihydro-9H-purin-9-yl)acetyl)-23-(4-aminobutyl)-6-(2-(5-methyl-2,4-dioxo-3,4-dihydropyrimidin-1(2H)-yl)acetyl)-4,10,16,22,25-pentaoxo-3,6,9,12,15,18,21,24-octaazatriacontyl)-2,5,11,17,23,29,35,41,44-nonaoxo-3,6,9,12,15,18,21,24,27,30,33,36,39,42,45-pentadecaazapentacontyl)-4-((E)-2-(5-cyano-1-methyl-1H-indol-3-yl)vinyl)pyridin-1-ium chloride



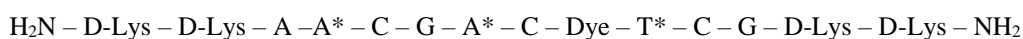
25.0 mg of a rink resin was used to synthesize BT 406. At the end of the synthesis sequence before deprotection, the resin was split in half. One part was stored in the fridge and the other part was treated with a 20%-solution of piperidine in DMF to remove the Fmoc protecting group. TFA was added to the resin (1 mL) and the mixture was shaken for 1 h. The crude product was precipitated in diethyl ether (10 mL). The resin was treated 3 times more with TFA to ensure the full cleavage of the oligo-PNA. The mixture was centrifuged and the liquid phase was removed *via* decantation. The crude product was dissolved in a minimum amount of water (~500 µl) and purified *via* semipreparative HPLC (water+0.1% TFA/acetonitrile+0.1% TFA 95/5 to 5/95, 30 min). 480 µg was obtained as a yellow solid.

MS (MALDI-TOF): m/z calc. for $\text{C}_{144}\text{H}_{192}\text{N}_{67}\text{O}_{31}$: 3355.5502 Da [M+], found: 3347.6569 Da.

HPLC: water+0.1% TFA/acetonitrile+0.1% TFA 95:5 to 5:95 in 30 min, flow rate: 1.00 mL/min, $t_{\text{ret}} = 10.5$ min.

BT 473

1-((16R,34R,43R,46R)-50-amino-9,27-bis(2-(4-amino-2-oxopyrimidin-1(2H)-yl)acetyl)-21-(2-(6-amino-4-oxo-4,5-dihydro-1H-imidazo[4,5-c]pyridin-1-yl)acetyl)-15,33,39-tris(2-(6-amino-9H-purin-9-yl)acetyl)-43-(4-aminobutyl)-46-carbamoyl-3-((11R,23R,26R)-26,30-diamino-12-(2-(4-amino-2-oxopyrimidin-1(2H)-yl)acetyl)-18-(2-(2-amino-6-oxo-1,6-dihydro-9H-purin-9-yl)acetyl)-23-(4-aminobutyl)-11-(3-guanidinopropyl)-6-(2-(5-methyl-2,4-dioxo-3,4-dihydropyrimidin-1(2H)-yl)acetyl)-4,10,16,22,25-pentaoxo-3,6,9,12,15,18,21,24-octaazatriacontyl)-16,34-bis(3-guanidinopropyl)-2,5,11,17,23,29,35,41,44-nonaoxo-3,6,9,12,15,18,21,24,27,30,33,36,39,42,45-pentadecaazapentacontyl)-4-((E)-2-(5-cyano-1-methyl-1H-indol-3-yl)vinyl)pyridin-1-ium chloride



25.0 mg of a rink resin was used to synthesize BT 473. At the end of the synthesis sequence before deprotection, the resin was split in half. One part was stored in the fridge and the other part was treated with a 20%-solution of piperidine in DMF to remove the Fmoc protecting group. TFA was added to the resin (1 mL) and the mixture was shaken for 1 h. The crude product was precipitated in diethyl ether (10 mL). The resin was treated 3 times more with TFA to ensure the full cleavage of the oligo-PNA. The mixture was centrifuged and the liquid phase was removed *via* decantation. The crude product was dissolved in a minimum amount of water (~500 µl) and purified *via* semipreparative HPLC (water+0.1% TFA/acetonitrile+0.1% TFA 95/5 to 5/95, 30 min). 480 µg was obtained as a yellow solid.

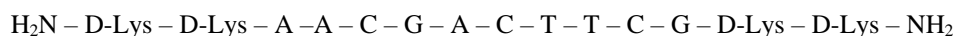
MS (MALDI-TOF): m/z calc. for $\text{C}_{156}\text{H}_{219}\text{N}_{76}\text{O}_{31}$: 3652.7891 Da $[\text{M}^+]$, found: 3647.7400 Da.

HPLC: water+0.1% TFA/acetonitrile+0.1%TFA 95:5 to 5:95 in 30 min, flow rate: 1.00 mL/min, $t_{\text{Ret}} = 11.0$ min.

NEW PRODUCTS

BT540

(R)-2,6-diamino-N-((5R,8R,71R)-1,75-diamino-12,18,60-tris(2-(4-amino-2-oxopyrimidin-1(2H)-yl)acetyl)-42,54,66-tris(2-(6-amino-9H-purin-9-yl)acetyl)-8-(4-aminobutyl)-5-carbamoyl-24,30,36,48-tetrakis(2-(5-methyl-2,4-dioxo-3,4-dihydropyrimidin-1(2H)-yl)acetyl)-7,10,16,22,28,34,40,46,52,58,64,70-dodecaoxo-6,9,12,15,18,21,24,27,30,33,36,39,42,45,48,51,54,57,60,63,66,69-docosaazapentaheptacontan-71-yl)hexanamide



25.0 mg of a rink resin was used to synthesize BT 540. At the end of the synthesis sequence before deprotection, the resin was split in half. One part was stored in the fridge and the other part was treated with a 20%-solution of piperidine in DMF to remove the Fmoc protecting group. TFA was added to the resin (1 mL) and the mixture was shaken for 1 h. The crude product was precipitated in diethyl ether (10 mL). The resin was treated 3 times more with TFA to ensure the full cleavage of the oligo-PNA. The mixture was centrifuged and the liquid phase was removed *via* decantation. The crude product was dissolved in a minimum amount of water (~500 µl) and purified *via* semipreparative HPLC (water+0.1% TFA/acetonitrile+0.1% TFA 95/5 to 5/95, 30 min). 364 µg was obtained as a white solid.

MS (MALDI-TOF): m/z calc. for $\text{C}_{131}\text{H}_{185}\text{N}_{61}\text{O}_{35}$: 3173.4572 Da [M+H], found: 3175.4103 Da.

HPLC: water+0.1% TFA/acetonitrile+0.1% TFA 95:5 to 5:95 in 30 min, flow rate: 1.00 mL/min, $t_{\text{ret}} = 9.3$ min.

BT 403 with linker and cleaver molecule

1-((10R,13R)-24,42-bis(2-(4-amino-2-oxopyrimidin-1(2H)-yl)acetyl)-54-((22R,25R)-29-amino-6-(2-(4-amino-2-oxopyrimidin-1(2H)-yl)acetyl)-12,18-bis(2-(6-amino-9H-purin-9-yl)acetyl)-22-(4-aminobutyl)-25-carbamoyl-2,8,14,20,23-pentaoxo-3,6,9,12,15,18,21,24-octaazanonacosyl)-18-(2-(2-amino-6-oxo-1,6-dihydro-9H-purin-9-yl)acetyl)-48-(2-(6-amino-9H-purin-9-yl)acetyl)-10,13-bis(4-aminobutyl)-1-(2-(2-(bis(2-(1H-benzo[d]imidazol-2-yl)ethyl)amino)ethyl)-1H-benzo[d]imidazol-6-yl)-30,36-bis(2-(5-methyl-2,4-dioxo-3,4-dihydropyrimidin-1(2H)-yl)acetyl)-1,8,11,14,20,26,32,38,44,50,55-undeca-oxo-2,9,12,15,18,21,24,27,30,33,36,39,42,45,48,51,54-heptadecaazahexapentacontan-56-yl)-4-((E)-2-(5-cyano-1-methyl-1H-indol-3-yl)vinyl)pyridin-1-ium chloride

H₂N – D-Lys – D-Lys – A – A – C – Dye – A – C – T – T – C – G – D-Lys – D-Lys – Linker – Cleaver

The aforementioned spared resin from BT403 was swollen in DCM for 1 h. After applying the linker molecule (6-aminohexanoic acid) and the cleaver (2-((2-(Bis(2-((1H-benzo[d]imidazol-2-yl)amino)ethyl)amino)ethyl)amino)-2,3-dihydro-1H-indene-5-carboxylic acid) under the same conditions as described in the general procedure, TFA was added to the resin (1 mL) and the mixture was shaken for 1 h. The crude product was precipitated in diethyl ether (10 mL). The resin was treated 3 times more with TFA to ensure the full cleavage of the oligo-PNA. The mixture was centrifuged and the liquid phase was removed *via* decantation. The crude product was dissolved in a minimum amount of water (~500 µl) and purified *via* semipreparative HPLC (water+0.1% TFA/acetonitrile+0.1% TFA 95/5 to 5/95, 30 min). 305 µg was obtained as a yellow solid.

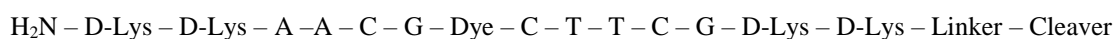
MS (MALDI-TOF): *m/z* calc. for C₁₇₇H₂₂₈N₇₃O₃₄: 3919.8351 Da [M⁺], found: 3925.6452 Da.

HPLC: water+0.1% TFA/acetonitrile+0.1% TFA 95:5 to 5:95 in 30 min, flow rate: 1.00 mL/min, *t*_{Ret} = 5.13 min.

NEW PRODUCTS

BT 404 with linker and cleaver molecule

1-((10R,13R)-48-((28R,31R)-35-amino-12-(2-(4-amino-2-oxopyrimidin-1(2H)-yl)acetyl)-6-(2-(6-amino-4-oxo-4,5-dihydro-1H-imidazo[4,5-c]pyridin-1-yl)acetyl)-18,24-bis(2-(6-amino-9H-purin-9-yl)acetyl)-28-(4-aminobutyl)-31-carbamoyl-2,8,14,20,26,29-hexaoxo-3,6,9,12,15,18,21,24,27,30-decaazapentatriacontyl)-24,42-bis(2-(4-amino-2-oxopyrimidin-1(2H)-yl)acetyl)-18-(2-(2-amino-6-oxo-1,6-dihydro-9H-purin-9-yl)acetyl)-10,13-bis(4-aminobutyl)-1-(2-(2-(bis(2-(1H-benzo[d]imidazol-2-yl)ethyl)amino)ethyl)-1H-benzo[d]imidazol-6-yl)-30,36-bis(2-(5-methyl-2,4-dioxo-3,4-dihydropyrimidin-1(2H)-yl)acetyl)-1,8,11,14,20,26,32,38,44,49-decaoxo-2,9,12,15,18,21,24,27,30,33,36,39,42,45,48-pentadecaazapentacontan-50-yl)-4-((E)-2-(5-cyano-1-methyl-1H-indol-3-yl)vinyl)pyridin-1-ium chloride



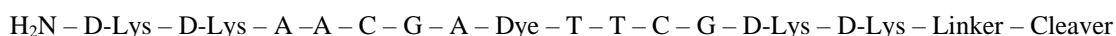
The aforementioned spared resin from BT404 was swollen in DCM for 1 h. After applying the linker molecule (6-aminohexanoic acid) and the cleaver (2-((2-(Bis(2-((1H-benzo[d]imidazol-2-yl)amino)ethyl)amino)ethyl)amino)-2,3-dihydro-1H-indene-5-carboxylic acid) under the same conditions as described in the general procedure, TFA was added to the resin (1 mL) and the mixture was shaken for 1 h. The crude product was precipitated in diethyl ether (10 mL). The resin was treated 3 times more with TFA to ensure the full cleavage of the oligo-PNA. The mixture was centrifuged and the liquid phase was removed *via* decantation. The crude product was dissolved in a minimum amount of water (~500 μ l) and purified *via* semipreparative HPLC (water+0.1% TFA/acetonitrile+0.1% TFA 95/5 to 5/95, 30 min). 432 μ g was obtained as a yellow solid.

MS (MALDI-TOF): m/z calc. for $\text{C}_{178}\text{H}_{229}\text{N}_{72}\text{O}_{35}$: 3934.8347 Da [M+], found: 3939.3311 Da.

HPLC: water+0.1% TFA/acetonitrile+0.1% TFA 95:5 to 5:95 in 30 min, flow rate: 1.00 mL/min, $t_{\text{ret}} = 5.01$ min.

BT 405 with linker and cleaver molecule

1-((10*R*,13*R*)-42-((34*R*,37*R*)-41-amino-18-(2-(4-amino-2-oxopyrimidin-1(2*H*)-yl)acetyl)-12-(2-(6-amino-4-oxo-4,5-dihydro-1*H*-imidazo[4,5-*c*]pyridin-1-yl)acetyl)-6,24,30-tris(2-(6-amino-9*H*-purin-9-yl)acetyl)-34-(4-aminobutyl)-37-carbamoyl-2,8,14,20,26,32,35-heptaoxo-3,6,9,12,15,18,21,24,27,30,33,36-dodecaazahentetracontyl)-24-(2-(4-amino-2-oxopyrimidin-1(2*H*)-yl)acetyl)-18-(2-(2-amino-6-oxo-1,6-dihydro-9*H*-purin-9-yl)acetyl)-10,13-bis(4-aminobutyl)-1-(2-(2-(bis(2-(1*H*-benzo[*d*]imidazol-2-yl)ethyl)amino)ethyl)-1*H*-benzo[*d*]imidazol-6-yl)-30,36-bis(2-(5-methyl-2,4-dioxo-3,4-dihydropyrimidin-1(2*H*)-yl)acetyl)-1,8,11,14,20,26,32,38,43-nonaoxo-2,9,12,15,18,21,24,27,30,33,36,39,42-tridecaazatetracontan-44-yl)-4-((*E*)-2-(5-cyano-1-methyl-1*H*-indol-3-yl)vinyl)pyridin-1-ium chloride



The aforementioned spared resin from BT405 was swollen in DCM for 1 h. After applying the linker molecule (6-aminohexanoic acid) and the cleaver (2-((2-(Bis(2-((1*H*-benzo[*d*]imidazol-2-yl)amino)ethyl)amino)ethyl)amino)-2,3-dihydro-1*H*-indene-5-carboxylic acid) under the same conditions as described in the general procedure, TFA was added to the resin (1 mL) and the mixture was shaken for 1 h. The crude product was precipitated in diethyl ether (10 mL). The resin was treated 3 times more with TFA to ensure the full cleavage of the oligo-PNA. The mixture was centrifuged and the liquid phase was removed *via* decantation. The crude product was dissolved in a minimum amount of water (~500 μ l) and purified *via* semipreparative HPLC (water+0.1% TFA/acetonitrile+0.1% TFA 95/5 to 5/95, 30 min). 366 μ g was obtained as a yellow solid.

MS (MALDI-TOF): m/z calc. for $\text{C}_{179}\text{H}_{229}\text{N}_{74}\text{O}_{34}$: 3958.8460 Da [M^+], found: 3951.9376 Da.

HPLC: water+0.1% TFA/acetonitrile+0.1%TFA 95:5 to 5:95 in 30 min, flow rate: 1.00 mL/min, $t_{\text{Ret}} = 5.01$ min.

NEW PRODUCTS

BT 406 with linker and cleaver molecule

1-((43R,46R)-50-amino-9,27-bis(2-(4-amino-2-oxopyrimidin-1(2H)-yl)acetyl)-3-((10R,13R)-24-(2-(4-amino-2-oxopyrimidin-1(2H)-yl)acetyl)-18-(2-(2-amino-6-oxo-1,6-dihydro-9H-purin-9-yl)acetyl)-10,13-bis(4-aminobutyl)-1-(2-(2-(bis(2-(1H-benzo[d]imidazol-2-yl)ethyl)amino)ethyl)-1H-benzo[d]imidazol-6-yl)-30-(2-(5-methyl-2,4-dioxo-3,4-dihydropyrimidin-1(2H)-yl)acetyl)-1,8,11,14,20,26,32-heptaaxo-2,9,12,15,18,21,24,27,30,33-decaazapentatriacontan-35-yl)-21-(2-(6-amino-4-oxo-4,5-dihydro-1H-imidazo[4,5-c]pyridin-1-yl)acetyl)-15,33,39-tris(2-(6-amino-9H-purin-9-yl)acetyl)-43-(4-aminobutyl)-46-carbamoyl-2,5,11,17,23,29,35,41,44-nonaaxo-3,6,9,12,15,18,21,24,27,30,33,36,39,42,45-pentadecaazapentacontyl)-4-((E)-2-(5-cyano-1-methyl-1H-indol-3-yl)vinyl)pyridin-1-ium chloride



The aforementioned spared resin from BT406 was swollen in DCM for 1 h. After applying the linker molecule (6-aminohexanoic acid) and the cleaver (2-((2-(Bis(2-((1H-benzo[d]imidazol-2-yl)amino)ethyl)amino)ethyl)amino)-2,3-dihydro-1H-indene-5-carboxylic acid) under the same conditions as described in the general procedure, TFA was added to the resin (1 mL) and the mixture was shaken for 1 h. The crude product was precipitated in diethyl ether (10 mL). The resin was treated 3 times more with TFA to ensure the full cleavage of the oligo-PNA. The mixture was centrifuged and the liquid phase was removed *via* decantation. The crude product was dissolved in a minimum amount of water (~500 μ l) and purified *via* semipreparative HPLC (water+0.1% TFA/acetonitrile+0.1% TFA 95/5 to 5/95, 30 min). 463 μ g was obtained as a yellow solid.

MS (MALDI-TOF): m/z calc. for $\text{C}_{178}\text{H}_{228}\text{N}_{75}\text{O}_{33}$: 3943.8463 Da $[\text{M}^+]$, found: 3948.6373 Da.

HPLC: water+0.1% TFA/acetonitrile+0.1%TFA 95:5 to 5:95 in 30 min, flow rate: 1.00 mL/min, $t_{\text{Ret}} = 7.29$ min.

BT 473 with linker and cleaver molecule

1-((16*R*,34*R*,43*R*,46*R*)-50-amino-9,27-bis(2-(4-amino-2-oxopyrimidin-1(2*H*)-yl)acetyl)-3-((10*R*,13*R*,25*R*)-24-(2-(4-amino-2-oxopyrimidin-1(2*H*)-yl)acetyl)-18-(2-(2-amino-6-oxo-1,6-dihydro-9*H*-purin-9-yl)acetyl)-10,13-bis(4-aminobutyl)-1-(2-(2-(bis(2-(1*H*-benzo[d]imidazol-2-yl)ethyl)amino)ethyl)-1*H*-benzo[d]imidazol-6-yl)-25-(3-guanidinopropyl)-30-(2-(5-methyl-2,4-dioxo-3,4-dihydropyrimidin-1(2*H*)-yl)acetyl)-1,8,11,14,20,26,32-heptaaxo-2,9,12,15,18,21,24,27,30,33-decaazapentatriacontan-35-yl)-21-(2-(6-amino-4-oxo-4,5-dihydro-1*H*-imidazo[4,5-*c*]pyridin-1-yl)acetyl)-15,33,39-tris(2-(6-amino-9*H*-purin-9-yl)acetyl)-43-(4-aminobutyl)-46-carbamoyl-16,34-bis(3-guanidinopropyl)-2,5,11,17,23,29,35,41,44-nonaaxo-3,6,9,12,15,18,21,24,27,30,33,36,39,42,45-pentadecaazapentacontyl)-4-((*E*)-2-(5-cyano-1-methyl-1*H*-indol-3-yl)vinyl)pyridin-1-ium chloride



The aforementioned spared resin from BT473 was swollen in DCM for 1 h. After applying the linker molecule (6-aminohexanoic acid) and the cleaver (2-((2-(Bis(2-((1*H*-benzo[d]imidazol-2-yl)amino)ethyl)amino)ethyl)amino)-2,3-dihydro-1*H*-indene-5-carboxylic acid) under the same conditions as described in the general procedure, TFA was added to the resin (1 mL) and the mixture was shaken for 1 h. The crude product was precipitated in diethyl ether (10 mL). The resin was treated 3 times more with TFA to ensure the full cleavage of the oligo-PNA. The mixture was centrifuged and the liquid phase was removed *via* decantation. The crude product was dissolved in a minimum amount of water (~500 μ l) and purified *via* semipreparative HPLC (water+0.1% TFA/acetonitrile+0.1% TFA 95/5 to 5/95, 30 min). 298 μ g was obtained as a yellow solid.

MS (MALDI-TOF): m/z calc. for $\text{C}_{190}\text{H}_{255}\text{N}_{84}\text{O}_{33}$: 4241.0852 Da [M^+], found: 4256.9969 Da.

HPLC: water+0.1% TFA/acetonitrile+0.1% TFA 95:5 to 5:95 in 30 min, flow rate: 1.00 mL/min, $t_{\text{ret}} = 7.50$ min.

NEW PRODUCTS

BT 540 with linker and cleaver molecule

***N*-((5*R*,8*R*,71*R*,74*R*)-1-amino-12,18,60-tris(2-(4-amino-2-oxopyrimidin-1(2*H*)-yl)acetyl)-42,54,66-tris(2-(6-amino-9*H*-purin-9-yl)acetyl)-8,71,74-tris(4-aminobutyl)-5-carbamoyl-24,30,36,48-tetrakis(2-(5-methyl-2,4-dioxo-3,4-dihydropyrimidin-1(2*H*)-yl)acetyl)-7,10,16,22,28,34,40,46,52,58,64,70,73,76-tetradecaoxo-6,9,12,15,18,21,24,27,30,33,36,39,42,45,48,51,54,57,60,63,66,69,72,75-tetracosazaahenooctacontan-81-yl)-2-(2-(bis(2-(1*H*-benzo[d]imidazol-2-yl)ethyl)amino)ethyl)-1*H*-benzo[d]imidazole-6-carboxamide**

H₂N – D-Lys – D-Lys – A – A – C – G – A – C – T – T – C – G – D-Lys – D-Lys – Linker – Cleaver

The aforementioned spared resin from BT540 was swollen in DCM for 1 h. After applying the linker molecule (6-aminohexanoic acid) and the cleaver (2-((2-(Bis(2-((1*H*-benzo[d]imidazol-2-yl)amino)ethyl)amino)ethyl)amino)-2,3-dihydro-1*H*-indene-5-carboxylic acid) under the same conditions as described in the general procedure, TFA was added to the resin (1 mL) and the mixture was shaken for 1 h. The crude product was precipitated in diethyl ether (10 mL). The resin was treated 3 times more with TFA to ensure the full cleavage of the oligo-PNA. The mixture was centrifuged and the liquid phase was removed *via* decantation. The crude product was dissolved in a minimum amount of water (~500 µl) and purified *via* semipreparative HPLC (water+0.1% TFA/acetonitrile+0.1% TFA 95/5 to 5/95, 30 min). 896 µg was obtained as a white solid.

MS (MALDI-TOF): *m/z* calc. for C₁₆₅H₂₂₁N₆₉O₃₇: 3760.7533 Da [M+H⁺], found: 3757.8200 Da.

HPLC: water+0.1% TFA/acetonitrile+0.1%TFA 95:5 to 5:95 in 30 min, flow rate: 1.00 mL/min, *t*_{ret} = 5.81 min.

6 Abbreviation index

Ac acetyl

ACN acetonitrile

Arg arginine

Ab azobenzene

Bn benzyl

cm⁻¹ wavenumber

DIPEA *N,N*-diisopropylethylamine

DMF *N,N*-dimethylformamide

DMSO dimethyl sulfoxide

DNA deoxyribonucleic acid

equiv. equivalents

Et ethyl

EtOAc EtOAc

FAB fast atom bombardment

Fmoc fluorenylmethoxycarbonyl

g grams

HBTU 2-(1H-Benzotriazol-1-yl)-1,1,3,3-tetramethyluronium-hexafluorophosphate
HOAt 1-hydroxy-7-azabenzotriazole

HPLC high performance liquid chromatography
Hz hertz

IR infrared

L-Ala *L*-alanine

ABBREVIATION INDEX

Lys	lysine
m/z	mass to charge ratio
Me	methyl
MeOH	methanol
MHz	megahertz
mL	millilitres
MS	mass spectrometry
NMP	<i>N</i> -methylpyrrolidone
NMR	nuclear magnetic resonance spectroscopy
Ph	phenyl
ppm	parts per million
rt	room temperature
SP	spiropyran
tBu	<i>tert</i> -butyl
TFA	trifluoroacetic acid
THF	tetrahydrofuran
TLC	thin-layer chromatography
T_m	melting point
TSTU	<i>N,N,N',N'</i> -Tetramethyl- <i>O</i> -(<i>N</i> -succinimidyl)uronium tetrafluoroborate
UV	ultraviolet
UV-Vis	ultraviolet and visible

7 Literature Index

1. Wadsworth, W.S. and W.D. Emmons, *The utility of phosphonate carbanions in olefin synthesis*. Journal of the American Chemical Society, 1961. **83**(7): p. 1733-1738.
2. Donnez, D., et al., *Bioproduction of resveratrol and stilbene derivatives by plant cells and microorganisms*. Trends in biotechnology, 2009. **27**(12): p. 706-713.
3. Baderschneider, B. and P. Winterhalter, *Isolation and characterization of novel stilbene derivatives from Riesling wine*. Journal of Agricultural and Food Chemistry, 2000. **48**(7): p. 2681-2686.
4. Miura, T., et al., *Antioxidative and prooxidative action of stilbene derivatives*. Pharmacology & toxicology, 2000. **86**(5): p. 203-208.
5. Condori, J., et al., *Induced biosynthesis of resveratrol and the prenylated stilbenoids arachidin-1 and arachidin-3 in hairy root cultures of peanut: Effects of culture medium and growth stage*. Plant Physiology and Biochemistry, 2010. **48**(5): p. 310-318.
6. Ono, M., et al., *¹¹C-labeled stilbene derivatives as A β -aggregate-specific PET imaging agents for Alzheimer's disease*. Nuclear Medicine and Biology, 2003. **30**(6): p. 565-571.
7. K Gill, R., et al., *A comprehensive review on combretastatin analogues as tubulin binding agents*. Current Organic Chemistry, 2014. **18**(19): p. 2462-2512.
8. Babii, O., et al., *Controlling biological activity with light: diarylethene - containing cyclic peptidomimetics*. Angewandte Chemie International Edition, 2014. **53**(13): p. 3392-3395.
9. Bossi, M., et al., *Reversible red fluorescent molecular switches*. Angewandte Chemie International Edition, 2006. **45**(44): p. 7462-7465.
10. Irie, M., *Diarylethenes for memories and switches*. Chemical Reviews, 2000. **100**(5): p. 1685-1716.
11. Yagi, K. and M. Irie, *Fluorescence property of photochromic diarylethenes with indole groups*. Bulletin of the Chemical Society of Japan, 2003. **76**(8): p. 1625-1628.
12. Pu, S., et al., *Photochromism of new unsymmetrical diarylethene derivatives bearing both benzofuran and thiophene moieties*. Dyes and Pigments, 2012. **94**(2): p. 195-206.
13. Pu, S., et al., *Synthesis and the effects of substitution upon photochromic diarylethenes bearing an isoxazole moiety*. Tetrahedron, 2011. **67**(7): p. 1438-1447.
14. Pu, S., et al., *Syntheses and properties of new photochromic diarylethene derivatives having a pyrazole unit*. Tetrahedron Letters, 2006. **47**(36): p. 6473-6477.
15. Xie, N. and Y. Chen, *Combination of fluorescent switch and electrochemical switch based on a photochromic diarylethene*. New Journal of Chemistry, 2006. **30**(11): p. 1595-1598.
16. Strizhak, A.V., et al., *Highly reactive bis-cyclooctyne-modified diarylethene for SPAAC-mediated cross-linking*. Organic & biomolecular chemistry, 2018. **16**(44): p. 8559-8564.
17. Irie, M., et al., *Photochromism of diarylethene molecules and crystals: memories, switches, and actuators*. Chemical Reviews, 2014. **114**(24): p. 12174-12277.
18. Roubinet, B., et al., *Fluorescent photoswitchable diarylethenes for biolabeling and single-molecule localization microscopies with optical superresolution*. Journal of the American Chemical Society, 2017. **139**(19): p. 6611-6620.

LITERATURE INDEX

19. Uno, K., et al., *Multicolour fluorescent "sulfide-sulfone" diarylethenes with high photo-fatigue resistance*. Chemical Communications, 2020. **56**(14): p. 2198-2201.
20. Diltthey, W. and H. Wübken, *Zur Kenntnis der Spiropyrane. (Heteropolare Kohlenstoffverbindungen, VI.)*. Berichte der deutschen chemischen Gesellschaft (A and B Series), 1928. **61**(5): p. 963-968.
21. Schiele, C. and G. Arnold, *Zum Verhalten 5-Ring-N-heterocyclischer Spiropyrane*. Zeitschrift für Naturforschung B, 1968. **23**(5): p. 628-637.
22. Alonso, M., et al., *Spiropyran derivative of an elastin-like bioelastic polymer: photoresponsive molecular machine to convert sunlight into mechanical work*. Macromolecules, 2000. **33**(26): p. 9480-9482.
23. Putri, R.M., et al., *Labelling Bacterial Nanocages with Photo - switchable Fluorophores*. ChemPhysChem, 2016. **17**(12): p. 1815-1818.
24. Lukyanov, B.S. and M.B. Lukyanova, *Spiropyrans: Synthesis, Properties, and Application. (Review)*. Chemistry of Heterocyclic Compounds, 2005. **41**(3): p. 281-311.
25. Kholmanskii, A.S. and M.D. Kirill, *The Photochemistry and Photophysics of Spiropyrans*. Russian Chemical Reviews, 1987. **56**(2): p. 136.
26. Wizinger, R. and H. Wenning, *Über intramolekulare Ionisation*. Helvetica Chimica Acta, 1940. **23**(1): p. 247-271.
27. Deniz, E., et al., *Fast and stable photochromic oxazines for fluorescence switching*. Langmuir, 2011. **27**(19): p. 11773-11783.
28. Kholmanskii, A.S., A.V. Zubkov, and M.D. Kirill, *The Nature of the Primary Photochemical Step in Spiropyrans*. Russian Chemical Reviews, 1981. **50**(4): p. 305.
29. Knippers, R., *Molecular Genetics*. Vol. 9. 2006, Stuttgart: Thieme-Verlag.
30. Wang, B., et al., *Photoresponsive nanogels synthesized using spiropyran - modified pullulan as potential drug carriers*. Journal of Applied Polymer Science, 2014. **131**(10).
31. Szymański, W., et al., *Reversible photocontrol of biological systems by the incorporation of molecular photoswitches*. Chemical reviews, 2013. **113**(8): p. 6114-6178.
32. Beharry, A.A. and G.A. Woolley, *Azobenzene photoswitches for biomolecules*. Chemical Society Reviews, 2011. **40**(8): p. 4422-4437.
33. Cattaneo, P. and M. Persico, *An ab initio study of the photochemistry of azobenzene*. Physical Chemistry Chemical Physics, 1999. **1**(20): p. 4739-4743.
34. Zhang, F., et al., *Structure-based approach to the photocontrol of protein folding*. Journal of the American Chemical Society, 2009. **131**(6): p. 2283-2289.
35. Bandara, H.D. and S.C. Burdette, *Photoisomerization in different classes of azobenzene*. Chemical Society Reviews, 2012. **41**(5): p. 1809-1825.
36. Samanta, S., et al., *Photoswitching azo compounds in vivo with red light*. Journal of the American Chemical Society, 2013. **135**(26): p. 9777-9784.
37. Knie, C., et al., *ortho - Fluoroazobenzenes: visible light switches with very long - lived z isomers*. Chemistry—A European Journal, 2014. **20**(50): p. 16492-16501.
38. Bleger, D., et al., *o-Fluoroazobenzenes as readily synthesized photoswitches offering nearly quantitative two-way isomerization with visible light*. Journal of the American Chemical Society, 2012. **134**(51): p. 20597-20600.
39. Goldau, T., et al., *Reversible Photoswitching of RNA Hybridization at Room Temperature with an Azobenzene C - Nucleoside*. Chemistry—A European Journal, 2015. **21**(7): p. 2845-2854.
40. Konrad, D.B., J.A. Frank, and D. Trauner, *Synthesis of redshifted azobenzene photoswitches by late - stage functionalization*. Chemistry—A European Journal, 2016. **22**(13): p. 4364-4368.

41. Watson, J.D. and F.H. Crick, *Molecular structure of nucleic acids*. Nature, 1953. **171**(4356): p. 737-738.
42. Suzuki, D.T., *Genetik*. 1991: VCH-Verlag-Ges.
43. Sinden, R.R., *DNA structure and function*. 2012: Elsevier.
44. Watson, J.D. and F.H. Crick, *Genetical implications of the structure of deoxyribonucleic acid*. Nature, 1953. **171**(4361): p. 964-967.
45. Franklin, R.E. and R.G. Gosling, *Evidence for 2-chain helix in crystalline structure of sodium deoxyribonucleate*. Nature, 1953. **172**(4369): p. 156-157.
46. Dickerson, R.E., et al., *The anatomy of a-, b-, and z-dna*. Science, 1982. **216**(4545): p. 475-485.
47. Dickerson, R.E., *Feinstruktur der DNA-Helix*. Spektrum der Wissenschaft, Heidelberg, 1984.
48. Hübscher, U., H.-P. Nasheuer, and J.E. Syväoja, *Eukaryotic DNA polymerases, a growing family*. Trends in biochemical sciences, 2000. **25**(3): p. 143-147.
49. Kornberg, A. and T. Baker, *DNA Replication*. WH Freeman and Company. New York, NY, 1992.
50. Stryer, L., J.L. Tymoczko, and J.M. Berg, *Biochemistry* Vol. 6. 2009, New York.
51. Wilke, C.O., *Selection for fitness versus selection for robustness in RNA secondary structure folding*. Evolution, 2001. **55**(12): p. 2412-2420.
52. Joyce, G.F., *The antiquity of RNA-based evolution*. Nature, 2002. **418**(6894): p. 214-221.
53. Brenner, S., F. Jacob, and M. Meselson, *An unstable intermediate carrying information from genes to ribosomes for protein synthesis*. Nature, 1961. **190**(4776): p. 576-581.
54. Jacob, F. and J. Monod, *Genetic regulatory mechanisms in the synthesis of proteins*. Journal of molecular biology, 1961. **3**(3): p. 318-356.
55. Varghese, R. and H.A. Wagenknecht, *Non-covalent Versus Covalent Control of Self-Assembly and Chirality of Nile Red-modified Nucleoside and DNA*. Chemistry—A European Journal, 2010. **16**(30): p. 9040-9046.
56. Buckup, T., et al., *Ultrafast time-resolved spectroscopy of diarylethene-based photoswitchable deoxyuridine nucleosides*. The journal of physical chemistry letters, 2015. **6**(23): p. 4717-4721.
57. Hoffmeister, M., et al., *Developmental neurogenesis in mouse and Xenopus is impaired in the absence of Nosip*. Developmental biology, 2017. **429**(1): p. 200-212.
58. Bill, B.R., et al., *A primer for morpholino use in zebrafish*. Zebrafish, 2009. **6**(1): p. 69-77.
59. Koshkin, A.A., et al., *LNA (locked nucleic acid): an RNA mimic forming exceedingly stable LNA: LNA duplexes*. Journal of the American Chemical Society, 1998. **120**(50): p. 13252-13253.
60. Kumar, R., et al., *The first analogues of LNA (locked nucleic acids): phosphorothioate-LNA and 2'-thio-LNA*. Bioorganic & medicinal chemistry letters, 1998. **8**(16): p. 2219-2222.
61. Singh, S.K., et al., *LNA (locked nucleic acids): synthesis and high-affinity nucleic acid recognition*. Chemical communications, 1998(4): p. 455-456.
62. Summerton, J. and D. Weller, *Morpholino antisense oligomers: design, preparation, and properties*. Antisense and Nucleic Acid Drug Development, 1997. **7**(3): p. 187-195.
63. Banack, S.A., et al., *Cyanobacteria produce N-(2-aminoethyl) glycine, a backbone for peptide nucleic acids which may have been the first genetic molecules for life on earth*. PLoS One, 2012. **7**(11).
64. Ørum, H., et al., *Single base pair mutation analysis by PNA directed PCR clamping*. Nucleic acids research, 1993. **21**(23): p. 5332-5336.

LITERATURE INDEX

65. Nielsen, P.E., et al., *Sequence-selective recognition of DNA by strand displacement with a thymine-substituted polyamide*. *Science*, 1991. **254**(5037): p. 1497-1500.
66. Autexier, C., *Telomerase as a possible target for anticancer therapy*. *Chemistry & biology*, 1999. **6**(11): p. R299-R303.
67. Evers, M.M., L.J. Toonen, and W.M. van Roon-Mom, *Antisense oligonucleotides in therapy for neurodegenerative disorders*. *Advanced drug delivery reviews*, 2015. **87**: p. 90-103.
68. Chen, C., et al., *Unique chromosome identification and sequence-specific structural analysis with short PNA oligomers*. *Mammalian Genome*, 2000. **11**(5):p. 384-391.
69. Stafforst, T. and D. Hilvert, *Modulating PNA/DNA hybridization by light*. *Angewandte Chemie International Edition*, 2010. **49**(51): p. 9998-10001.
70. Zhang, L., G. Linden, and O. Vázquez, *In search of visible-light photoresponsive peptide nucleic acids (PNAs) for reversible control of DNA hybridization*. *Beilstein journal of organic chemistry*, 2019. **15**(1): p. 2500-2508.
71. Sonar, M.V., et al., *Fluorescence detection of KRAS2 mRNA hybridization in lung cancer cells with PNA-peptides containing an internal thiazole orange*. *Bioconjugate chemistry*, 2014. **25**(9): p. 1697-1708.
72. Koppelhus, U. and P.E. Nielsen, *Cellular delivery of peptide nucleic acid (PNA)*. *Advanced drug delivery reviews*, 2003. **55**(2): p. 267-280.
73. Koppelhus, U., et al., *Improved cellular activity of antisense peptide nucleic acids by conjugation to a cationic peptide-lipid (CatLip) domain*. *Bioconjugate chemistry*, 2008. **19**(8): p. 1526-1534.
74. Hamilton, S.E., et al., *Cellular delivery of peptide nucleic acids and inhibition of human telomerase*. *Chemistry & biology*, 1999. **6**(6): p. 343-351.
75. Zhou, P., et al., *Novel binding and efficient cellular uptake of guanidine-based peptide nucleic acids (GPNA)*. *Journal of the American Chemical Society*, 2003. **125**(23): p. 6878-6879.
76. Sahu, B., et al., *Synthesis and characterization of conformationally preorganized,(R)-diethylene glycol-containing γ -peptide nucleic acids with superior hybridization properties and water solubility*. *The Journal of organic chemistry*, 2011. **76**(14): p. 5614-5627.
77. Lohse, J., O. Dahl, and P.E. Nielsen, *Double duplex invasion by peptide nucleic acid: a general principle for sequence-specific targeting of double-stranded DNA*. *Proceedings of the National Academy of Sciences*, 1999. **96**(21): p. 11804-11808.
78. McNeer, N.A., et al., *Nanoparticles deliver triplex-forming PNAs for site-specific genomic recombination in CD34+ human hematopoietic progenitors*. *Molecular Therapy*, 2011. **19**(1): p. 172-180.
79. Janowski, B.A., J. Hu, and D.R. Corey, *Silencing gene expression by targeting chromosomal DNA with antigene peptide nucleic acids and duplex RNAs*. *Nature protocols*, 2006. **1**(1): p. 436.
80. Imamura, Y., et al., *A peptide nucleic acid to reduce type I collagen production by fibroblast cells*. *Open Journal of Medicinal Chemistry*, 2015. **5**(01): p. 1.
81. Alagpulinsa, D.A., et al., *A peptide nucleic acid targeting nuclear RAD51 sensitizes multiple myeloma cells to melphalan treatment*. *Cancer biology & therapy*, 2015. **16**(6): p. 976-986.
82. Akisawa, T., Y. Ishizawa, and F. Nagatsugi, *Synthesis of peptide nucleic acids containing a crosslinking agent and evaluation of their reactivities*. *Molecules*, 2015. **20**(3): p. 4708-4719.
83. Thomas, S.M., et al., *Antitumor effects of EGFR antisense guanidine-based peptide nucleic acids in cancer models*. *ACS chemical biology*, 2013. **8**(2): p. 345- 352.

84. Dragulescu-Andrasi, A., et al., *Cell-permeable GPNA with appropriate backbone stereochemistry and spacing binds sequence-specifically to RNA*. Chemical communications, 2005(2): p. 244-246.
85. Vermorken, J.B., et al., *Overview of the efficacy of cetuximab in recurrent and/or metastatic squamous cell carcinoma of the head and neck in patients who previously failed platinum - based therapies*. Cancer: Interdisciplinary International Journal of the American Cancer Society, 2008. **112**(12): p. 2710- 2719.
86. Loeffler-Ragg, J., et al., *EGFR inhibition as a therapy for head and neck squamous cell carcinoma*. Expert opinion on investigational drugs, 2008. **17**(10): p. 1517- 1531.
87. Bolarinwa, O., et al., *Structure and Function of AApeptides*. Biochemistry, 2017. **56**(3): p. 445-457.
88. Marr, A.K., W.J. Gooderham, and R.E. Hancock, *Antibacterial peptides for therapeutic use: obstacles and realistic outlook*. Current opinion in pharmacology, 2006. **6**(5): p. 468-472.
89. Zasloff, M., *Antimicrobial peptides of multicellular organisms*. nature, 2002. **415**(6870): p. 389-395.
90. Bahal, R., et al., *In vivo correction of anaemia in β -thalassemic mice by γ PNA-mediated gene editing with nanoparticle delivery*. Nature communications, 2016. **7**(1): p. 1-14.
91. Huang, M.L., et al., *A comparison of linear and cyclic peptoid oligomers as potent antimicrobial agents*. ChemMedChem, 2012. **7**(1): p. 114-122.
92. Kang, S.-J., et al., *Antimicrobial peptides: therapeutic potentials*. Expert review of anti-infective therapy, 2014. **12**(12): p. 1477-1486.
93. Narayana, J.L. and J.-Y. Chen, *Antimicrobial peptides: possible anti-infective agents*. Peptides, 2015. **72**: p. 88-94.
94. Guilhelmelli, F., et al., *Antibiotic development challenges: the various mechanisms of action of antimicrobial peptides and of bacterial resistance*. Frontiers in microbiology, 2013. **4**: p. 353.
95. Nijnik, A. and R. Hancock, *Host defence peptides: antimicrobial and immunomodulatory activity and potential applications for tackling antibiotic-resistant infections*. Emerging health threats journal, 2009. **2**(1): p. 7078.
96. Padhee, S., et al., *Non-hemolytic α -AApeptides as antimicrobial peptidomimetics*. Chemical communications, 2011. **47**(34): p. 9729-9731.
97. Malina, A. and Y. Shai, *Conjugation of fatty acids with different lengths modulates the antibacterial and antifungal activity of a cationic biologically inactive peptide*. Biochemical Journal, 2005. **390**(3): p. 695-702.
98. Henriksen, J.R., et al., *Side chain hydrophobicity modulates therapeutic activity and membrane selectivity of antimicrobial peptide mastoparan-X*. PLoS one, 2014. **9**(3).
99. Niu, Y., et al., *Lipo- γ -AApeptides as a new class of potent and broad-spectrum antimicrobial agents*. Journal of medicinal chemistry, 2012. **55**(8): p. 4003-4009.
100. Gupta, A., A. Mishra, and N. Puri, *Peptide nucleic acids: Advanced tools for biomedical applications*. Journal of Biotechnology, 2017. **259**: p. 148-159.
101. Maekawa, K., et al., *Antisense peptide nucleic acid-peptide conjugates for functional analyses of genes in Pseudomonas aeruginosa*. Bioorganic & medicinal chemistry, 2015. **23**(22): p. 7234-7239.
102. Nölling, J., et al., *Duplex DNA-invading γ -modified peptide nucleic acids enable rapid identification of bloodstream infections in whole blood*. MBio, 2016. **7**(2): p. e00345-16.
103. Kolevzon, N., et al., *Use of peptide nucleic acids to manipulate gene expression in the malaria parasite Plasmodium falciparum*. PLoS One, 2014. **9**(1).

LITERATURE INDEX

104. Goh, S., et al., *Oxacillin sensitization of methicillin-resistant Staphylococcus aureus and methicillin-resistant Staphylococcus pseudintermedius by antisense peptide nucleic acids in vitro*. BMC microbiology, 2015. **15**(1): p. 262.
105. Hansen, A.M., et al., *Antibacterial peptide nucleic acid–antimicrobial peptide (PNA–AMP) conjugates: Antisense targeting of fatty acid biosynthesis*. Bioconjugate chemistry, 2016. **27**(4): p. 863-867.
106. Sadeghizadeh, M., et al., *Cellular Morphology and Immunologic Properties of Escherichia coli Treated With Antimicrobial Antisense Peptide Nucleic Acid*. Iranian Journal of Pathology, 2009. **4**(1): p. 13-18.
107. Kurupati, P., et al., *Inhibition of gene expression and growth by antisense peptide nucleic acids in a multiresistant β -lactamase-producing Klebsiella pneumoniae strain*. Antimicrobial agents and chemotherapy, 2007. **51**(3): p. 805-811.
108. Sawada, S., et al., *Design of tail-clamp peptide nucleic acid tethered with azobenzene linker for sequence-specific detection of homopurine DNA*. Molecules, 2017. **22**(11): p. 1840.
109. Li, J., et al., *The hybridization between peptide nucleic acid containing azobenzene and DNA labeled nanoparticle on chip surfaces studied by atomic force microscopy*. Chinese Science Bulletin, 2008. **53**(19): p. 3077-3080.
110. Hövelmann, F. and O. Seitz, *DNA Stains as Surrogate Nucleobases in Fluorogenic Hybridization Probes*. Accounts of Chemical Research, 2016. **49**(4): p. 714-723.
111. Merino, E., *Synthesis of azobenzenes: the coloured pieces of molecular materials*. Chemical Society Reviews, 2011. **40**(7): p. 3835-3853.
112. Zellmann, F., et al., *Site-Specific Cleavage of RNAs Derived from the PIM1 3' - UTR by a Metal-Free Artificial Ribonuclease*. Molecules, 2019. **24**(4): p. 807.
113. Silver, J.E., et al., *Optimized flash chromatography gradient methods*. Abstracts of Papers of the American Chemical Society, 2013. **246**.
114. Still, W.C., M. Kahn, and A. Mitra, *Rapid Chromatographic Technique for Preparative Separations with Moderate Resolution*. Journal of Organic Chemistry, 1978. **43**(14): p. 2923-2925.
115. Pothukanuri, S., Z. Pianowski, and N. Winssinger, *Expanding the scope and orthogonality of PNA synthesis*. European Journal of Organic Chemistry, 2008. **2008**(18): p. 3141-3148.
116. Pettersson, M., et al., *8-Triazolylpurines: Towards fluorescent inhibitors of the MDM2/p53 interaction*. PloS one, 2015. **10**(5).
117. Shahani, V.M., et al., *Identification of purine-scaffold small-molecule inhibitors of Stat3 activation by QSAR studies*. ACS medicinal chemistry letters, 2011. **2**(1): p. 79-84.
118. Wojciechowski, F. and R.H. Hudson, *A convenient route to N-[2-(Fmoc) aminoethyl] glycine esters and PNA oligomerization using a Bis-N-Boc nucleobase protecting group strategy*. The Journal of organic chemistry, 2008. **73**(10): p. 3807-3816.
119. Dai, D., et al., *Supramolecular assembly-induced emission enhancement for efficient mercury (II) detection and removal*. Journal of the American Chemical Society, 2019. **141**(11): p. 4756-4763.
120. Milic, D. and Prato, M. *Fullerene Unsymmetrical Bis – Adducts as Models for Novel Peptidomimetics*. European Journal of Organic Chemistry. 2010, **2010**(3) p. 476-483.
121. Di Gioia, M., et al., *N-Urethane protection of amines and amino acids in an ionic liquid*. RSC Advances, 2015. **5**(78): p. 63407-63420.
122. Lawton, G.R. and D.H. Appella, *Nonionic side chains modulate the affinity and specificity of binding between functionalized polyamines and structured RNA*. Journal of the American Chemical Society, 2004. **126**(40): p. 12762-12763.

123. Gaudelli, N.M. and C.A. Townsend, *Stereocontrolled syntheses of peptide thioesters containing modified seryl residues as probes of antibiotic biosynthesis*. The Journal of organic chemistry, 2013. **78**(13): p. 6412-6426.
124. Pianowski, Z., et al., *Imaging of mRNA in live cells using nucleic acid-templated reduction of azidorhodamine probes*. Journal of the American Chemical Society, 2009. **131**(18): p. 6492-6497.
125. Guedira, N.E. and R. Beugelmans, *Ambident behavior of ketone enolate anions in SNAr substitutions on fluorobenzonitrile substrates*. The Journal of Organic Chemistry, 1992. **57**(21): p. 5577-5585.
126. Karcher, J., *Photomodulation of Supramolecular Systems Containing Bioactive Small Molecules and Biopolymers*, in IOC. 2019, KIT: Karlsruhe.
127. Al-Horani, R.A., A.Y. Mehta, and U.R. Desai, *Potent direct inhibitors of factor Xa based on the tetrahydroisoquinoline scaffold*. European journal of medicinal chemistry, 2012. **54**: p. 771-783.
128. Schwechheimer, C., *Struktur-Reaktivitätsbeziehung von Cyanin-Styryl-Farbstoffen und deren Anwendung in der fluoreszenten Bioanalytik lebender Zellen*, in IOC. 2019, KIT: Karlsruhe.

8 Appendix

8.1 Curriculum Vitae



Name: Tobias Bantle
Date of birth: 08 November 1989, Karlsruhe

Personal information

E-mail: Tobias_Bantle2@web.de
Nationality: German

Profession

01/2016 – 10/2019 PhD-student: “Peptide Nucleic Acids (PNA) as a versatile tool for modulation of biological systems with visible light”
Dr. Pianowski, Karlsruhe Institute of Technology
Supervision 3 bachelor’s students, 2 interns and many students as a part of their training.
Research Training Groups GRK 2039 Conferences 5 posters

University

04/2015 – 03/2017 Master of Science Chemistry 1.9
Key competences in Organic and Inorganic Chemistry
10/2010 – 03/2015 Bachelor of Science Chemistry, 2.6
-Karlsruhe Institute of Technology

Military service

07/2009 – 03/2010 Basic training at Dornstadt
-Motorist at the logistics Bataillon 471

School

09/2000 – 07/2009 A-Levels, Ludwig Marum Gymnasium Pfinztal

Languages

German native speaker
English fluent
Latin intermediate

Skills

Software

MS-Office, Excel and Origin

Analytics

MS, IR, CD, SEC, HPLC, NMR,

UV-Vis, and fluorescence spectroscopy

Craftsmanship

Repairs of technical devices e.g. HPLC

Driver's license

Car

Interests

Sports (e.g. Volleyball), history, reading, cooking

Karlsruhe, 10 June 2020

9 Acknowledgements

In the end I would like to express my sincere thanks to some people and institutions without whom this work would not have been possible.

First of all I would like to thank my mother and father who brought me to where I am today. Especially my mother, who had a hard time with me after my father died. At this point a special thanks to G. Faude who was like a substitute father for me. He always gave me advice how he would have given it to his own children. May they both rest in peace.

A big thank you goes to the GRK 2039/1 for financing the first 2 1/2 years of the doctorate.

Furthermore, I would like to thank the group of Prof. Dr. Bräse at the Institute of Organic Chemistry at KIT for the infrastructure provided and the unrestricted use of the internal analytical equipment.

Many thanks to my colleagues, especially M. Stahlberger, S. Kirchner, A.-L. Leistner, C. Herlan, J. Karcher, and N. Rosenbaum for the good laboratory atmosphere. It was always a pleasure to work with you and to discuss emerging problems.

Thanks to all family members and friends, especially M. Rutschmann, X. Robin, F. and R. Falk, B. Bitterer, J. Fartak, E. Mittmann, A. and T. Fritz, C. Bickmann, F. und D. Reinhardt, J. Hütig, K. and P. Munz, P. Henkenhaf and K. Albrecht, who have motivated and inspired me all the way and have accompanied me through difficult times.

The greatest thanks goes to Dr. Z. L. Pianowski for the opportunity to do a doctorate in his small group. Thank you for the years of support and the confidence you have shown in us to work on this topic.